NASA/USRA UNIVERSITY ADVANCED DESIGN PROGRAM 1992-1993

PROJECT CENTER MENTOR: NASA-AMES DRYDEN FLIGHT RESEARCH FACILITY

FINAL DESIGN PROPOSAL

The Bunny

A Simulated Commercial Air Transportation Study

April 1993

Department of Aerospace and Mechanical Engineering
University of Notre Dame
Notre Dame, IN 46556

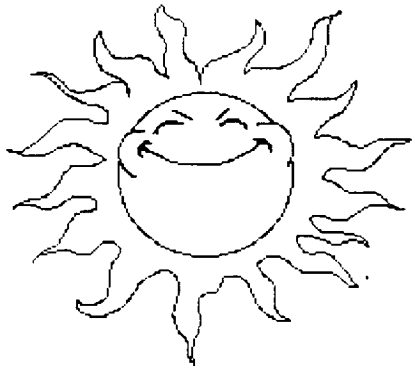

Sunshine
Aeronautics
a division of AE441 Inc.

David Fulton
Patrick Gallagher
William Grannan
Jennifer Martin
Nicole Mastej
Brett Wujek

Final Design Proposal
4/8/93

The Bunny

Table of Contents

List of Figures

List of Tables

List of Nomenclature

$\frac{X_{ac}}{\bar{c}}$	Aerodynamic center location in % of mean chord (from leading edge)
ϕ	Bank Angle
$\frac{d\varepsilon}{d\alpha}$	Change in downwash with angle of attack
$C_{m\delta e}$	Change in pitching moment coefficient with elevator deflection
$\frac{d\sigma}{d\beta}$	Change in the sidewash angle with sideslip
Γ	Dihedral angle
$C_{n\beta}$	Directional stability derivative
S_e	Elevator area
δ_e	Elevator deflection
τ	Flap effectiveness parameter
$C_{m_{\alpha f}}$	Fuselage contribution to pitching moment coefficient slope
$C_{L_{\alpha}}$	Fuselage lift curve slope
AR_H	Horizontal tail aspect ratio
S_H	Horizontal tail area
η	Horizontal tail efficiency
$C_{L_{\alpha}}$	Horizontal tail lift curve slope
V_H	Horizontal tail volume ratio
$C_{l\beta}$	Lateral stability derivative
C_L	Lift coefficient
$\frac{R}{C_{max}}$	Maximum Rate of Climb
$\frac{X_{np}}{\bar{c}}$	Neutral point location in percent of mean chord (measured from leading edge)
C_m	Pitching moment coefficient
C_{mac}	Pitching moment coefficient about the aerodynamic center
$C_{m_{\alpha}}$	Pitching moment coefficient slope
P_{av}	Power Available
P_{re}	Power Required
$C_{l\delta r}$	Roll control power
C_{lp}	Roll Damping Derivative
S_r	Rudder area
δ_r	Rudder deflection
β	Sideslip angle
p_{ss}	Steady State Roll Rate

i_t	Tail incidence (measured from fuselage reference line)
l_t	Tail moment arm
S_v	Vertical tail area
η_v	Vertical tail efficiency
$C_{L\alpha v}$	Vertical tail lift curve slope
V_v	Vertical tail volume ratio
AR	Wing aspect ratio
S_w	Wing area
$C_{L_{\alpha w}}$	Wing lift curve slope
α_{stallw}	Wing stall angle
Λ	Wing sweep
λ	Wing taper ratio
$C_{n\beta wf}$	Wing-fuselage contribution to directional stability derivative
$C_{n\delta r}$	Yaw moment coefficient due to rudder deflection
α	Angle of attack
$\alpha_{L=0}$	Zero-lift angle
A_π	Component area
$\alpha stall)_\delta$	Aircraft stall angle due to flap deflection
$\alpha_{stallA/C}$	Aircraft stall angle
c.g.	Center of gravity location in percent of chord (from the leading edge)
C_D	Drag coefficient
C_{D0}	Parasite drag coefficient
$C_{D\pi}$	Component parasite drag coefficient
C_f	Skin friction coefficient
c_f/c	Flap chord ratio
$C_{L\alpha})_\delta$	Aircraft lift curve due to flap deflection
$C_{L\alpha A/C}$	Aircraft lift curve slope
$C_{L\alpha w})_\delta$	Wing lift curve slope due to flap deflection
$C_{L\alpha wf}$	Wing-fuselage lift curve slope
C_{Lo}	Lift coefficient at zero angle of attack
$C_{Lo})_\delta$	Aircraft lift coefficient at zero angle of attack due to flap deflection
C_{Lowf}	Wing-fuselage lift coefficient at zero angle of attack
C_{Lwing}	Wing lift coefficient
CPSPK	Cost per seat per 1000 feet
c_r	Root chord
c_t	Tip chord

ΔC_L	Change in lift coefficient due to flap deflection
ΔC_{Lw}	Change in wing lift coefficient due to flap deflection
d_f	Fuselage reference diameter
δ_f, df	Flap deflection angle
DOC	Direct Operating Cost
D_p	Propeller diameter
D_{TO}	Take-off distance
e	Oswald efficiency factor
e_{fus}	Fuselage efficiency factor
e_{wing}	Wing efficiency factor
i_w	Wing incident angle
k_{cw}	Wing-canard interference factor
K_{wf}	Wing-fuselage interference factor
k_{wh}	Wing-horizontal tail interference factor
L/D	Lift to drag ratio
LD	Landing Distance
n	Load Factor
PL	Avionics Package Location
ρ	Freestream density
S	Wing planform area
S_H/S	Tail to wing area ratio
SM	Static margin in percent of mean chord
S_{ref}	Reference area
S_{wet}	Aircraft wetted surface area
t	Airfoil thickness
t/c	Airfoil thickness in % chord
V	Freestream velocity
WL	Wing Location
x/c	Chordwise location in % chord

1.0 EXECUTIVE SUMMARY

The Bunny is a single-engine, 100 passenger commercial transport designed to serve the high density short-to-medium range markets in AEROWORLD. The aircraft's design range is 10,000 feet at a cruise velocity of 30 ft/s. With a take-off distance of 16 feet at the maximum take-off weight of 5.3 lbs., the aircraft is capable of serving all airports in AEROWORLD.

The aircraft features a low wing which incorporates polyhedral for roll control. Yaw and pitch control are accomplished by a rudder and elevator, respectively. Propulsion is provided by a nose-mounted Astro 15 electric motor powered by thirteen 1.2 V, 1000 mah batteries with a Zinger 12-6 propeller. The aircraft is structurally designed with a safety factor of 1.5 and is constructed primarily of balsa, bass, and birch wood. Passenger seating is arranged on two levels, with three-abreast on the lower level and two-abreast on the upper level.

The factors which had the most significant influence on the final design were the direct operating cost and the take-off distance. Since this aircraft will be in competition with the existing HB-40, it must offer AEROWORLD airlines a distinct advantage in order to be marketable. In a competitive economic environment, the most attractive feature of a new aircraft is lower operating costs, described in terms of the cost per seat per thousand feet (CPSPK). The large capacity of *The Bunny* helps to reduce the CPSPK, since the total costs are divided among more revenue passengers. In addition, attempts were made to reduce the fuel costs by decreasing the overall weight and increasing the lift to drag ratio. The Astro 15 motor was chosen for its light weight and low cost. The wing features a moderate aspect ratio of 8.5 in order to reduce structural weight, as well as slight taper to reduce induced drag. The Wortmann FX 63-137 airfoil has a high lift-to-drag ratio; in addition, the fuselage shape is trapezoidal to reduce frontal area and features rounded corners to reduce parasite drag. Since one of the primary missions of *The Bunny* is the ability to operate in all cities in AEROWORLD, take-off distance became one of the other driving factors. In order to meet a maximum take-off distance of 20 feet, *The Bunny* was designed with plain flaps spanning the inboard half of the wing. In addition, the Wortmann airfoil was utilized to provide a high C_{Lmax}. With respect to this design goal, the flaps and the high-lift airfoil are critical technologies.

The primary strength of *The Bunny* is its ability to compete economically with the HB-40. At full capacity and mid-range fuel costs, the CPSPK of this aircraft is 25% less than the HB-40. At 75% capacity, it can operate with the same CPSPK as the HB-40 at full capacity. Thus *The Bunny* offers a strong economic advantage in addition to its ability to reach new markets. Another principal strength is its ability to operate in all

airports in AEROWORLD. Also, *The Bunny's* two-piece removable wing is an advantage from a transportability standpoint.

However, *The Bunny* also has some weaknesses which may effect its success. The manufacturing of the wing is more complicated than the competition's due to its high-lift airfoil and flaps. The inability to precisely manufacture the airfoil shape may lead to a decrease in aerodynamic performance from the design values. The use of dihedral instead of ailerons couples the roll control with the lateral/directional stability; as a result, *The Bunny's* roll response may be slow, although it should feature good stability. The stability and control requirements also dictated large tail surfaces; these are a weakness since they cause increased drag.

Figure 1.1: External View - Isometric

Aircraft Dimensions:

Length	=	58 in
Width(top)	=	4.5 in
(bottom)	=	7.5 in
Span	=	9.22 ft

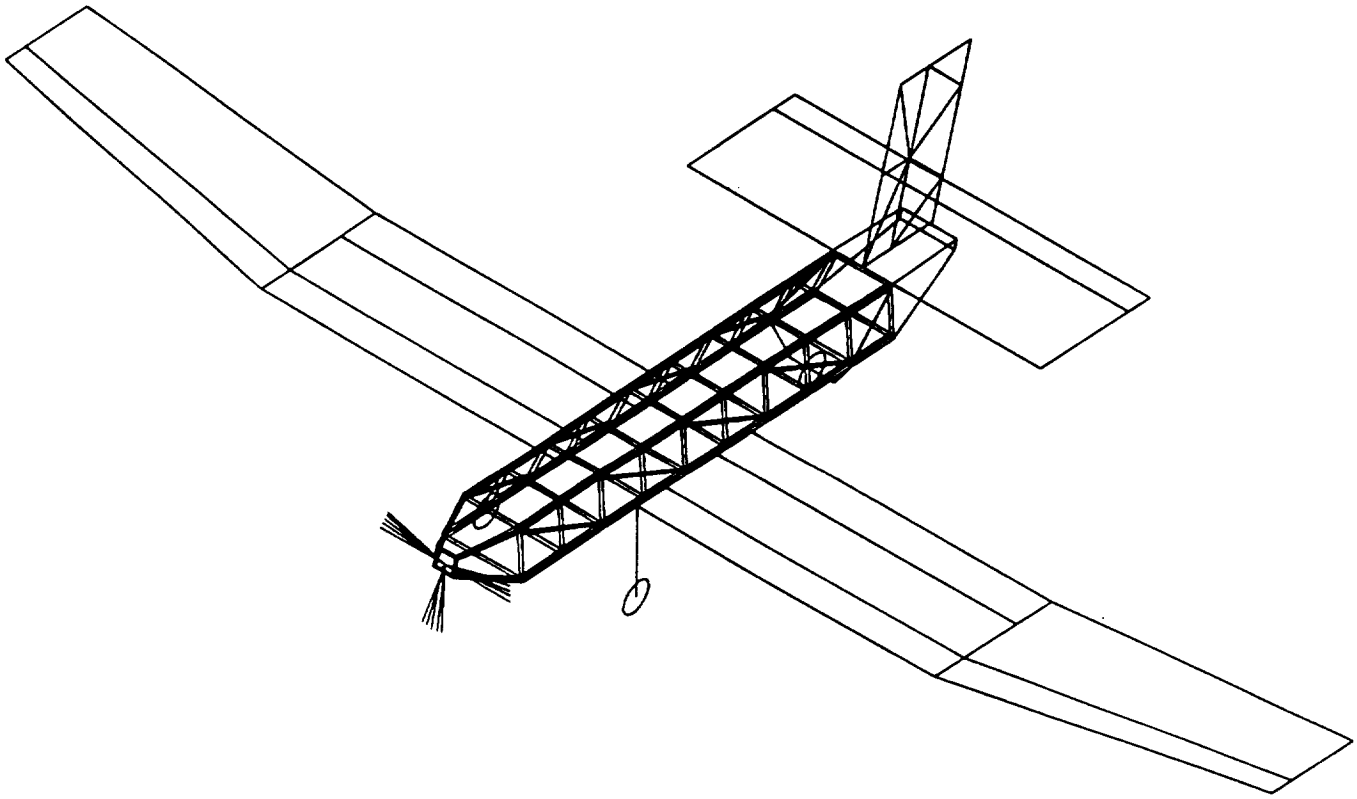

Figure 1.2: External View - Three-view

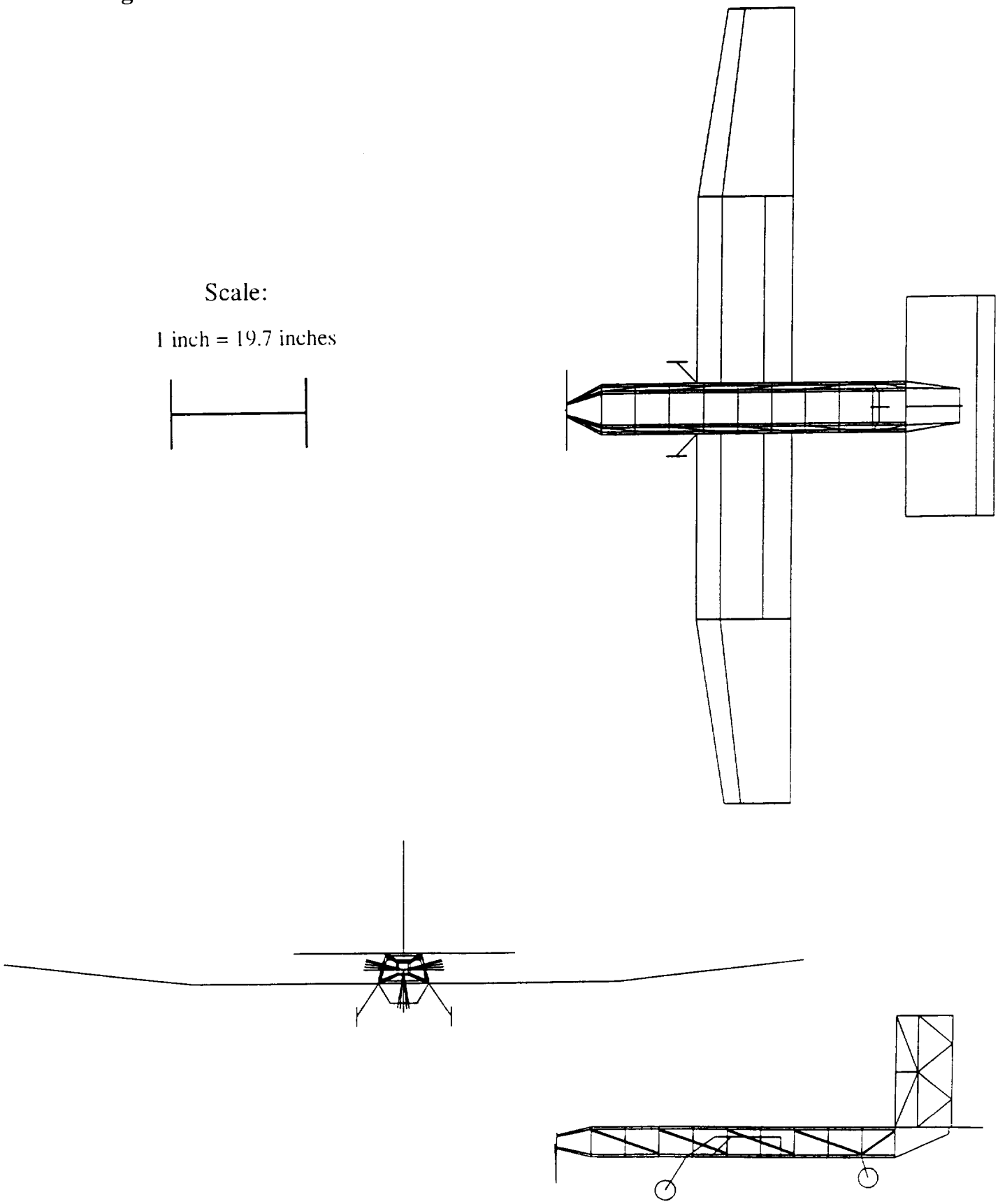

Figure 1.3: Internal View

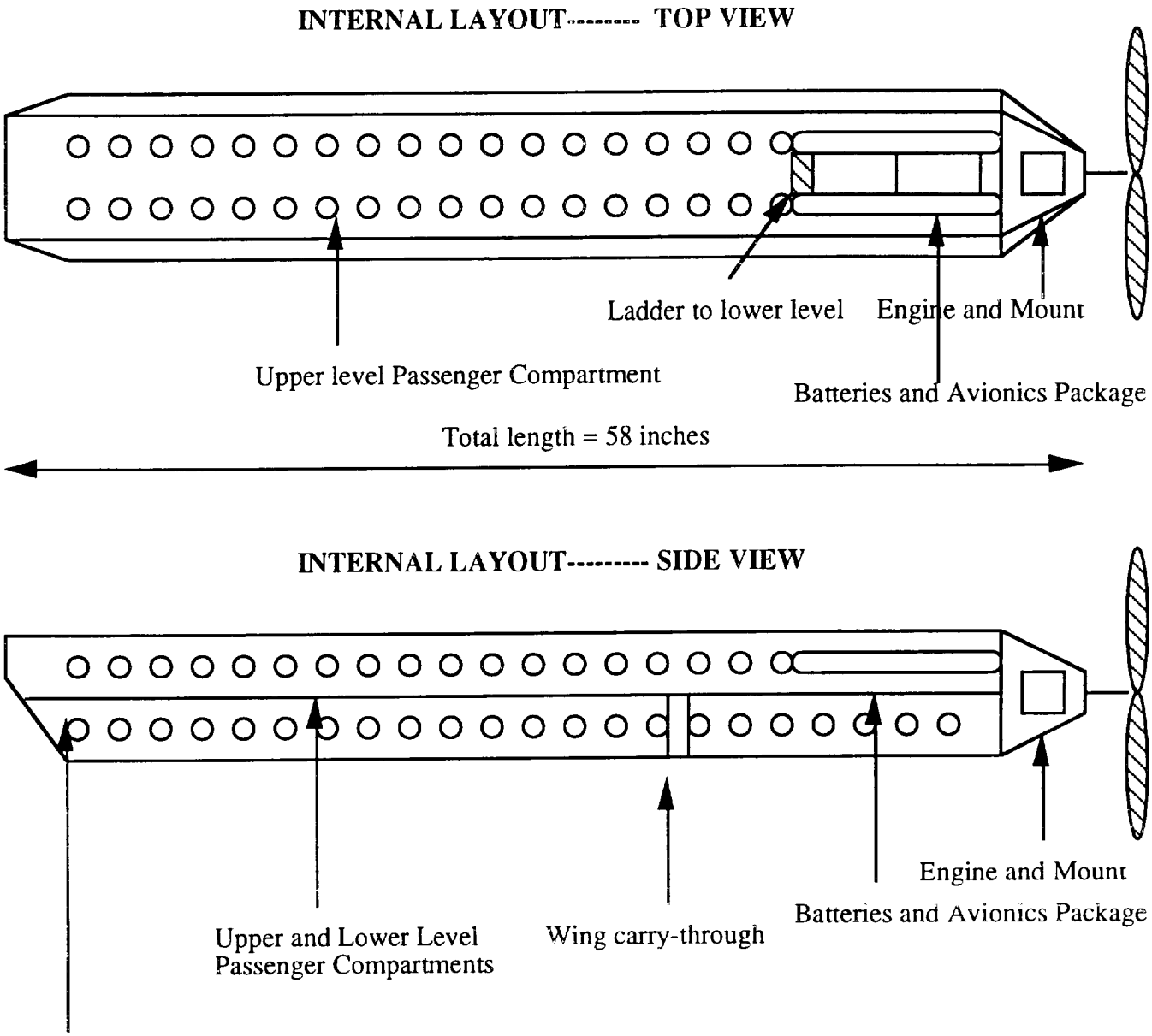

Three passenger rows on the lower deck and two passenger rows on the upper deck

The cockpit and crew are situated below the battery pack and avionics and are separated from the passengers by a main bulkhead

POST FLIGHT MANAGEMENT REVIEW: **The Bunny**

April 30, 1993

The following observations were made during the flight test validation for this aircraft design. This assessment is obviously quite qualitative and is based primarily upon the pilot's comments and instructor's observations.

1. Final flight weight was rather heavy (approx. 6.7 lbs).

2. Good first flight take-off performance with no flaps.

3. It was trimmed at takeoff although C.G. position was not noted. It was assumed to be at the design point.

4. Flew well but appeared to be underpowered although this may be attributable to the heavy takeoff weight.

5. Problems encountered with the speed controller in flight and the aircraft was still controllable. The speed controller was replaced.

6. Second flight with take-off with 1/2 flaps and it appeared to be very underpowered. Inconclusive as to if this was a problem with the speed controller, batteries or that the drag increment was that large.

7. Successful validation of basic flight concept. Flew under control through entire closed course at approximately the required loiter speed. Landing and take-off performance was acceptable based upon the requirements.

Table 1.1: *The Bunny* Specification Summary

Aerodynamics	
Wing Area	10 ft^2
Aspect Ratio	8.5
Mean Chord	12.96 inches
Root Chord	14.04 inches
Span	9.22 ft
Taper Ratio	0.7
Sweep	8.6 degrees
Polyhedral	6 degrees
Cdo (aircraft)	0.031
Airfoil Section	Wortmann FX 63-137
Wing incidence angle	2.5 degrees
Performance	
Take-off distance	16.1 ft
Velocity at take-off	21.7 ft/sec
Velocity in cruise	30 ft/sec
Range (cruise)	14325 ft
Endurance (cruise)	478 sec
Max Range	14728 ft
Max Endurance	478 sec
Max Rate of Climb	9.27 ft/sec
Minimum Turn Radius	33.6 ft
Empennage	
Horizontal Tail section	flat plate
Vertical Tail section	flat plate
Horizontal Tail area	2.98 ft^2
Elevator area	0.60 ft^2
Elevator max deflection	18 degrees
Vertical Tail area	0.97 ft^2
Rudder Area	0.58 ft^2
Rudder max deflection	30 degrees
Propulsion	
Engine	Astro 15
Propeller	Zinger 12-6
Number of Batteries	13
Battery pack voltage	15.6 V
Battery capacity	1000 mah
Cruise prop RPM	4653
Structure	
Weight	5.3 lbs
Fuselage length	58 in
Fuselage Width (max)	7.5 in
Fuselage Height	4.5 in
Economics	
DOC (per flight)	$6.26 - $7.25
CPSPK	.626 - .725 cts

Table 1.2: Critical Data Summary

Parameter	
DESIGN GOALS:	
V cruise	30 ft/s
Max # of passengers	100
#passengers-coach	100
# passengers-1st class	0
# crew	5
Max Range at Wmax	14,325.3 ft
Altitude cruise	20 ft
Minimum turn radius	33.6 ft
Max range at Wmin	14,728 ft
Maximum TO Weight-WMTO	5.3 lbs
Minimum TO Weight - Wmin	4.75 lbs
Total Cost per Aircraft	$1,948.69
DOC	$6.26-$7.25
CPSPK(max design conditions)	.626-.725 cts
BASIC CONFIGURATION	
Wing Area	10 sq ft
Maximum TO Weight-WMTO	5.3 lbs
Empty Flight Weight	4.75 lbs
Wing Loading(WMTO)	8.05 ozs/sq ft
max length	58 inches
max span	9.22 ft
max height	14 inches
Total Wetted Area	5366.1 sq in
WING	
Aspect Ratio	8.5
Span	9.22 ft
Area	10 sq ft
Root Chord	14.04 inches
Tip Chord	9.83 inches
Taper Ratio	0.7(at .25 b)
C mac-MAC	12.96 inches
leading edge Sweep	8.61 degrees
1/4 chord Sweep	8.61 degrees
Dihedral	6 deg (poly)
Twist(washout)	0
Airfoil section	FX63-137
Design Reynolds number	160,000
t/c	0.14
Incidence angle(root)	2.5 degrees
Hor. pos of 1/4 MAC	22.5
Ver. pos of 1/4 MAC	0
e-Oswald efficiency	0.8
CDo-wing	0.0145
CLo-wing	0.36
Clalpha-wing	.078/degree
FUSELAGE	
Length	58 inches
Cross section shape	trapezoid
Nominal Cross Section Area	29.25 sq in
Finess Ratio	8.9
Payload volume	1300 cu in
Frontal area	29.25 sq in
CDo -fuselage	0.00241
CLalpha-fuselage	4.68e-5/ deg

EMPENNAGE	
Horizontal tail	
Area	2.98 sq ft
Span	2.73 ft
Aspect Ratio	2.5
Root chord	1.09 ft
Tip chord	1.09 ft
Average chord	1.09 ft
Taper ratio	1
l.e. sweep	0
1/4 chord sweep	0
incidence angle	0
hor. pos. of 1/4 MAC	52.8 inches
ver. pos. of 1/4 MAC	0
Airfoil section	flat plate
CLalpha - horizontal	.061/degree
CLde - horizontal	
CM mac-horizontal	-0.15
Vertical tail	
Area	1.18 sq ft
Aspect ratio	2
root chord	9.22 inches
tip chord	9.22 inches
average chord	9.22 inches
taper ratio	1
l.e. sweep	0
1/4 chord sweep	0
hor. pos. of 1/4 MAC	54.8 inches
vert. pos. of 1/4 MAC	0
Airfoil section	flat plate
SUMMARY AERODYNAMICS	
Cl max (airfoil)	1.58
CL max(aircraft) w/o flaps	1.45
CL max(aircraft) w/ flaps	1.9
lift curve slope(aircraft)	.086/degree
CDo (aircraft)	0.031
efficiency-e(aircraft)	0.8
Alpha stall(aircraft) w/o flaps	9.5 degrees
Alpha stall(aircraft) w/ flaps	9.2 degrees
Alpha zero lift (aircraft)	7/-13 deg
L/D max(aircraft)	13.1/11.8
Alpha L/D max(aircraft)	3 deg/5 deg
WEIGHTS	
Weight total (empty)	4.75 lbs
C. G. most forward-x&y	21.23
C. G. most aft-x&y	23.3
Avionics	2.75 ounces
Payload-Crew and Pass-max	8.8 ounces
Engine & Engine controls	12.25 ounces
Propeller	.69 ounces
Fuel(battery)	16 ounces
Structure	
Wing	14.4 ounces
Fuselage/emp	11.68/6.3 ozs
Landing gear	6.0 ounces

PROPULSION	
Type of engines	Astro-15
number	1
placement	4 inches
Pavil max at cruise	103.94 Watts
Preq cruise	28.62 Watts
max current draw at TO	11.85 amps
cruise current draw	5.25 amps
Propeller type	Zinger 12-6
Propeller pitch	6 degrees
Number of blades	2
cruise prop. rpm	4653.42
max thrust	3.06 lbs
cruise thrust	.454 lbs
battery type	P90-SCR
number	13
individual capacity	1000 mah
individual voltage	1.2
pack capacity	1000 mah
pack voltage	15.6

STABILITY AND CONTROL	
Neutral point	.59c
Static margin %MAC	0.2
Hor. tail volume ratio	0.69
Vert. tail volume ratio	0.032
Elevator area	.596 sq ft
Elevator max deflection	18 degrees
Rudder area	.71 sq ft
Rudder max deflection	30 degrees
Cm alpha	.008/degree
Cn beta	.138/rad
Cl alpha tail	.061/degree
Cl delta e tail	.01/rad

PERFORMANCE	
Vmin at WMTO	15.95 ft/s
Vmax at WMTO	50 ft/s
Vstall at WMTO	15.95 ft/s
Range max at WMTO	14,355 ft
Endurance @Rmax	495 sec
Endurance Max at WMTO	615 sec
Range at Emax	11,700 ft
Range max at Wmin	14,717 ft
ROC max at WMTO	9.27 ft/s
Min Glide angle	3.97 deg
T/O distance at WMTO	16.1 ft

SYSTEMS	
Landing gear type	tail dragger
Main gear position	20 inches
Main gear length	7 inches
Main gear tire size	1.5 inches
nose/tail gear position	50 inches
n/t gear length	6.5 inches
n/t gear tire size	1 inch
engine speed control	throttle

TECHNICAL	
Max Take-off Weight	5.3 lbs
Empty Operating Weight	4.75 lbs
Wing Area	10 sq ft
Hor. Tail Area	2.98 sq ft
Vert. Tail Area	1.18 sq ft
C. G. position at WMTO	23.3 inches
1/4 MAC position	22.5 inches
static margin %MAC	0.2
V takeoff	30 ft/s
Range max	14,728 ft
Airframe struc. weight	33.5 ounces
Propulsion sys. weight	26.19 ounces
Avionics weight	2.75 ounces
Landing gear weight	6 ounces

ECONOMICS	
raw materials cost	$68.69
propulsion system cost	$146.00
avionics system cost	$284.00
production manhours	100
personnel costs	$1,000.00
tooling costs	$350.00
total cost per aircraft	$1,948.69
Flight crew costs	$.3/flight
mantenance costs	$.063/flight
operation costs per flight	$0.36
current draw at cruise WMTO	5.25 amps
flight time-design Range max	453.3 secs
DOC	$6.26-$7.25
CPSPK	.626-.725 cts

2.0 MISSION DEFINITION

In order to be competitive in the commercial aircraft industry, a new airplane concept must offer the airlines a product which is better than what is currently on the market. This "edge" can be manifested through design characteristics such as greater capacity or longer range, or economic factors such as lower operating cost. A market study which identifies which areas of the market are not currently being served will help identify a target market, and study of the current aircraft will help determine potential improvements. The results of these studies can then be used to define a mission for the aircraft and specify the design requirements and objectives.

2.1 Market Analysis

Data for the AEROWORLD market was supplied by G-Dome Enterprises (Reference 1). The data was obtained in terms of range between cities and the number of passengers traveling between each pair of cities. A standard model for the frequency of flights between each city pair was employed, and this information was used to reduce the total passenger load to passengers per flight on each of the routes. Figure 2.1 depicts the AEROWORLD market in terms of the number of passengers per flight on a given route versus the length of the route in feet.

Figure 2.1: Market Assessment

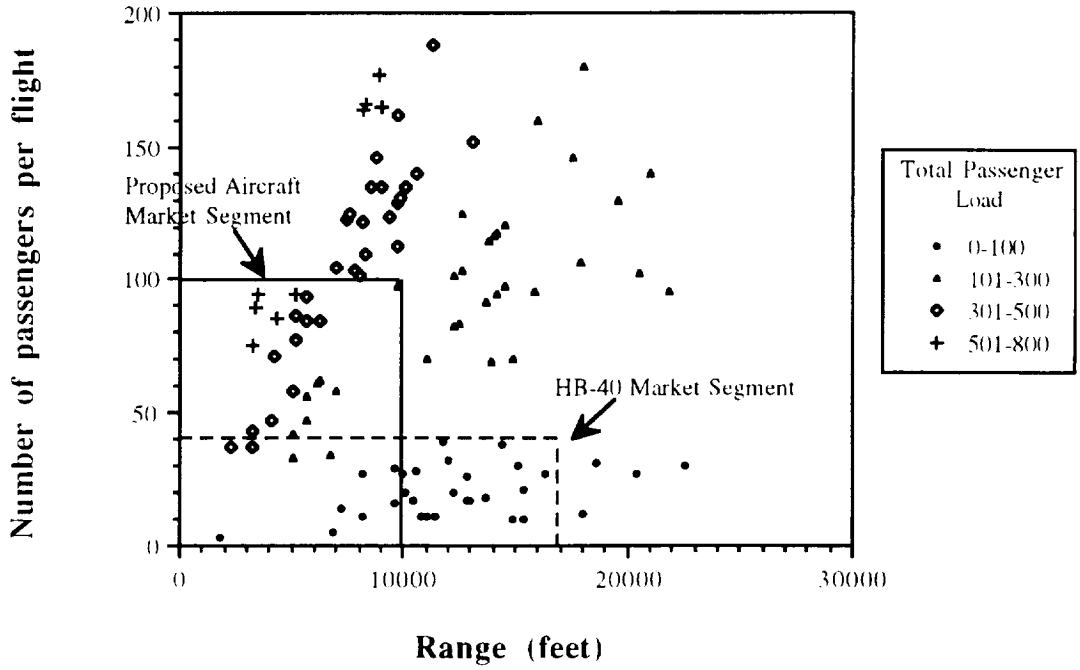

The only aircraft currently serving AEROWORLD is the HB-40, a 40-passenger aircraft with a range of 17000 feet. The market segment which the HB-40 currently serves is summarized in Table 2.1.

Table 2.1: Market served by the HB-40
31 city pairs served 2650 passengers per day in market 8 routes can be operated at 75% capacity or greater

In order to be profitable, the proposed aircraft configuration must be able to serve a segment of the market more efficiently than the competition. The symbols in Figure 2.1 are divided into categories according to the total number of passengers needing to travel a particular route per day, regardless of the number of passengers per flight. Examining the HB-40's market segment as depicted in Figure 2.1, it can be seen that the HB-40 currently serves low-density markets, i.e. the total number of passengers needing to travel on the 31 routes which the HB-40 can serve is only 2650. In addition, Table 2.1 indicates that only 26% of the total possible routes of the HB-40 (8 routes) have a need such that the aircraft will be at least 75% full on any given flight.

Further study of Figure 2.1 reveals that there are a number of shorter range, higher capacity routes which have a greater number of passengers needing to travel per day. In order to study the possibility of a candidate aircraft serving this portion of the market, six proposed configurations were compared. The configurations range from 65 to 100 passengers and have a range of 8000 to 10000 feet. A comparative study shown in Table 2.2 indicates that for larger capacity aircraft, more passengers per day can be included in the target market. Also, for a given size aircraft, extending the range to 10000 feet adds a few more possible routes, although the target market is not significantly increased.

Table 2.2: Comparison of Candidate Configurations			
Range (feet)	**Capacity (passengers)**	**# of City Pairs Served**	**Total # of Passengers per Day**
8000	65	17	4330
8000	80	20	5980
8000	100	28	10580
10000	65	22	4690
10000	80	23	6340
10000	100	34	11240

In order to efficiently serve the market, it is desired that the aircraft size match the demand on the routes as closely as possible. Thus, the operating costs of the aircraft are

distributed among more revenue passengers. However, as an aircraft manufacturer it is advantageous to build an aircraft which has the potential to accommodate future market expansion. With this in mind, the 100-passenger, 10000 foot range aircraft was chosen as the proposed aircraft configuration, since it can serve the most routes and also captures the largest target market. In addition, 32% of the proposed aircraft's routes can be operated at 75% capacity or better. Thus, the proposed aircraft offers a slight improvement over the HB-40 in terms of serving the market efficiently, while offering a significant increase in total target market . The final configuration chosen for the proposed aircraft and the market it will serve are summarized in Table 2.3.

Table 2.3: Proposed Aircraft's Size and Target Market
100 passenger capacity 10000 foot range
34 city pairs served 11240 passengers per day in market
11 routes can be operated at 75% capacity or greater

The proposed aircraft will serve 12 routes on which the HB-40 currently operates, while adding an additional 22 routes that the HB-40 cannot serve. The aircraft will be designed to minimize fuel and manufacturing costs, so that its cost advantage over the HB-40 can be maximized.

2.2 Design Requirements and Objectives

The goal of *Sunshine Aeronautics* with regard to the current project is threefold:

- to serve the travel needs of the target AEROWORLD market through the design of a large capacity, medium range civil transport;
- to serve the economic needs of AEROWORLD passengers by reducing the costs associated with production, manufacturing, and waste;
- and to serve the environmental needs of AEROWORLD through the proper disposal and reduction of waste materials.

In order to accomplish these goals certain technical and manufacturing design requirements and objectives were established and are specified as follows:

REQUIREMENTS:

- Limited to $190 to purchase raw materials by management directive.
- Must allow for 8 cubic inches per passenger to ensure passenger comfort.
- Must include two person flight crew.
- Must include three attendants to serve 100 passengers.
- Perform a 60 foot radius turn at 25 ft/sec.
- Loiter for 2 minutes.
- Design prototype to take off and land under its own power.
- Ensure altitude does not exceed 25 feet .
- Install removable radio control and propulsion system in under 20 minutes.
- Utilize no more than four servos.
- Follow safe life design philosophy for all structural components.
- Transport prototype in 8'x4' space to ensure compatibility with transport vehicle.
- Construct prototype within two week period.

Note: All requirements are per AEROWORLD regulations unless otherwise specified.

OBJECTIVES:

Aircraft Configuration:

Internal:

- Large capacity aircraft - 100 passengers in coach seating (from market analysis).
- Separate cockpit area to accommodate two crew members and area to accommodate three flight attendants.
- Area to accommodate propulsion system and radio control system.
- Two level passenger seating arranged two abreast on the top level and three abreast on the lower level with at least 1.5 inch aisle spacing on each level.
- Internal volume of approximately 1300 cubic inches to accommodate passengers and equipment.

External:

- Trapezoidal fuselage for drag reduction, propeller blockage reduction and ease in manufacturing.
- Three control surfaces consisting of elevator and rudder for control and flaps for increased C_L on take-off.
- Tricycle/tail dragger landing gear with pivoting rear wheel which provides adequate ground clearance for the propeller.

- Easy access to batteries and radio control system.
- Tapered tail and nose section for drag reduction.
- Rounded fuselage edges for drag reduction.
- Overall prototype length of approximately 56 inches to accommodate passenger section and nose and tail sections.

Propulsion:

- Single engine battery powered aircraft for reduced complexity and weight.
- Provide sufficient thrust for take off and cruise at maximum payload weight.
- Propeller diameter greater than 10 inches to reduce fuselage blockage effects.
- Flexibility in battery placement to allow for CG control.
- Variable throttle control to allow pilot control of aircraft speed.

Structures:

- Use of lightweight and available materials consistent with AEROWORLD technology.
- Maximum empty weight of 6 pounds.
- Maximum operating weight of 6.5 pounds.
- Supporting structure provided for a wing carry-through design.
- Safe life design throughout a cycle of 400 flights.
- Landing gear able to absorb impact of landing.

Aerodynamics, Stability and Control:

Wing:

- Tapered wing to provide a more elliptical wing loading and thus a higher L/D.
- Polyhedral to provide roll control in the absence of ailerons.
- Flaps controlled by servo motor to provide greater C_L during take-off.

Horizontal Tail:

- Elevator controlled by servo motor to provide pitch control about the c.g.

Vertical Tail:

- Rudder controlled by servo motor to provide yaw and roll control.
- Rudder and pivoting rear wheel to provide ground maneuverability.

Performance:

- Range of 13, 000 feet to allow for operation between cities of 10, 000 foot range and a two minute loiter consisting of 3000 feet.

- Target cruise speed of 30 ft/s.
- Maximum take off distance of 20 feet to serve all cities in target market.
- Minimum take off speed of 15-20 ft/s.
- Maximum airfoil L/D of approximately 30 with flaps deflected.

Cost and Manufacturing:

- CPSPK 25% less than that of the HB-40.
- Projected total cost of prototype $2, 225.
- Maximum total person hours of 100.

The final design did not require any exceptions to the design requirements and objectives.

3.0 CONCEPT SELECTION

For a given aircraft mission and specified design requirements and objectives, there are many different concepts which are appropriate. Before preliminary design studies can commence, each candidate concept must be evaluated in order to determine the final concept. Strengths and weaknesses of each concept must be discussed so that the final concept represents the best possible configuration. The final concept for *The Bunny* is a hybrid of three different concepts which were evaluated as discussed below.

3.1 Aileron Design

One of the first designs considered was a high-wing aircraft with ailerons, illustrated in Figure 3.1. Passenger seating was arranged three-abreast on a single level. Dihedral was not incorporated due to the use of ailerons in combination with the high-wing design. The wing was of rectangular planform with a moderate aspect ratio.

The primary advantage of this design was the fuselage volume efficiency offered by its three-abreast seating configuration. For a given capacity, seating passengers three-abreast requires less aisle space than a two-abreast design. A four-abreast configuration would require even less aisle space, but would result in a short, wide fuselage, which could cause stability problems. Another advantage of this concept was the use of ailerons, which ensure proper roll control without excessive lateral stability, as can be the case for a dihedral design. However, there were also several important disadvantages. In order to accommodate 100 passengers as dictated by the aircraft's mission, the fuselage was very long, necessitating a stronger fuselage structure and therefore adding weight. In addition, the design requirement of a maximum take-off distance of 20 feet may require the use of flaps. However, flaps were not possible on this design with the standard 4-channel radio transmitters, since the ailerons, rudder, elevator and speed control occupy all available channels.

3.2 Tapered Wing Design

Another candidate concept was a high-wing, tapered planform design, shown in Figure 3.2. Seating for this concept was arranged two-abreast on two levels. The fuselage shape was trapezoidal, with a tapered lower deck. The nose and tail sections were also tapered. A removable, one-piece wing was employed.

This concept offered several key advantages. The tapered wing offered less induced drag for improved aerodynamic performance. Although the taper would require airfoil sections to be of different sizes, this was not seen as a significant manufacturing problem. The trapezoidal fuselage with its rounded edges was seen as a potential

Figure 3.1: Aileron Design

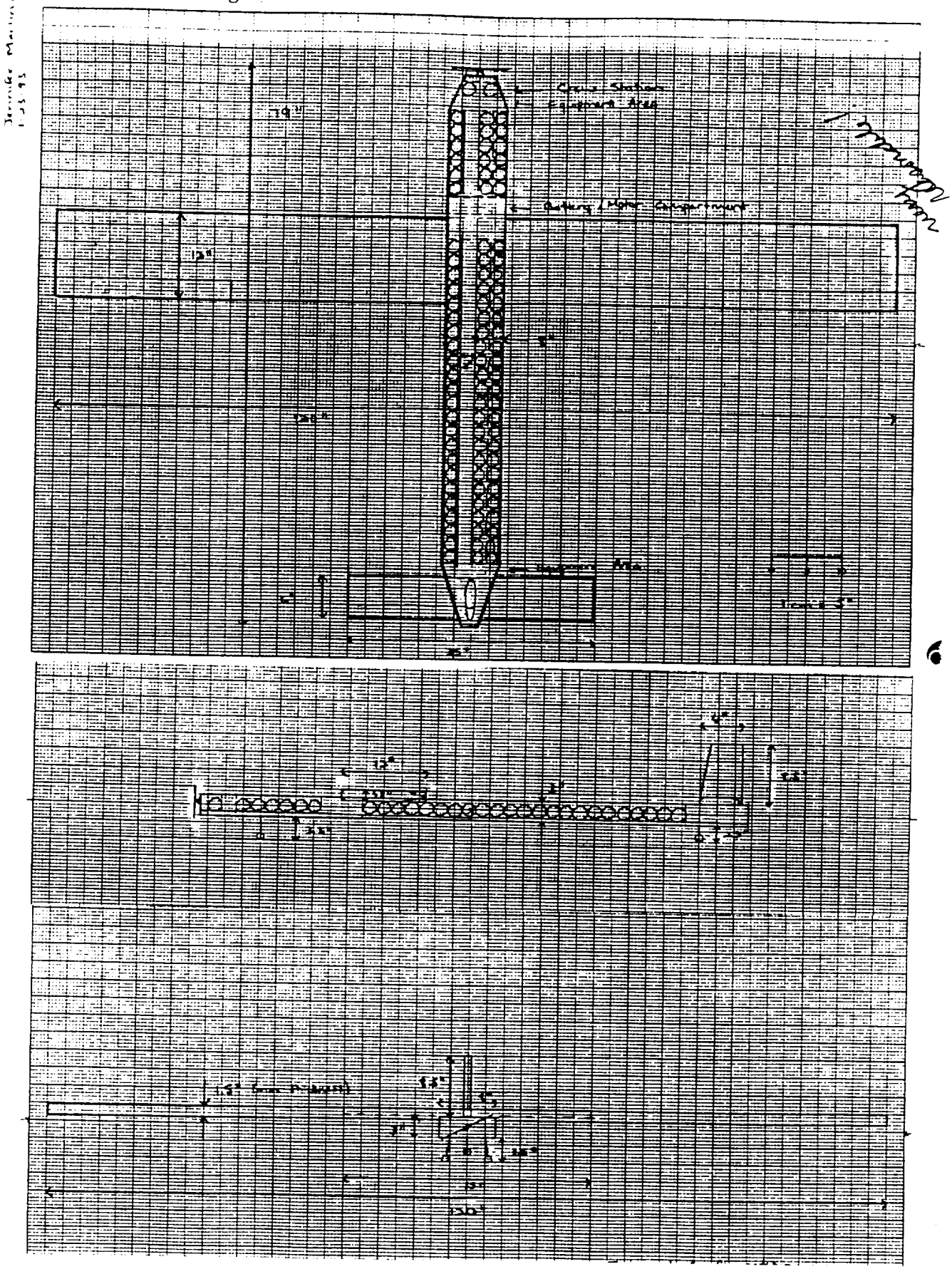

Figure 3.2: Tapered Wing Design

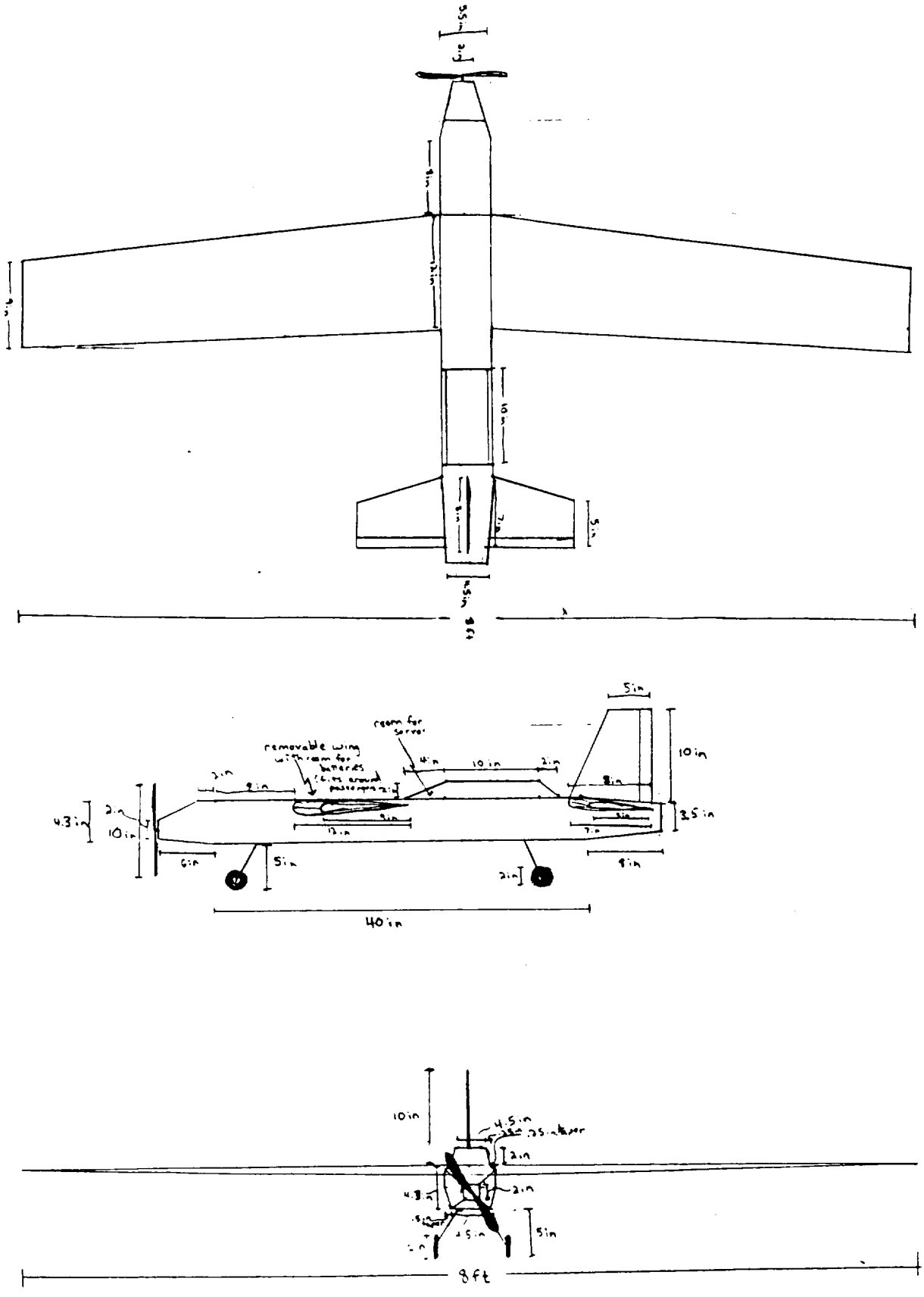

advantage if combined with a seating arrangement of three-abreast on one level and two-abreast on the other level. For this type of configuration, with an odd number of passengers per cross section, the trapezoid would have less frontal area than a rectangular fuselage and would thus offer a drag reduction. The double-level seating provided greater capacity with a moderate fuselage length. However, a disadvantage was seen in the one-piece removable wing, since transportability requirements would limit the wing span to eight feet.

3.3 Triple-deck Design

A third concept considered was the three-level, two abreast passenger seating design depicted in Figure 3.3. This aircraft featured a square fuselage with a high wing. Dihedral was included for roll control, with a flat center section for ease of attachment to the fuselage. The nose and tail sections were tapered as for the tapered wing design.

The main advantage of this design was the potential for high capacity due to the three-level passenger seating deck. However, a disadvantage was also associated with this design feature. Since a capacity of 100 passengers has been targeted, a three-deck design leads to a relatively short fuselage and thus a short tail moment arm. This was a significant concern, since the tail moment arm has a prominent effect on stability and control. In addition, the three-level fuselage required an additional aisle and led to less efficient use of fuselage volume.

3.4 *The Bunny*

The final concept chosen for *The Bunny* strives to incorporate the primary strengths of the candidate configurations while eliminating the weaknesses. Table 3.1 summarizes these specific strengths and weaknesses.

Table 3.1: Primary Strengths and Weaknesses of Candidate Concepts

Concept	Strengths	Weaknesses
Aileron Design	Three-abreast design uses cabin space efficiently	Long fuselage leads to increased structural weight
		Inclusion of ailerons uses all available radio channels
Tapered-wing Design	Tapered wing reduces induced drag	One-piece wing may be difficult to transport
	Trapezoidal fuselage with rounded edges reduces drag	
Triple-deck Design	Three-level design allows higher capacity	Short fuselage may create insufficient tail moment arm

Figure 3.3: Triple-deck Design

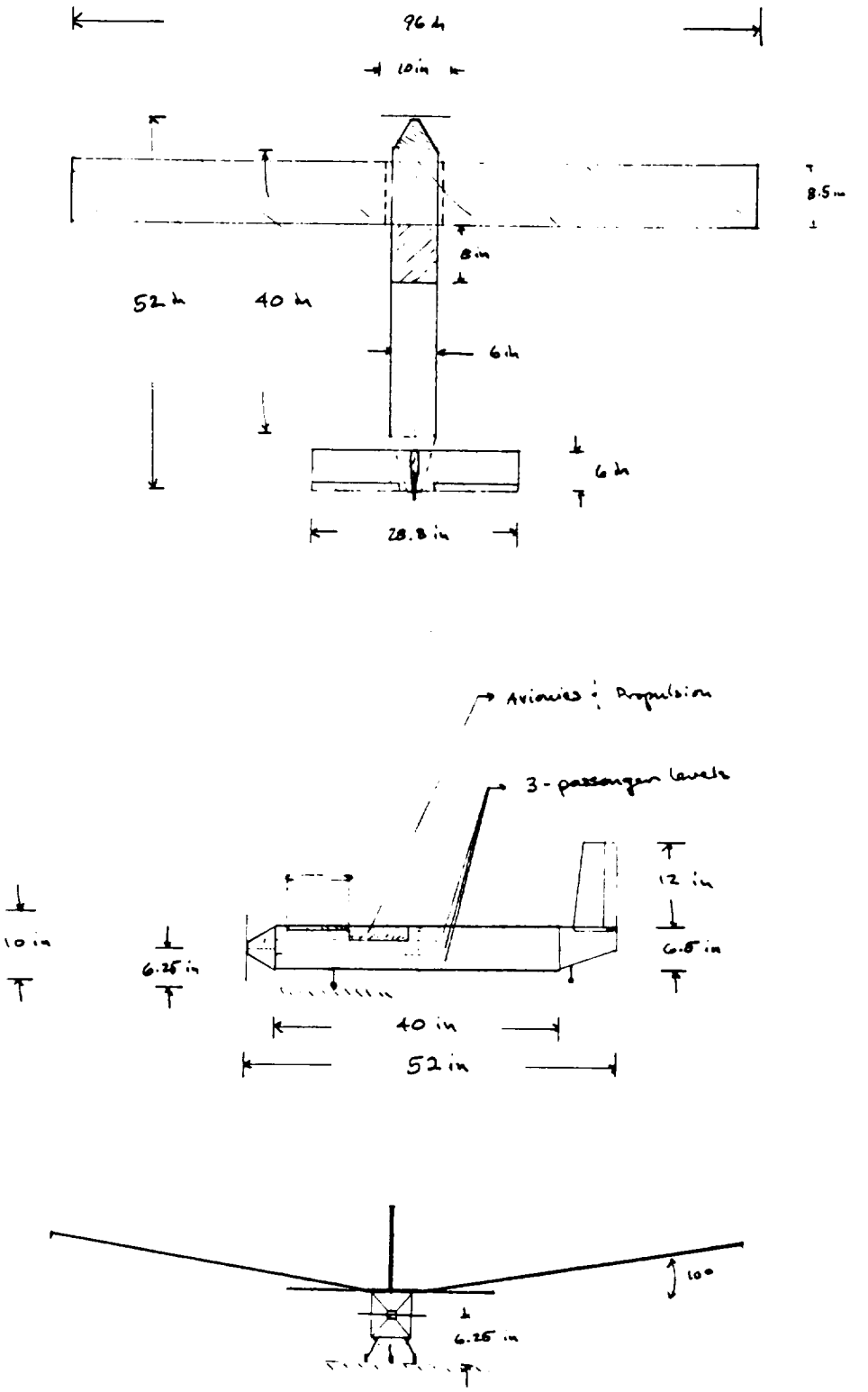

The Bunny features double-level seating to provide a capacity of 100 passengers while maintaining a moderate fuselage length. This allows a trade-off between minimum structural weight and maximum tail moment arm. The passenger seating arrangement incorporates the drag reduction advantage of a trapezoidal fuselage with fuselage volume efficiency by using three-seats-abreast on the bottom level and two-abreast on the top. This single-class arrangement represents the highest capacity seating available on *The Bunny*. Future designs may feature areas of two-abreast first class seating on the lower level, but the total capacity will be reduced. Alternate seating arrangements will be designed according to individual airlines' needs. The nose and tail sections will be tapered to minimize drag. In order to meet the maximum take-off distance requirement, flaps will be utilized; therefore, dihedral rather than ailerons will be used for roll control. Since the flaps will span the inner half of the wing, a three-panel polyhedral design will be used, such that the flapped portion of the wing will be flat. This will maximize the effect of the flaps and increase the ease of construction. The outboard portion of the wing will be slightly tapered to improve aerodynamic performance. A two-piece removable low wing design will be used to ensure adequate transportability. Accessibility of the battery/servo compartment will be maintained by placing these components on the top level. Tail-dragger landing gear will be employed such that the main gear can be attached to the wing carry-through structure, eliminating the need for additional structural build-up. Diagrams of *The Bunny's* external and internal configurations can be found in Figures 1.1, 1.2, and 1.3.

4.0 AERODYNAMIC DESIGN DETAIL

The major contributing factors in the aerodynamic design of *The Bunny* include both economic and performance requirements. In order to reduce fuel costs and meet the take-off, range and endurance performance requirements, obtaining maximum lift became the most significant factor behind the aerodynamic design. By providing a take-off distance less than 20 ft., *The Bunny* aims to serve all passenger markets within Aeroworld. To serve these goals, a high-lift airfoil and flaps have been incorporated into the design of the main wing. Minimizing drag, and hence the costs associated with the propulsion system, was another major factor in the aerodynamic design. To serve this goal, tapered wing tips and a low-wing attachment were incorporated in the wing design. Through this combination of aerodynamic features, *The Bunny* proves to be a viable competitor in the low Reynolds number, high-volume passenger transport market of Aeroworld.

4.1 Airfoil Selection

The selection of a low Reynolds number (Re=1.6E+05) airfoil section for the main wing involved four primary considerations. First, due to a high volume fuselage section (100 passengers) and a take-off requirement of under 20 ft, an airfoil section with high lift characteristics is necessary. Second, in order to reduce overall drag, the airfoil section must exhibit low drag characteristics. Third, a high airfoil L/D is necessary to reduce propulsion requirements and increase the range and endurance performance of the aircraft. Finally, the geometry of the airfoil section must be considered. The airfoil cross-section must be thin enough to reduce the overall weight of the wing, yet it must provide adequate thickness in order to allow for structural support. The thickness of the airfoil section near the trailing edge must also be considered due to the implementation of flap devices. For $c_f/c=0.3$ and $x/c=0.7$, an airfoil cross-section thickness of at least 1/4 in. is required to provide adequate structural support for the flap section.

Figures 4.1-4.3 illustrate the lift, drag, and L/D characteristics versus angle of attack for four different airfoils commonly selected for use in gliders, RPV's, and other low Reynolds number aircraft designs. These airfoils were selected for their relatively high lift and L/D capabilities. Note the differences in Reynolds number for each set of airfoil section data [2]. Based on its high lift, low drag, and high L/D characteristics the Wortmann FX 63-137 airfoil section offers our design the best aerodynamic performance. As illustrated in Figures 4.1 and 4.3, the FX 63-137 demonstrates significantly higher lift and L/D capabilities than the other airfoils.

Fig. 4.1: Cl vs. Alpha for Various 2-D Airfoil Sections

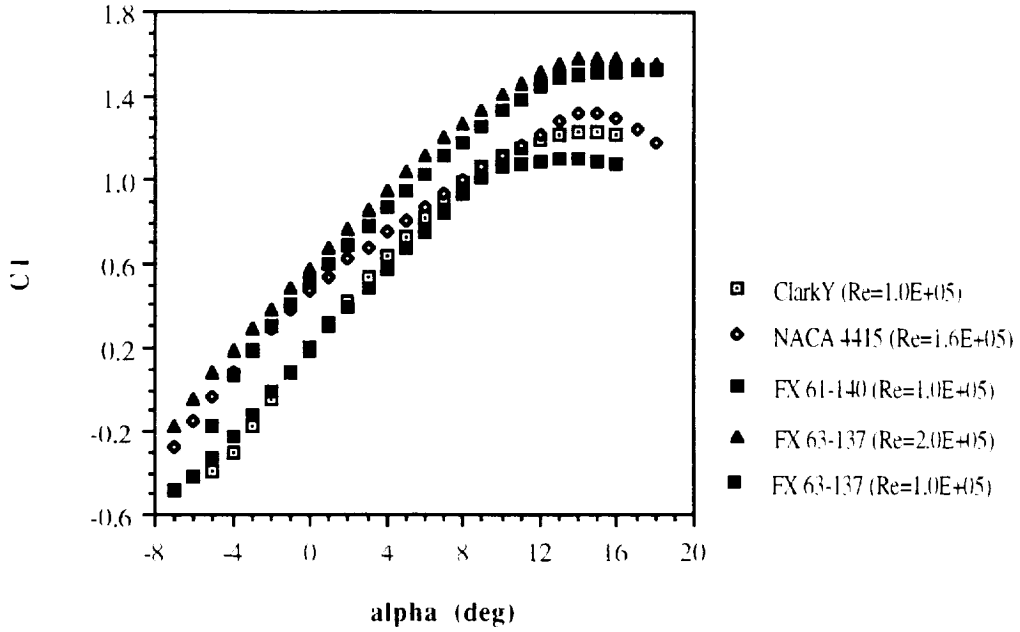

Fig. 4.2: Cd vs. Alpha for Various 2-D Airfoil Sections

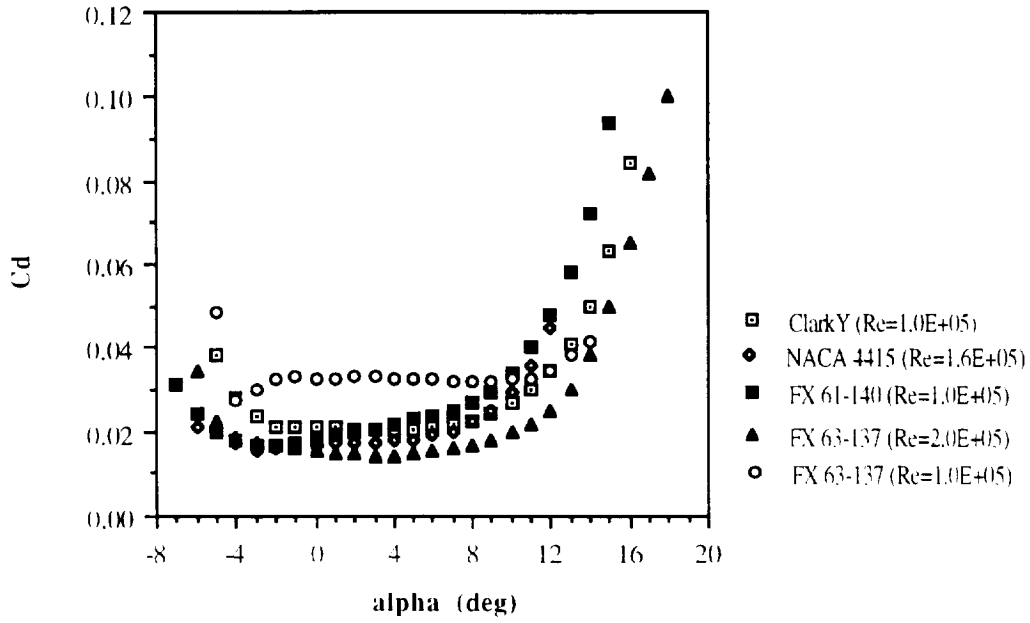

Fig. 4.3: Cl/Cd vs. Alpha for Various 2-D Airfoil Sections

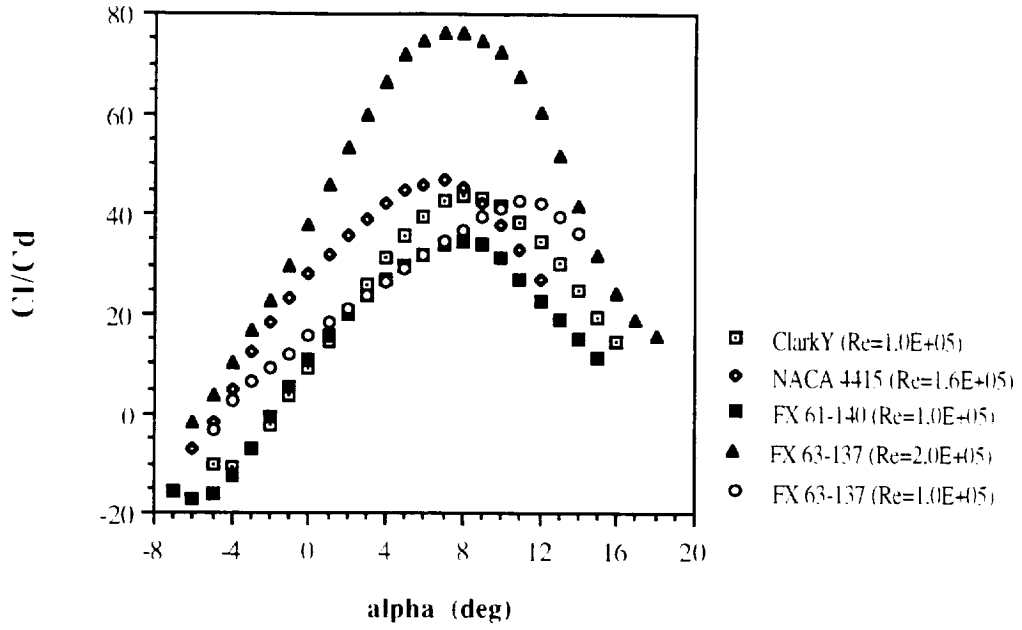

However, the data for the FX 63-137 also shows the effect of Reynolds number on airfoil lift and drag performance. For the data sets given in Figures 4.1-4.3 (Re=1.0 and 2.0E+05) the FX 63-137 exhibits significant changes in aerodynamic performance. Whereas Figure 4.1 illustrates only a slight decrease in C_l due to a lower Reynolds number, Figures 4.2 and 4.3 illustrate the significant drag increases due to lower Reynolds number. Although *The Bunny* shall operate at a cruise Reynolds number in between these data sets (Re=1.6E+05), design considerations must take into account the increased drag with decreasing Reynolds number. Design of *The Bunny* must compensate for drag losses at conditions other than cruise where low Reynolds numbers will be encountered (larger chord to increase effective Reynolds number, high AR to reduce induced drag, etc.), yet it is recommended that further development stages of *The Bunny* investigate the effect of Reynolds number on the specific performance and propulsion requirements of *The Bunny*.

The aerodynamic performance of the remaining airfoils, although offering the advantage of ease of manufacturing due to their relatively flat lower surfaces and "simple" geometries, are considerably lower than that of the FX 63-137. Both the NACA 4415 and the Clark Y airfoils have flat lower surfaces and thick trailing edges making them relatively easier to produce and capable of supporting a flap structure, yet neither achieves the high lift performance of the FX 63-137. Table 4.1 summarizes the aerodynamic performance

and geometric characteristics for each of the airfoils considered for *The Bunny*. Figure 4.4 illustrates the lift and drag characteristics of our design airfoil, the FX 63-137.

Table 4.1: Airfoil Aerodynamic and Geometric Summary						
Airfoil Section	**C_{Lmax}**	**C_{Dmin}**	**l/dmax**	**t/c**	**$\alpha_{L=0}$**	**t (x/c=0.7)**
Clark Y	1.23	0.021	43.8	0.117	-2.0 deg	1.05 in
NACA 4415	1.32	0.015	46.8	0.150	-5.0 deg	1.28 in
FX 61-140	1.10	0.017	34.8	0.140	-2.0 deg	1.01 in
FX 63-137	1.58	0.014	78.0	0.137	-5.5 deg	0.88 in

Fig. 4.4: Cl & Cd vs. Alpha for FX 63-137 Airfoil

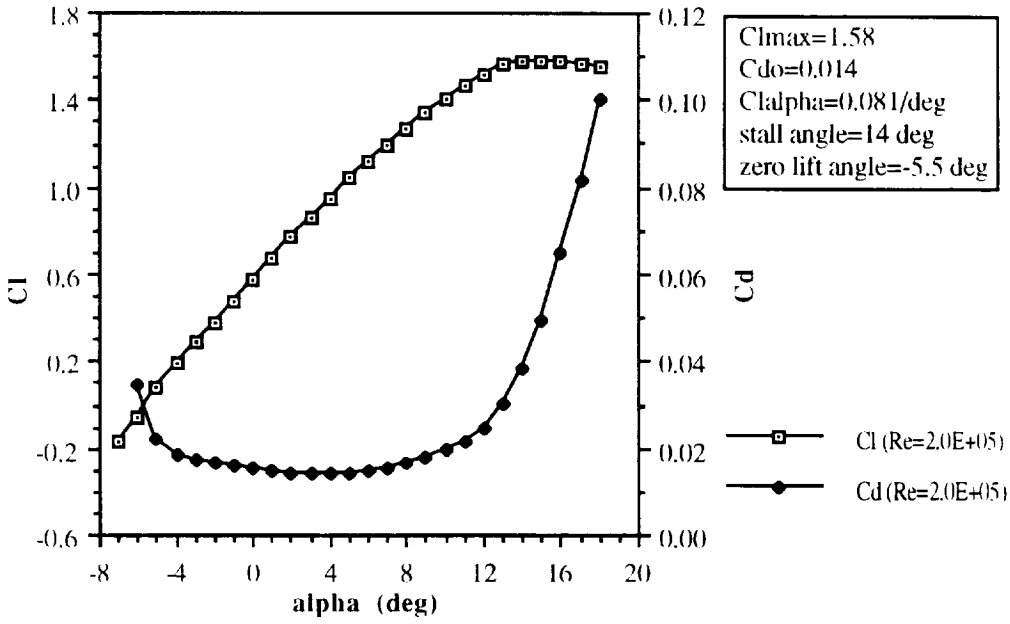

4.2 Wing Design

The design of the wing was approached in order to maximize the lift potential of our high lift airfoil section while at the same time minimizing drag losses. The incorporation of several aerodynamic features including flaps, tapered wing tip sections, a polyhedral configuration and low wing placement have made the analysis of such an advanced wing rather complex. The Lin-Air software package was used extensively as a tool in determining aerodynamic performance parameters for our wing design. Although very

useful in determining the lift and lift-induced drag coefficients for our design model. Lin-Air is unable to compute viscous effects. In general, Lin-Air was used in several trade studies in order to determine design variables which would maximize our aerodynamic performance. The results of these trade studies that eventually led to our final design are outlined below. Yet, several design decisions for our wing were made without adequate aerodynamic analysis. The rationale behind these design choices are mentioned below as well, and it is strongly suggested that further aerodynamic analyses be performed in these areas as development of *The Bunny* progresses.

4.2.1 Wing Sizing, Aspect Ratio & Taper

A driving consideration in the selection of wing area was to meet our take-off requirement of 20 ft, thus serving all cities in the Aeroworld passenger transport market. Wing area can be related directly to take-off distance through the approximation:

$$D_{TO}=\frac{1.44W^2}{\rho S C_{Lmax}(T-(D+\mu(W-L)))0.7L}$$

By fixing values of W, T, μ, and D at preliminary estimates (6 lbs, 3 lbs, 0.15 kg/m·s, and 2 lbs, respectively) the relationship between C_{Lmax}, take-off distance, and the necessary planform area could be determined. Figure 4.5 illustrates this relationship for a variety of wing planform areas. Clearly a larger planform area results in reduced take-off distance. Yet, Figure 4.5 also illustrates the need for high lift devices. In order to achieve a take-off distance of under 20 ft with a planform area of 10 ft^2, a C_{Lmax} of 1.35 is required. This high C_L requirement is beyond the capabilities of our airfoil section at reasonable angles of incidence, and thus flaps must be developed in order to achieve this goal.

Fig. 4.5: CL vs. Take-Off Distance (various wing areas)

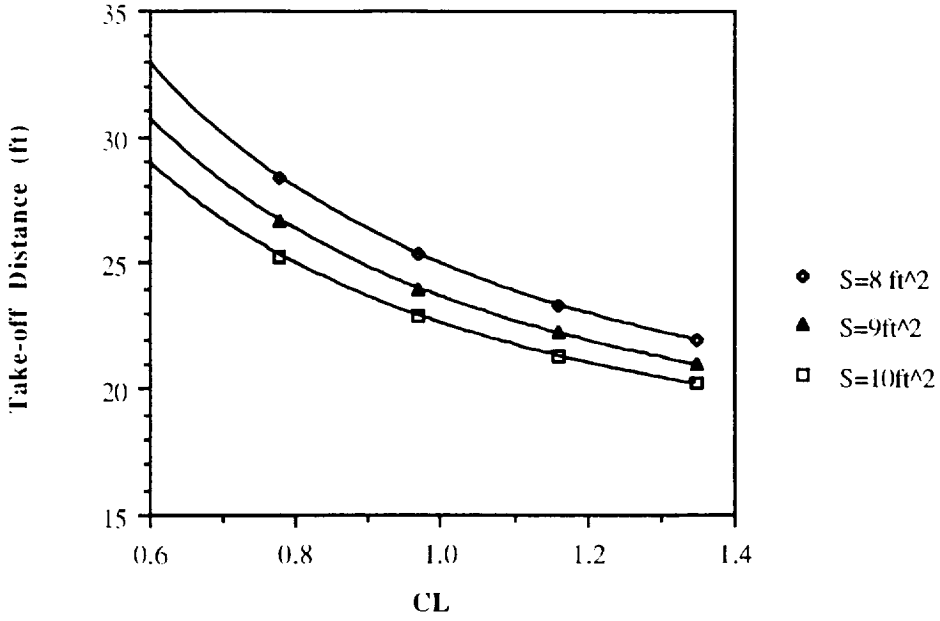

In order to reduce the overall drag of the aircraft, trade studies relating aspect and taper ratios to induced drag were conducted. Lin-Air was used to determine the induced drag coefficient for a wing model of constant planform area while varying the aspect and taper ratios. Figures 4.6 and 4.7 illustrate the effect of these design parameters on C_{Di}. Figure 4.6 illustrates that for λ=0.7, induced drag effects can be decreased by approximately 2% versus that of a rectangular planform. Even more significant to the reduction of induced drag is the influence of aspect ratio, as illustrated in Figure 4.7. Here it can be seen that for a constant wing planform, C_{Di} can be significantly reduced through the implementation of a large aspect ratio wing. Database analysis revealed a range of RPV aspect ratios from 7 to 11. Yet in order to achieve an acceptable wing geometry, reasonable wing span, and adequate wing cross-section thickness for the implementation of flap surfaces (b=9.22 ft, c_r=14.04 in, c_t=9.83 in, S=10.0 ft^2), our design aspect ratio was chosen to be 8.5. See Figure 4.8 for an illustration of *The Bunny* wing design.

Figure 4.6:

Relationship Between Induced Drag and Taper

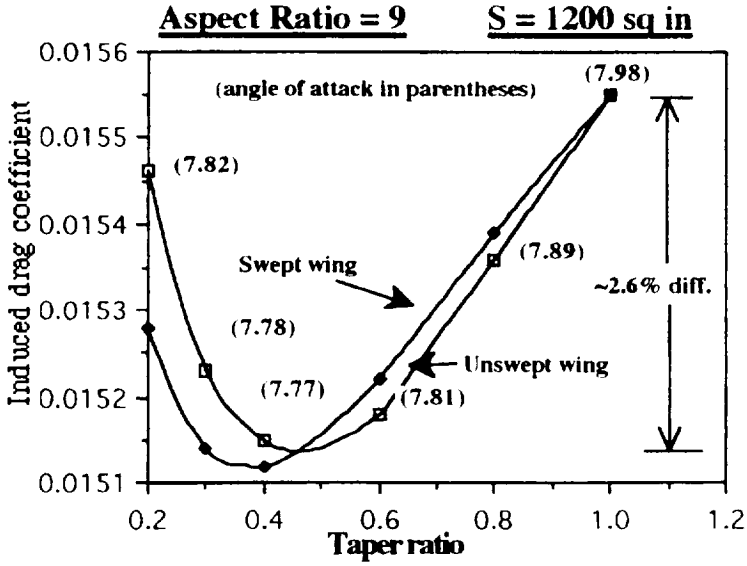

Figure 4.7:

Induced Drag Dependency on Aspect Ratio

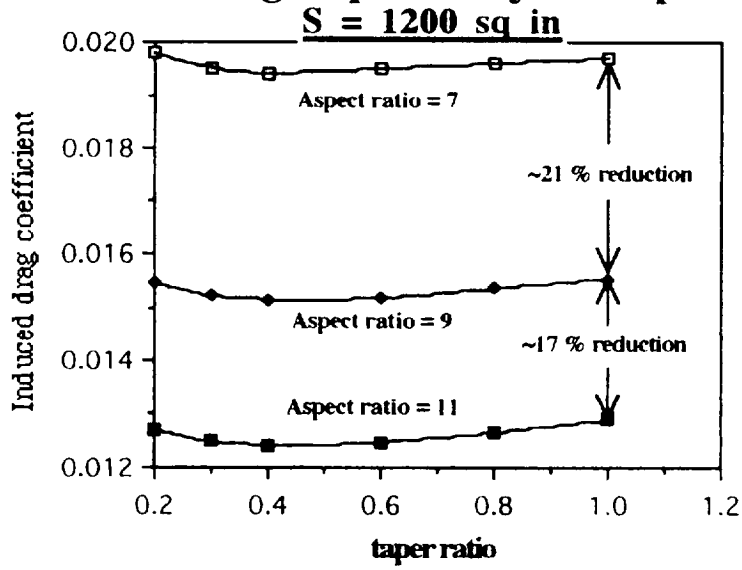

4.2.2 Polyhedral & Low-Wing Placement

A polyhedral wing configuration was incorporated in order to provide necessary roll and lateral stability for the aircraft in lieu of ailerons. Utilizing 4-channels of radio

operation for flaps, elevator, rudder and throttle, ailerons were neglected in order to provide the pilot ease of operation. A combination of rudder deflection along with a polyhedral angle of approximately 6° shall allow for adequate roll control and lateral stability. See Section 7.3 for further discussion of the stability and control performance of the polyhedral wing.

The placement of the wing along the length of the fuselage was governed primarily by weight balance and stability and control considerations (see Sections 7 & 8), yet the placement of the wing with respect to the height of the fuselage was governed by drag considerations. Due to the trapezoidal fuselage cross-section, the angle between the wing and the fuselage varies between the high-wing and low-wing locations. In the high-wing configuration the angle is acute, thus producing a significantly large wing-fuselage interference drag. In the low-wing configuration however, this angle is obtuse, thus reducing the interference drag at the wing-fuselage connection.

Fig. 4.8:
The Bunny Wing Design

Top View

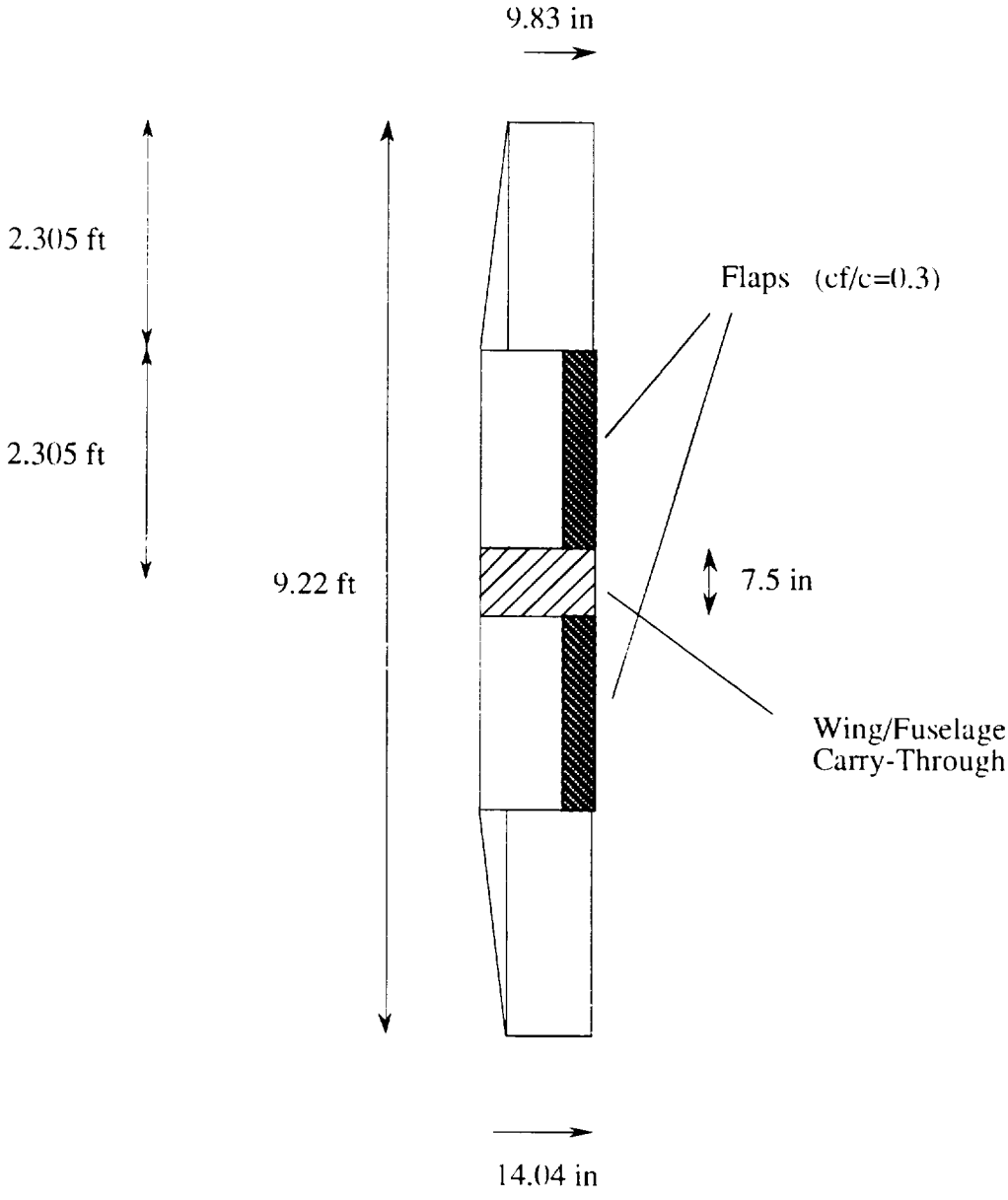

Front View

4.2.3 Flaps

Flaps are valued for their ability to increase the lift characteristics of the wing, yet at the same time can greatly increase the drag of the entire aircraft. The variance in the lift and drag characteristics of the wing due to flaps can be achieved through several design parameters including the type of flap surface, flap deflection angle (δ_f), and the flap to wing chord ratio (c_f/c). Lin-Air was again used to model the wing and flap surfaces, where the lift and induced drag characteristics of the wing could be analyzed. Due to the significant camber of the FX 63-137 airfoil, the wing model used in Lin-Air consisted of 4 elements to approximate the mean camber line of the airfoil section. In this way, deflection of a plain flap could be easily incorporated into the aerodynamic study of the wing simply by deflecting the trailing edge element relative to the three other elements.

Figure 4.9 illustrates the increased lift performance with increasing flap deflection angle. It is important to note that Lin-Air solves for the lift distribution along the span of the wing through the linear superposition of discrete line vortices, and thus does not account for viscous effects. Hence, stall and the loss in lift associated with stall is not accounted for in a Lin-Air analysis. Local stall occuring at the flap section and the associated losses in flap effectiveness would need to be analyzed in the further stages of development, especially in the regions of large flap deflections ($\delta_f > 20^o$). For our design case of maximum flap deflection ($\delta_f = 20^o$), Lin-Air provides a much more accurate estimation of the wing lift characteristics. Note: for the following graphs illustrating the effects of flap deflection, δ_f is symbolized by df.

Fig. 4.9: CLwing vs. Alpha (with flap deflection)

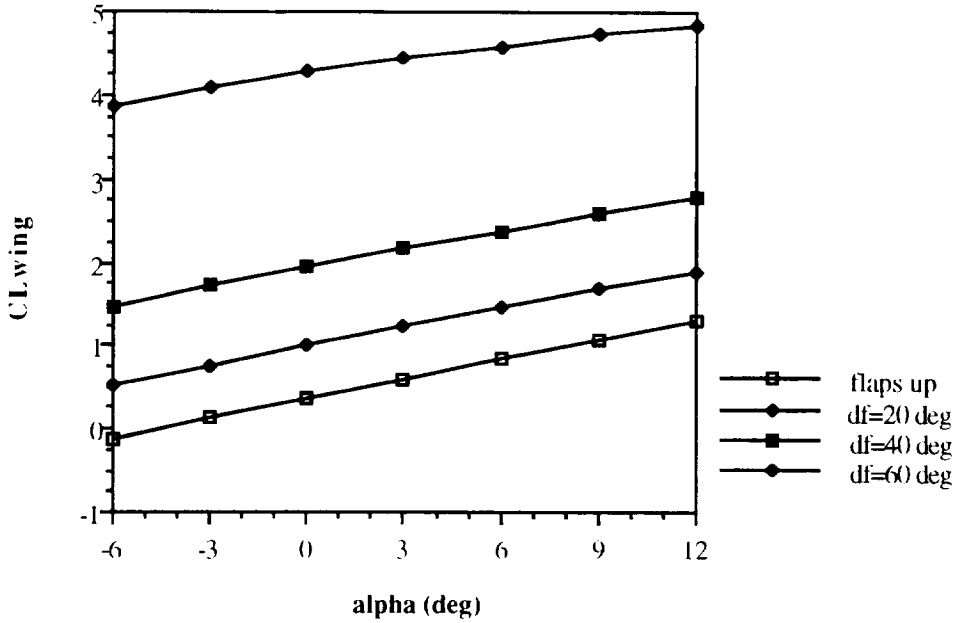

According to Figure 4.9 ΔC_L can be seen to vary from approxiamtely 0.7 to 3.7 depending on the angle of flap deflection. It can be clearly seen that a larger flap deflection angle results in maximizing C_{Lmax} (4.0-5.0 for $\delta_f=60^o$). However, Figs 4.10-4.11 illustrate that increases in flap deflection angle also significantly effect the wing drag performance and thus may not be practical for the design of *The Bunny*. Figure 4.10 shows that C_D may increase by as much as 1200% through a flap deflection of 60^o. These increses in drag performance would simply require too much added propulsion weight, power, and fuel to be considered for a lightweight, low-Reynolds number aircraft design. Rather, for a smaller flap deflection of 20^o, the drag characteristics only increase slightly (on the order of 50%). Figure 4.11 illustrates the influence of the increased drag due to flap deflection on the wing L/D. Although the wing obtains its greatest C_L performance at high flap deflection angles, L/D performance is inversely related to flap deflection. A wing L/D_{max} of approximately 14.0 is obtained with no flap deflection ($\alpha=6^o$), yet for $\delta_f=20^o$ the wing L/D_{max} only decreases by about 11% to 12.5 ($\alpha=0^o$). For deflection angles greater than 20^o, L/D_{max} decreases significantly and thus should not be considered.

Figure 4.12 illustrates the relationship between flap sizing and lift performance. Clearly a larger flap surface shall result in a greater wing C_{Lmax} for each flap deflection. Figure 4.13 illustrates the reduction in wing L/D_{max} for larger flap sizes. For a flap size of $c_f/c=0.3$ and $\delta_f=20^o$, C_{Lmax} increases by nearly 50% over the flaps up configuration (1.90 vs. 1.30), while only suffering a 11% reduction in L/D_{max} (14.0 vs. 12.5). For this reason, the wing design shall incorporate flaps of $c_f/c=0.3$ with a maximum deflection

angle of 20°, primarily to provide the needed lift during take-off. Figure 4.14 illustrates the wing lift curve and aerodynamic performance characteristics for both a flaps up and flaps deflected configuration.

Fig. 4.10: CDwing vs. Alpha (with flap deflection)

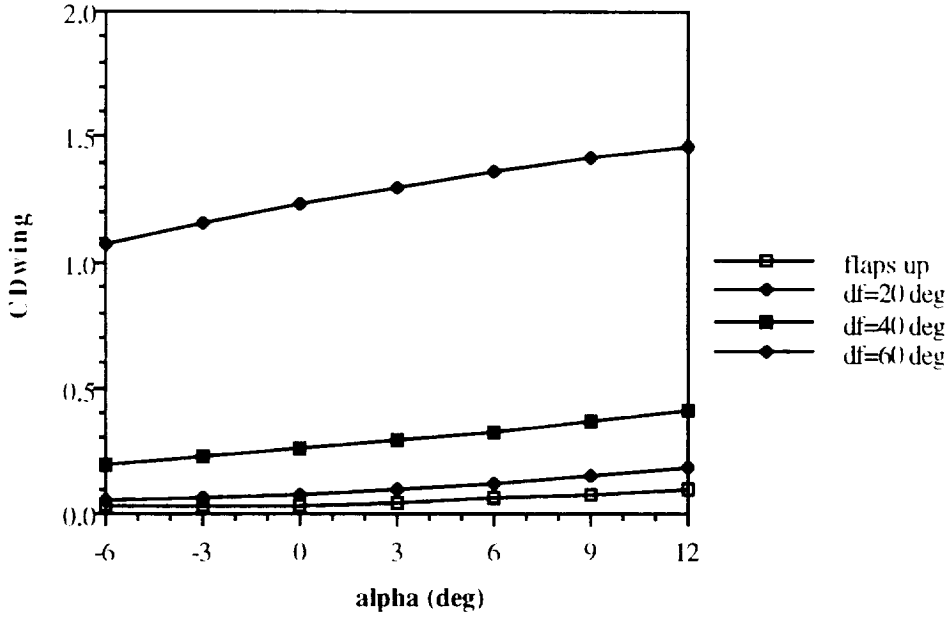

Fig. 4.11: Wing L/D vs. Alpha (with flap deflection)

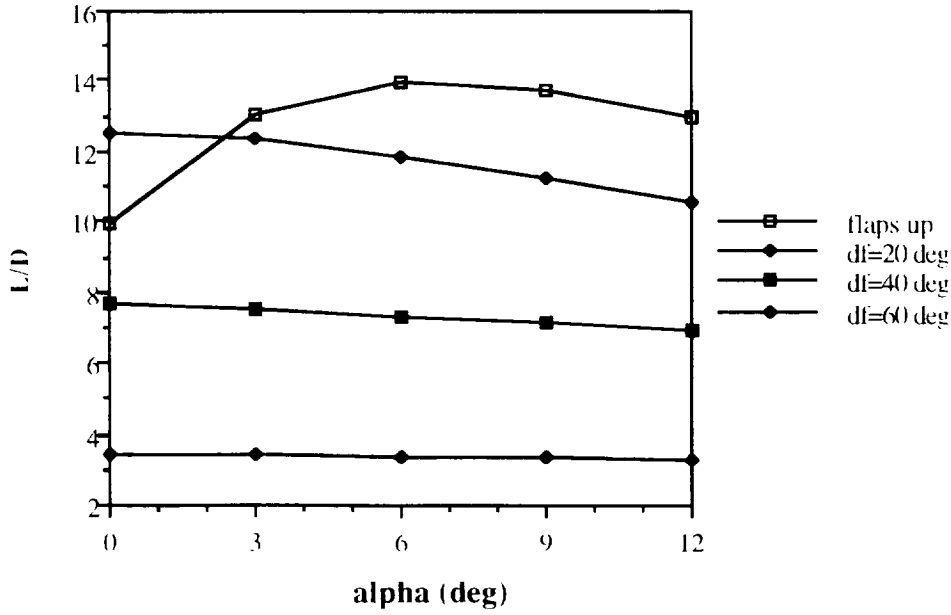

Fig. 4.12: CLmax vs. Flap Deflection Angle (various cf/c)

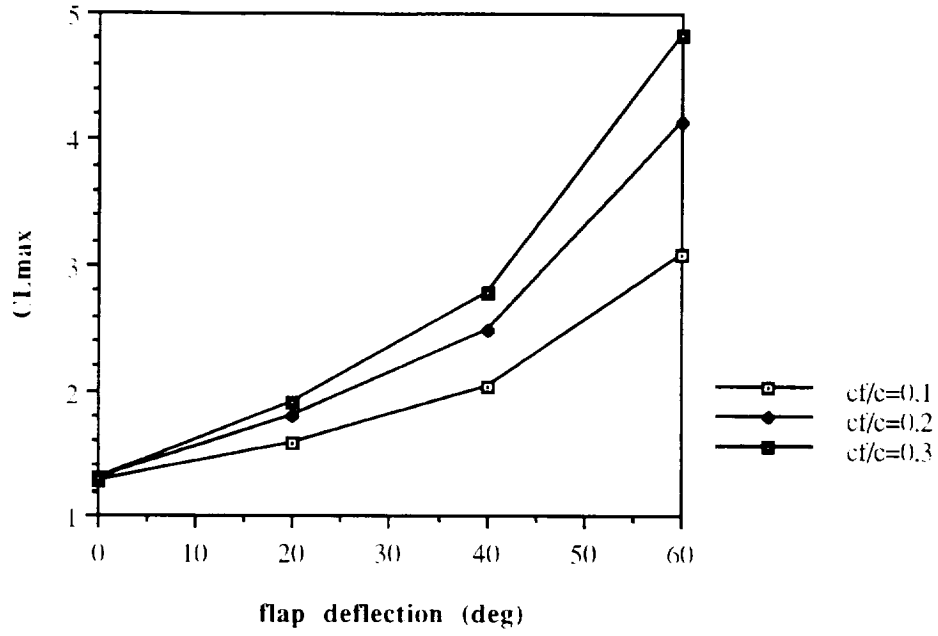

Fig. 4.13: Max L/D vs. Flap Deflection Angle (various cf/c)

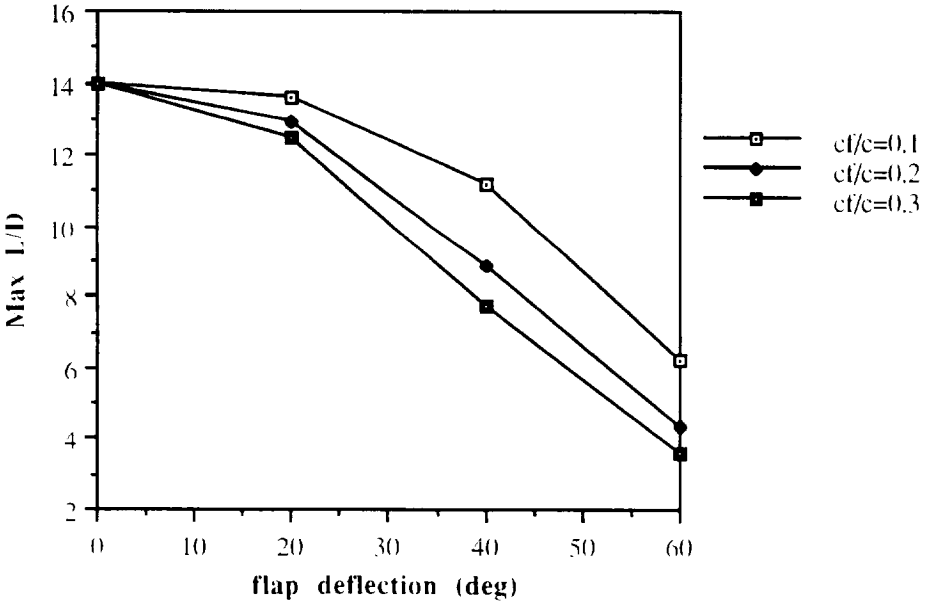

Fig. 4.14: CLwing vs. Alpha (w/flap deflection)

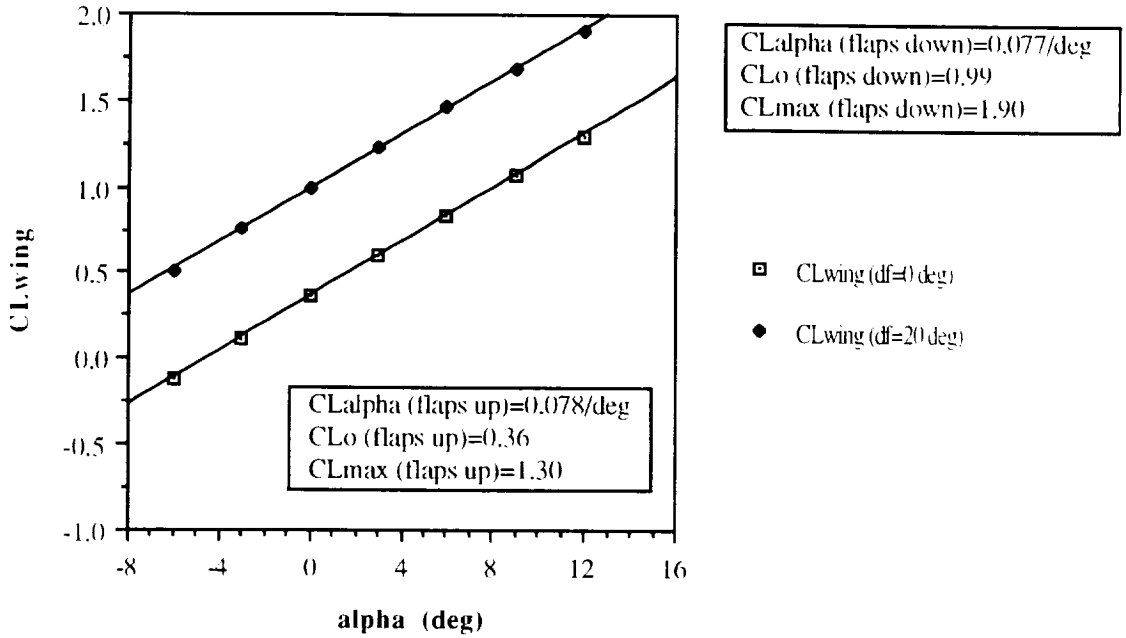

4.2.4 Wing Design Specifications & Aircraft Lift Curve

Table 4.2 below lists the design parameters for the finalized *Bunny*wing and horizontal tail configuration. Factors governing the design criteria of the horizontal tail and the wing incident angle are summarized in Section 7 under Stability and Control.

Table 4.2: Bunny Wing and Horizontal Tail Configurations

	wing	horizontal tail
Airfoil Section	FX 63-137	Flat Plate
Aspect Ratio	8.5	2.5
Planform Area	10.0 ft^2	2.98 ft^2
Span	9.22 ft	2.73 ft
Chord	1.17 ft	1.09 ft
Incident Angle	2.5^o	0.0^o
Flap/Elevator Chord Ratio	0.3	0.2
Max Flap/Elevator Deflection	20^o	18^o

Using the above design parameters for the wing and horizontal tail along with the C_{Lw} performance data obtained from Lin-Air (see Figure 4.14), the aircraft lift curve was constructed using the methods illustrated in [3], Sections 8.1.5-8.1.6. The methods outlined in [3] facilitate conversion of wing lift curve data to a corresponding aircraft lift curve for both the flaps up and flaps deflected configurations (see Figure 4.15). Tables 4.3-4.4 summarize the necessary parameters and important results of the conversion.

Table 4.3: Wing to Aircraft Conversion Parameters		
S_H/S=0.289	i_w=2.5°	$d\varepsilon/d\alpha$=0.335
i_t=0.0°	$\alpha_{L=0w}$=-5.5°	$\alpha_{L=0}$=-7.0°
P_{av}=0.038 hp	$C_{L\alpha w}$=0.078/deg	ΔCLw=0.63
D_p=0.917 ft	d_f=6.33 in	k_{cw}=1.0
ρ=0.00238 slugs/ft^3	K_{wf}=1.0006	k_{wh}=0.8
V=30 ft/s	AR_H=2.5	$C_{L\alpha w})_\delta$=0.077/deg
ε_h=0.0°	$C_{L\alpha t}$=0.050/deg	η=3.62

Table 4.4: Wing to Aircraft Conversion Results		
CLowf=0.624	α_{stallw}=12°	$C_{Lo})_\delta$=1.11
$C_{L\alpha wf}$=0.0781/deg	$\alpha_{stallA/C}$=9.5°	$C_{L\alpha})_\delta$=0.0863/deg
$C_{LoA/C}$=0.624	C_{Lmax}=1.45	ΔC_{Lmax}=0.450
$C_{L\alpha A/C}$=0.0873/deg	$\Delta C_L)_\delta$=0.486	$\alpha_{stall})_\delta$=9.2°

Fig. 4.15: Aircraft CL vs. Alpha (w/flap deflection)

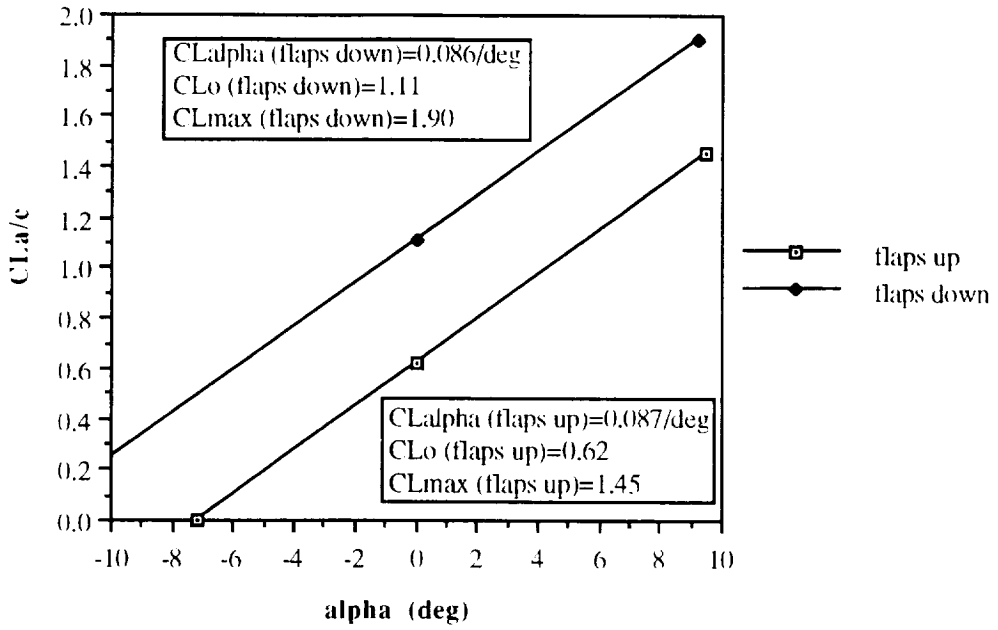

4.3 Drag Prediction

The drag prediction for *The Bunny* was performed through the use of two widely used methods for low Reynolds number aircraft. The first drag estimation utilized a Method I approach as outlined in Daniel T. Jensen's *Drag Prediction Methodology for Low Reynolds Number Flight Vehicles* [4]. A second approach utilized the drag breakdown method as presented by Dr. Robert C. Nelson in his AE 348 Flight Mechanics lecture notes [5]. Due to the similarity between Jensen's Method II approach and Nelson's method, these methods were actually performed in conjunction with each other, combining Nelson's drag breakdown for all aircraft components besides the main wing, and Jensen's formulation for the parasite drag contibution of the wing.

According to Jensen's Method I, the aircraft drag coefficient can be expressed as a summation of parasite drag (pressure and skin friction drag) and lift-induced drag contributions. This drag model can be expressed as:

$$C_D = C_{D_0} + \frac{C_L^2}{\pi e AR}$$

where the Oswald efficiency factor, e, accounts for the 3-D effects of a finite wing as well as the fact that pressure and skin friction drag are not independent of lift or angle of attack

as the model suggests. According to Method I, the parasite drag coefficient, C_{D_0}, can be estimated through the expression:

$$C_{D_0}=\frac{C_f S_{wet}}{S_{ref}}$$

where S_{wet} is the aircraft wetted surface area, and S_{ref} is the planform area of the main wing (1440 in^2). C_f, the equivalent skin friction coefficient, is suggested by Jensen to equal 0.0055 for the class of low Reynolds number RPV's. Jensen's Method I approach assumes drag to be a function only of the aircraft surface area and thus neglects an analysis of landing gear and added drag contribution due to flap deflection. To account for these shortcomings, data from [3] was substituted whenever applicable. Table 4.5 lists the component wetted areas, drag contributions, and composite parasite drag coefficient computed using Jensen's Method I.

Table 4.5: Jensen's Method I Drag Estimation

component	S_{wet} (in^2)	C_{D_0} Contribution	% Total C_{D_0}
wing	2880.0	0.0110	40.1
fuselage	1288.0	0.0049	17.9
horizontal tail	858.0	0.0032	11.7
vertical tail	340.0	0.0012	4.4
landing gear	--	0.0071	25.9
TOTAL		**0.0274**	

According to Nelson's drag breakdown method, the parasite drag coefficient, C_{D_0}, can be estimated by performing the summation:

$$C_{D_0}=\frac{\sum C_{D\pi} A_\pi}{S_{ref}}$$

where $C_{D\pi}$ represents the parasite drag coefficient of an individual component of the aircraft and A_π symbolizes the area which $C_{D\pi}$ is based upon. The reference area, S_{ref}, was again taken to be the wing planform area. With values for $C_{D\pi}$ provided in Nelson's method, the component contributions to C_{D_0} for the entire aircraft were calculted and are illustrated in Table 4.6. Jensen's Method II approach suggests that the wing contribution to the aircraft parasite drag coefficient be based on the C_{dmin} for the airfoil section, and not

an arbitrary $C_{D\pi}$. Thus, substituting C_{dmin}=0.0143 for the wing contribution to C_{Do}, Table 4.7 summarizes a more detailed drag breakdown. In each of these cases a percentage of the composite drag was added to account for interferences and roughness/protuberances. According to [5] these percentages were taken as 5% and 10%, respectively. An overall parasite drag coefficient of C_{Do}=0.031 was obtained from the combined average of all three drag prediction methods.

Table 4.6: Nelson's Component Drag Breakdown Estimation

component	$C_{D\pi}$	A_π (in^2)	C_{Do} Contribution	% C_{Do}
wing	0.007	1440.0	0.0070	24.5
fuselage	0.110	31.5	0.0024	8.4
horizontal tail	0.008	429.0	0.0024	8.4
vertical tail	0.008	170.0	0.0009	3.1
landing gear	0.014	1440.0	0.0140	49.0
interferences			0.0006	2.1
roughness/protuberances			0.0013	4.5
TOTAL			**0.0286**	

Table 4.7: Combined Nelson/Jensen Method II Drag Breakdown Estimation

component	$C_{D\pi}$	A_π (in^2)	C_{Do} Contribution	% C_{Do}
wing	0.007	1440.0	0.0143	38.6
fuselage	0.110	31.5	0.0024	6.5
horizontal tail	0.008	429.0	0.0024	6.5
vertical tail	0.008	170.0	0.0009	2.4
landing gear	0.014	1440.0	0.0140	37.8
interferences			0.0010	2.7
roughness/protuberances			0.0020	5.4
TOTAL			**0.0370**	

Calculation of the induced drag contribution to the aircraft drag coefficient reqires the determination of the Oswald efficiency factor, e. Nelson and Jensen both propose the following calculation in order to determine e:

$$\frac{1}{e} = \frac{1}{e_{fus}} + \frac{1}{e_{wing}} + \frac{1}{e_{other}}$$

where e_{fus} and e_{other} have been obtained from data presented in Nelson's method. For our particular design these values have been calculated to be 33.5 and 20.0, respectively. In order to determine e_{wing}, Lin-Air was used to solve for the induced drag effects for our wing design. Solving for C_{Lw} and C_{Di} over a range of angles of attack, Lin-Air was used to solve for e_{wing} through the expression:

$$e_{wing}=\frac{C_{Lw}^2}{C_{Di}\pi AR}$$

Although e_{wing} was found to vary slightly with angle of attack, an average value of e_{wing}=0.85 was obtained. Combining these component Oswald efficiency factors, an overall value of e=0.80 was obtained for *The Bunny*. Along with the value for C_{Do} computed above, the equation for the overall drag of the design can be expressed as:

$$C_D=0.031+0.047C_L^2$$

which is graphically represented as the aircraft drag polar in Figure 4.16. Combining the lift curve for the aircraft given in Figure 4.15 with the above aircraft drag polar allows the L/D characteristics of the aircraft to be determined versus angle of attack. Figure 4.17 illustrates that for a flaps up configuration our L/D_{max} is approximately equal to 13.1, while our L/D_{cruise} is approximately equal to 12.7.

Fig. 4.16: Aircraft Drag Polar

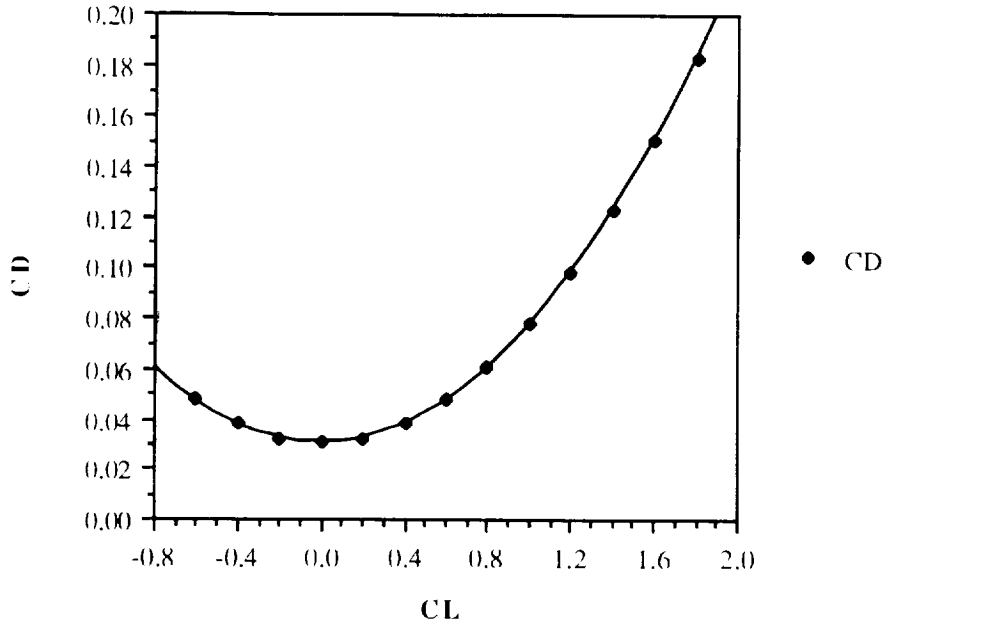

Fig. 4.17: Aircraft L/D vs. Alpha

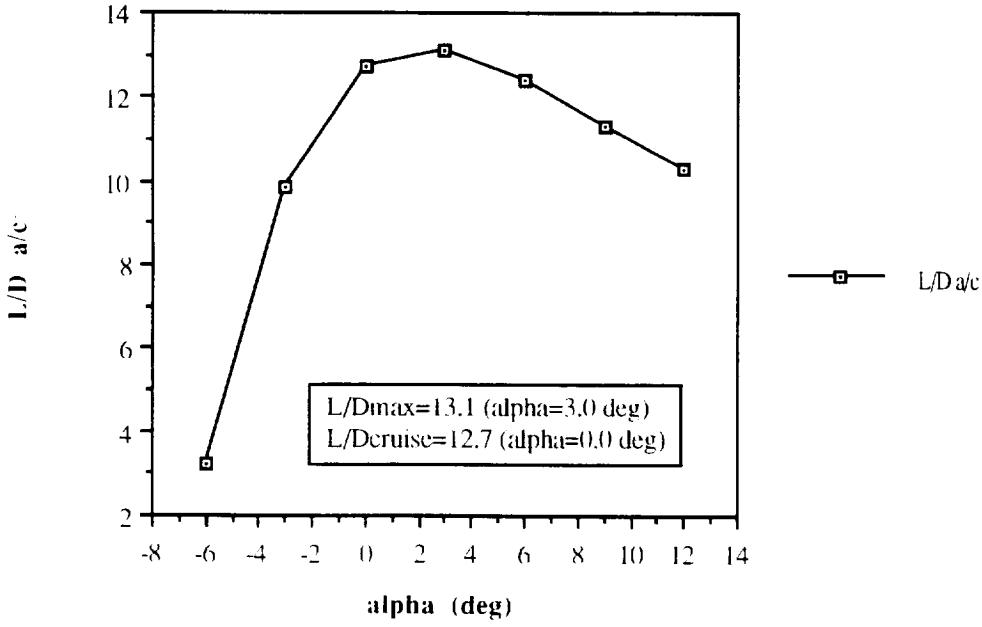

5.0 PROPULSION SYSTEM

5.1 Requirements and Objectives

Design Requirements:

1. Environmentally safe.
2. Take off and land under own power.
3. Maximum take-off distance of 40 feet.
4. Loiter for 2 minutes.
5. Maximum altitude of 25 feet.
6. Installation performed in under 20 minutes.

Design Objectives:

1. Maximum take-off distance of 20 feet.
2. $V_{take\text{-}off}$ greater than 1.3 V_{stall} for safety.
3. Reduce fuselage blockage effects.
4. Flexible battery placement for CG control.
5. Variable throttle control.

5.2 System Selection

The mission requirements dictate that the propulsion system for the technology demonstrator be environmentally safe. This effectively limits the selection to a small number of propulsion options. The two considered by *Sunshine Aeronautics* are electrical power and stored mechanical energy such as rubber band propulsion. Given the relatively short period of time allotted to prepare this proposal, ease of analysis necessarily played a major role in the propulsion systems studied. Electric propulsion was chosen because of the large data base accumulated from past years' projects and the extensive experience of the program advisors with the common electric propulsion systems.

One motor, mounted in the front of the fuselage, is being employed to meet the power needs of the aircraft. This is a reasonable decision since several of the motor choices suggested provide the necessary power for takeoff and cruise with maximum payload. The structural difficulty in mounting two motors, either on the sides of the fuselage or by suspending them from the wings, also discouraged the idea of a plane with more than one motor. Questions have been raised about the difficulty of synchronizing more than one motor at identical RPM settings in order to produce even, parallel thrust vectors to keep the aircraft in straight and level flight. The necessity of minimizing weight in order to minimize take-off distance also recommends a single-motor design.

Three two-blade propellers were considered in conjunction with the available motors, and were chosen based on availability and projected thrust requirements. Only two-blade propellers were considered because of weight considerations and the availability of an extensive data base.

The battery selection was based on the necessary voltage, discharge rates, range and endurance objectives, as well as cost considerations.

The following design values were used in all performance calculations:

Table 5.1: Key Design Variables

weight	5.3 lbf
wing area	10 ft^2
efficiency	0.60
Cl_{max}	1.8
$Cl_{take\text{-}off}$	1.07
Cd	1.1

5.3 Motor Selection

The driving factor in the motor and propeller choice was the desire to meet the take-off distance objective of 20 ft. This will enable *Sunshine Aeronautics* to serve all of the cities in the AEROWORLD market. For this reason a motor which produces a large amount of thrust was chosen in order to accelerate the plane to the take-off velocity quickly. The primary analytical tool used to determine take-off performance for a particular motor/propeller combination was the program provided by Dr. Batill [Reference 6] which estimates take-off characteristics based on input of propeller thrust and power coefficients, and motor characteristics. The motor manufacturers provided lists of RPM, current, voltage and torque. The motor parameters t_{loss}, k_v, and k_t were obtained from graphs of these quantities. Using the plot of effective voltage versus motor RPM, the value of k_v can be estimated. As can be seen in Figure 5.1, the plot of RPM vs. current for the Astro-15, the value of k_v is about 8.1×10^{-6} V/rpm. The parameter k_t is the slope of the torque vs. current curve for a given motor, while t_{loss} is the intercept of the same curve. For the Astro-15, the graph of torque versus current is shown in Figure 5.2, along with the corresponding values of k_t and t_{loss}.

Figure 5.1

Variation in Torque with Current for Astro-15 Motor

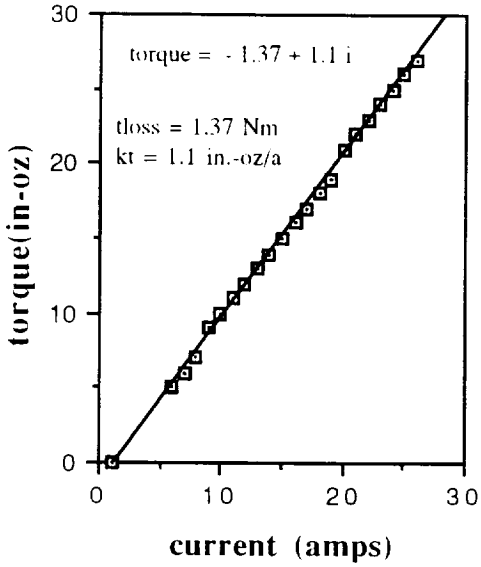

Figure 5.2

Effective Voltage vs. Motor Speed

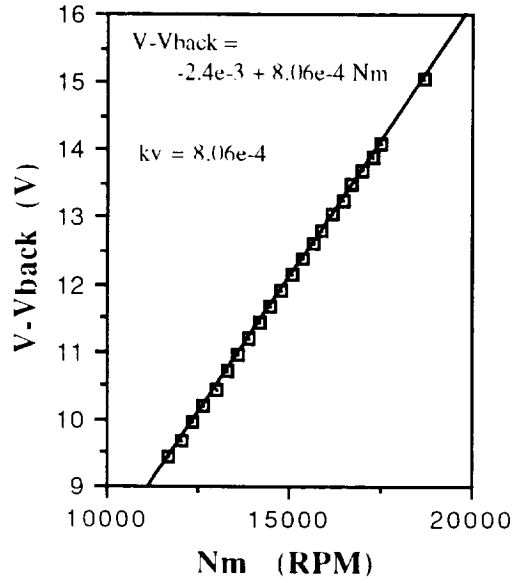

A wide range of motors were considered including the Astro 05, 05 FAI, 15, 25, and 40. The large weight of the Astro 40 series motor system (45 oz.) indicated that using this motor would entail sacrificing the take-off distance goal based on the sensitivity of take-off performance to weight. A comprehensive study was done of the remaining motors. First a take-off analysis was done, which indicated that the Astro 05 and 05 FAI would have to be operated at an excessive RPM in order to take-off, with a current draw larger than the fuse setting of 20 amps. Both the Astro 15 and Astro 25 motors produced sufficient thrust to ensure a take-off distance of 20 feet. The Astro 25 drew less current than the 15, but the 4.0 oz. weight increase made it a less attractive choice. The flaps which *The Bunny* will employ at take-off provide a high lift coefficient so that the Astro-15 can provide the power necessary to meet our take-off objective. For these reasons *Sunshine Aeronautics* has chosen the Astro Cobalt 15 as the motor for the technology demonstrator.

Analysis of the cruise and take-off performance of *The Bunny* indicates that there is a strong dependency on gear ratio. For instance, it was found that lower gear ratios yielded shorter take-off distances. Manufacturer's information lists three possible gear ratios for the Astro-15: 1.84, 2.21 and 2.38. Although the 1.84 would be preferred, the motor we have been provided with has a gear ratio of 2.21. For optimum take-off performance it is recommended that in the future *The Bunny* be outfitted with the Astro-15 with a gear ratio of 1.84.

The following are the motor characteristics for the Astro-15 motor which will be installed in *The Bunny* based on a fuse-amperage of 20 amps and a maximum voltage of 15.6 V.

Table 5.2: Motor Characteristics

type	electric powered
name	Astro Cobalt 15
max power	185 watts
internal resistance	0.12 Ω
gear ratio	31:14
weight	7.5 oz.

5.4 Propeller Selection

The propeller coefficients were obtained using the propeller code developed by B.N. Young on the Apple IIe [Reference 7]. The propeller geometry of the Zinger propellers was provided from measurements conducted by Ms. Elena Quirk, and the characteristics of the Top-Flight 13x7 propeller were taken from Reference 8. Corrections for induced velocity and tip losses were included, although no correction for low Reynold's number was employed. This omission could produce erroneous results, and before production begins further testing should be conducted to determine accurate propeller performance.

Three propellers were considered for *The Bunny* based on preliminary take-off performance calculations conducted using their thrust and power coefficients. These were the Zinger 12x4 and 12x6 propellers, and the Top Flight 13x7 propeller. As can be seen in Figure 5.3, over the range of advance ratios at which *The Bunny* operates, the Zinger 12x6 has the best efficiency. At our cruise advance ratio of 0.385, $\eta_{prop} = 0.68$ for the Zinger 12x6 propeller, by far the best efficiency of the propellers studied.

Figure 5.3

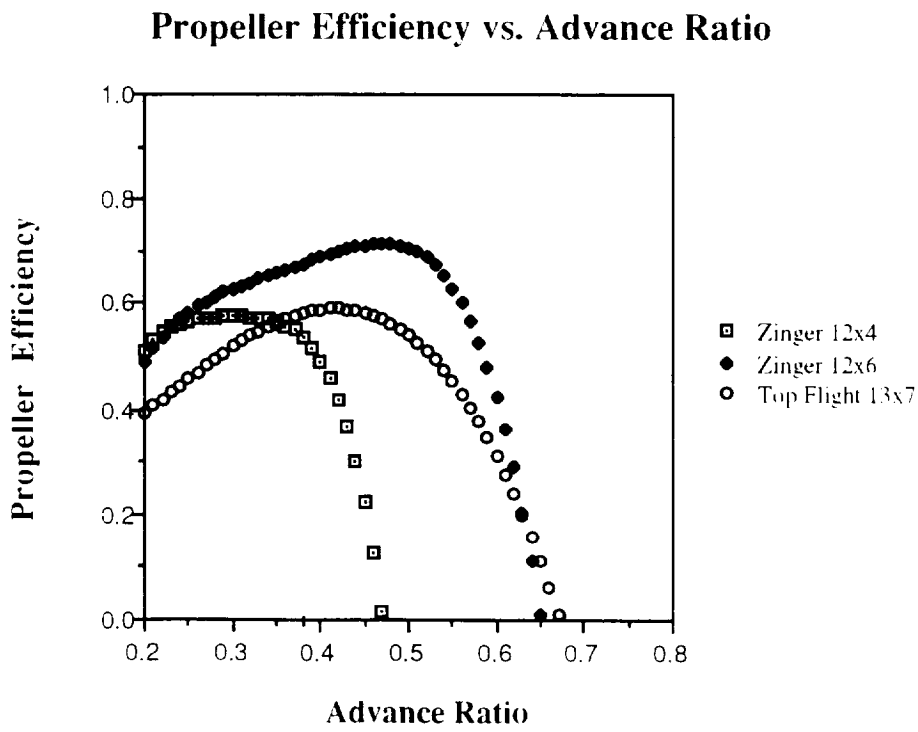

One of the benefits of the Zinger 12x6 propeller is a large diameter, which will produce large amounts of thrust at the tips, indicating that the interference of the fuselage will be small. This is a concern given the large (6.5 ") width of *The Bunny's* fuselage. A smaller propeller would have to turn at a higher RPM setting in order to produce the same thrust level, while a larger propeller would need more torque to be turned. The Zinger 12x6 propeller is capable of producing approximately 3 lbf. of thrust at takeoff, and of cruising with a small current draw and a high propeller efficiency at V_{cruise} = 30 ft/s.

The propeller selection was limited by the relatively small number of propellers available for analysis at the design facility. Furthermore, propeller geometry could not be determined accurately using the measuring equipment available. In the future the compilation of a data base including manufacturer's propeller specifications would be very useful in the design process.

5.5 Battery Pack Selection

The conventional battery pack chosen for the Astro 15 is 12 1.2 volt batteries in series, yielding a net voltage of 14.4 volts. Unfortunately, the take-off distance was estimated to be 21 feet using only 12 batteries. However, the Astro 15 motor is rated at a peak voltage of 16.3 V, which suggests that the addition of a thirteenth battery, bringing the total voltage to 15.6 volts, would be acceptable. This additional voltage significantly improves the take-off performance of the aircraft, with only a small penalty in weight and cost.

Thirteen Panasonic P-100SCR batteries were chosen to provide the fuel for *The Bunny*. These are high rate discharge and rapid charge batteries which will enable *The Bunny* to accelerate quickly for take-off and to be recharged quickly for the next flight. The battery pack holds a total charge of 1000 mahrs which leaves over 200 mahrs of charge for ground maneuvering and emergency operation given the cruise characteristics of *The Bunny*. Approximately 850 mahr batteries would be ideal to enable *The Bunny* to meet its range objective at the lowest fuel cost, but only a finite number of battery options were available. The 1000 mahr batteries chosen are the smallest available which fulfill the range objective. There are numerous more expensive, heavier battery packs which have higher capacity and lower impedance which could provide improved range, but cost and weight considerations dictate that the least expensive system which meets the design requirements and objectives be chosen. The following table indicates the characteristics of the battery pack chosen for *The Bunny*.

Table 5.3: Battery Characteristics		
	1 battery	13 cell pack
type	Panasonic P-100SCR	
voltage	1.2 V	15.6 V
capacity	1000 mahrs	1000 mahrs.
internal impedance	7 mΩ	91 mΩ
weight	1.23 oz.	16 oz.
cost	$3.00	$39.00

5.6 Propulsion Performance Predictions

Making accurate predictions of the performance of the chosen propulsion system proves difficult because of the uncertainty of several parameters. An accurate weight total for *The Bunny* will not be determined until manufacturing is complete. This is true because of the inherent difficulties in predicting accurately how much structure is necessary for structural integrity.

Several trade studies were conducted in order to estimate the take-off performance of *The Bunny*. A take-off analysis code provided by Dr. Batill was used for many of these calculations. This code does a detailed numerical integration based on motor characteristics and propeller performance coefficients from Mr. Young's program. The program assumes full throttle and uses an estimate of the thrust coefficient at V = 0.0. The main drawback of Dr. Batill's take-off performance code is that it does not include t_{loss}, the torque loss due primarily to friction. This could lead to an overestimation of the power available. T_{loss} should be included in subsequent power analysis to insure valid results. Based on the current design variables, the following are the take-off results according to the take-off performance code provided by Dr. Batill.

Table 5.4: Predicted Take-off Performance	
take-off distance	16.1 feet
take-off velocity	20.7 feet/sec.
time for run	1.65 sec.
current draw	13.4 amps
battery drain	5.3 mahrs.

A FORTRAN code which calculates the cruise characteristics for an RPV was developed in AE-454 (Propulsion) in order to analyze RPV propulsion. This code uses a iteration scheme to find the voltage and current at which the power available equals the power required. At this point there is no excess power, therefore the rate-of-climb is equal to zero (cruise). The input to this program included the motor and propeller characteristics indicated above. The endurance at cruise was calculated using the net battery capacity and the cruise current draw. The net battery capacity is the capacity remaining for cruise after subtracting the capacity used during take-off, climb to altitude and landing. The maximum range and endurance were calculated by using the power code at a wide range of cruise velocities.

$$\text{Endurance} = \frac{\text{Net Battery Capacity}}{\text{Cruise Current Draw}} \qquad \text{Range} = \text{Cruise Velocity} \times \text{Endurance}$$

Table 5.5: Predicted Cruise Performance

cruise velocity	30 feet/sec.
range	14,344 feet
endurance	478 sec. = 7 min. 58 sec.
current draw	6.5 amps
voltage	9.5 volts
power required = available	28 watts = 0.0375 Hp.
motor RPM	10303
propeller RPM	4653
η_{prop}	0.68
advance ratio (J)	0.39

5.7 Motor Control

During take-off the maximum power output of the motor is desired for the minimum take-off distance. Conversely, a comparatively small power output is necessary during cruise. The

necessity of different velocity and power settings means that a speed controller must be used in conjunction with the radio-control system. This throttle control will be on the Futaba radio control. For take-off the pilot will hold the throttle all of the way open until the plane lifts off of the ground and achieves a safe altitude. The pilot will then try to trim the aircraft with the elevator while reducing the power to that necessary for cruise at 30 ft/s. This corresponds to a throttle setting of approximately 0.6 based on the maximum velocity of 50 ft/s.

These propulsion characteristics were calculated using the latest design values for *The Bunny*. It is imperative that the calculations be reevaluated if estimates of weight, drag or other design variables change during subsequent design iterations.

6.0. WEIGHT ANALYSIS

6.1 Preliminary Estimation

An estimation of the weight of *The Bunny* was very important in the initial stages of the design as it is of considerable concern with regard to aerodynamics and propulsion. However, basing an estimation merely on a concept is a very difficult task. Therefore, based on the size of the aircraft and the goal range for which *The Bunny* was being designed, rough component weight estimations were made by referring to the compiled database of previous RPV designs of similar sizes and ranges listed in Appendix C. For example, an RPV with a similar range and payload would most likely require a similar size motor and number of batteries. Also, wing and fuselage weights were plotted against fuselage volume as a means of obtaining a range for their individual weights. It was decided that high weight estimates would be more beneficial in the early stages of the design since lower actual weights would improve the performance in most cases. Also, observing the weight percentages, it was noted that the areas for the greatest improvement (reduction) in weight were in the fuselage and wing structures (considering the propulsion system variation to be rather limited due to the design goal range). The initial estimates resulted in an overall prototype weight of 94.8 ounces (5.95 lbs) when fully loaded. (See Table 6.1).

6.2 Final Values and Estimates

As the design evolved, actual weights of certain components were obtained with a propulsion system selection and structural analysis and the overall prototype weight was refined. Commitment to the Astro 15 engine and 13 P-90SCR batteries to achieve the necessary takeoff voltage set those weights at 7.5 ounces and 18 ounces respectively, and the Zinger 12-6 propeller selected weighs .69 ounces. The use of flaps in our design required an extra servo adding 0.6 ounces. Finally, the structural analysis discussed in Section 9 provided more dependable values for wing (14.4 ounces), empenage (6.3 ounces), and fuselage weights (11.68 ounces), although these values are still estimates. As was expected, the updated value of the prototype weight was much (15%) lower than the original estimated value, at 80.49 ounces (5.03 lbs) fully loaded. (Note: An estimation of Monokote skin weight (4.3 ounces) was made post-analysis, resulting in an overall weight estimation of 84.8 ounces (5.3 lbs)). Although the possibility exists for an increase in this weight through manufacturing considerations (glue, screws, added structural supports, etc.), there is plenty of room for added weight as 6 lbs was consistently used throughout all preliminary performance and aerodynamic calculations. (See Table 6.1).

Table 6.1: Component Weight Estimates

Component	Prelim. Estimate (ounces)	Weight Fraction (%)	Final Estimate (ounces)	Weight Fraction (%)
Propulsion:				
engine	9.0	9.49	7.5	9.32
propeller	0.5	.53	.69	.86
avionics package:		27.43		29.82
speed controller	3.25		3.25	
servos	1.8		1.8	
receiver	.95		.95	
batteries	20.0		18.0	
Structure:				
wing	16.0	21.1	14.4	22.86
fuselage	24.0	25.32	11.68	14.51
empenage	4.0	4.22	6.3	7.83
landing gear	5.0	1.05	6.0	2.48
engine mount	1.5	1.58	1.12	1.39
Empty Totals	86.0		71.69	
Passenger load	8.8	9.28	8.8	10.93
Full Totals	94.8	100%	80.49	100%

6.3 Center of Gravity

The center of gravity of the airplane is a crucial design consideration for stability and control purposes. A major advantage of *The Bunny* is the fact that its internal layout allowed placement of the batteries and avionics equipment anywhere on the upper deck along the entire length of the passenger portion of the fuselage. It was determined that this package, consisting of 13 batteries, 3 servos, a receiver, and a speed controller, could be contained in 6 inches of fuselage length (2 inches deep, 5.5-6.5 inches wide) with room to spare for wire and control rod connections. Thus, the center of gravity (cg) could be moved to a desired location (determined by stability and control analysis) by properly positioning this package.

However, in the initial stages of the design the wing location was also variable. Therefore, using the initial component weight estimates and positions for a fully loaded airplane in the equation for the center of gravity, and leaving wing and package locations variable, the relationship

pckg loc. = 2.937 wing loc. - 65.462 (inches from the nose)

was found by setting the cg position at the quarter-chord of the wing (it should be noted that the wing location was defined as the wing half-chord location). From this relationship it was determined that the farthest forward the wing could be placed for the avionics package to be out of the nose section (10 inches from the nose) was 26 inches. Although points further back were also examined which moved the package back even further (PL=WL at 34 inches), this forward wing location was chosen for stability and control reasons.

Using this wing location and the resulting package location, the center of gravity for both a full and an empty airplane was found to be 23.3 and 21.23 inches from the nose, respectively. The weight balance diagram in Figure 6.1 shows the positioning of the component weights and the resulting cg location. A weight balance diagram is shown in Figure 6.2, illustrating the cg travel which results from different passenger loads. The cg for the fully loaded configuration was considered to be the aft cg limit as weight estimates were high and removing passengers or decreasing component weights which are still variable in the design would move the cg forward. In the event of changes in final component weights, a study was done to determine the amount of cg movement with 10 and 20 % changes in individual component weights. It was found that the most the cg would move with a 20% change in the fuselage weight (the greatest component weight percentage) was approximately 1.5 inches forward or aft (decreasing or increasing weight), or about 10% of the chord. Yet, any such additional movement could be accounted for by moving the avionics package slightly in the opposite direction of the cg movement.

Figure 6.1: Component Layout Diagram

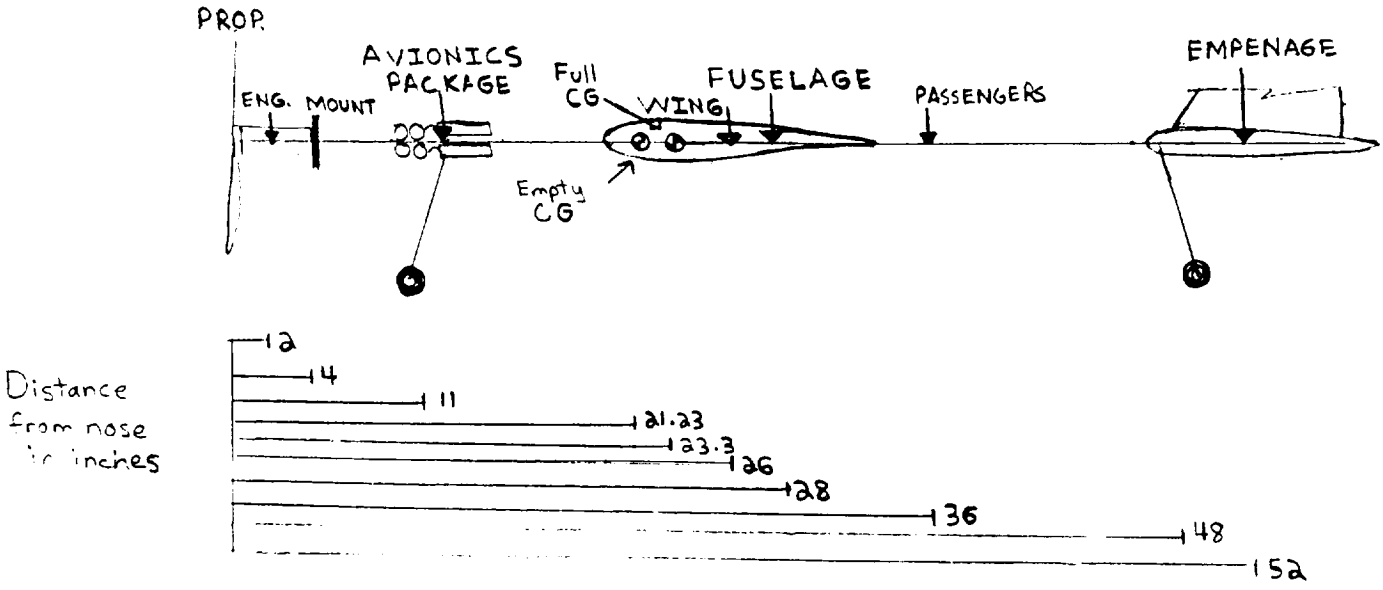

Figure 6.2: Weight Balance Diagram

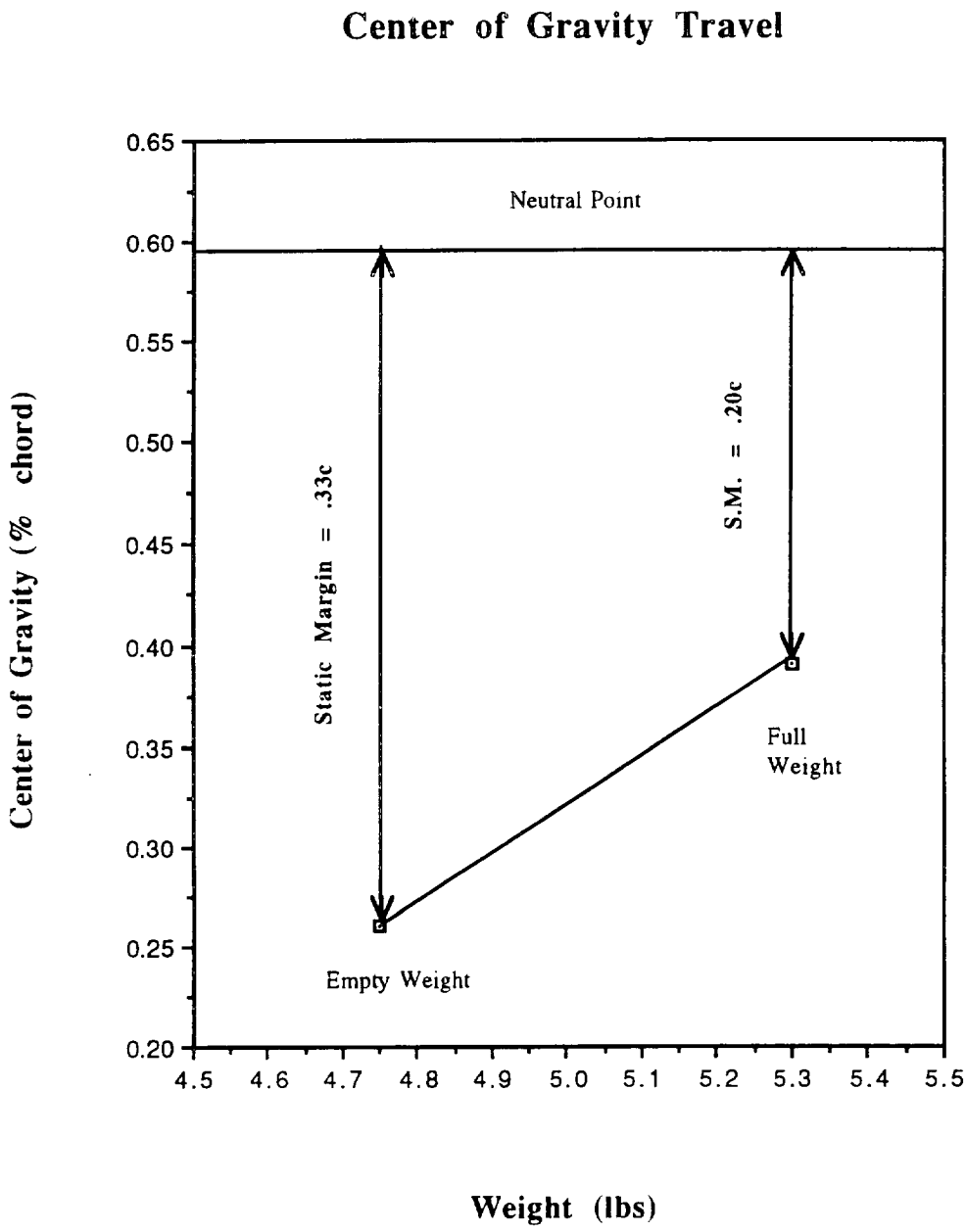

7.0 STABILITY AND CONTROL

The Bunny must exhibit the following characteristics:

1) longitudinal stability through the horizontal tail
2) longitudinal control for maneuvering and trim through the elevator
3) lateral stability through dihedral
4) directional stability through the vertical tail
5) lateral/directional control through rudder-dihedral interaction

At this stage, primary design consideration will be given to static stability. The design issues and trade-offs necessary to meet these requirements are described below. The analysis methods used for the design can be found in Appendix B.

7.1 Longitudinal Stability

Longitudinal stability is critical for the airplane's flying qualities. Without sufficient longitudinal stability, the aircraft will be extremely difficult to handle. Desirable longitudinal stability corresponds to a negative slope of the pitching moment coefficient versus alpha curve: for a nose up change in angle of attack, the moment developed is negative and thus rotates the nose downward. Since the proposed aircraft concept is remotely piloted, stability is especially important since a remote pilot's response time is relatively long.

Static margin is a typical measure of the amount of longitudinal stability of an aircraft. Static margin (SM) is defined as the distance between the center of gravity and the neutral point in percent of chord. A typical aircraft needs a static margin of 5-10% to be sufficiently stable; for an RPV, it is recommended that the SM be increased to 20%.

The method indicated in Appendix B was used to obtain the horizontal tail sizing. The design point was taken to be the aftmost c.g. location, which corresponds to the maximum capacity configuration. The design SM was set at .2 and the horizontal tail was sized to produce a neutral point which corresponded to this SM. The tail moment arm was set by the fuselage length and a flat plate design was chosen for ease of construction. A high aspect ratio was desired in order to increase the lift curve slope of the tail; however, increasing the aspect ratio leads to increased structural weight for the tail. Therefore a moderate aspect ratio of 2.5 was chosen. With these parameters fixed, the necessary horizontal tail area was calculated. The resulting horizontal tail configuration is given in Table 7.1.

Table 7.1: Horizontal Tail Configuration
$\frac{S_H}{S_w} = .298$
$V_H = .69$
AR = 2.5
$C_{L_\alpha} = .061 / ^\circ$
l_t = 30 in.
$i_t = 0^\circ$

LinAir was used to determine the stability characteristics of this tail configuration. Although there are certain limitations inherent in LinAir, it provides a convenient way to calculate the pitching moment coefficient for various incidences of the wing, tail and elevator. However, these limitations must be noted because they may cause inaccuracies in the results. The wing was modeled without dihedral or taper due to constraints on the number of elements. Also, the fuselage was not included. In order to include the airfoil section's characteristics, the wing was modeled with 5 elements at various incidences to simulate camber; however, the exact camber of the complicated Wortmann airfoil could not be modeled. Thus the effect of the pitching moment coefficient about the a.c. at zero angle of attack may not be accurate.

It is desirable from drag considerations that the aircraft be in trim at cruise in a level attitude with zero elevator deflection. This can be accomplished by setting the tail incidence. However, Figure 7.1 illustrates that as the tail incidence becomes more negative to provide zero net moment, the download on the tail causes the overall C_L to decrease. In order to regain the desired C_L, the wing incidence must be increased, disturbing the moment balance. Thus the solution must be obtained through iteration, in this case using LinAir. Since the drag increases as the angle of attack of the wing or tail is increased, it is also desirable to keep the incidences as small as possible. The design point for *The Bunny* was taken to be cruise at the aft c.g. location with flaps up and a fuselage angle of attack of zero. A wing incidence angle of 2.5 degrees with a tail incidence angle of zero degrees provided the proper trim at this condition while maintaining cruise C_L. Note that LinAir yields results specified to 5 significant digits. Due to the iterative nature of the design process, the desired C_m and C_L values of 0.0 and 0.6, respectively, could not be obtained exactly. However, the design point indicated on Figure 7.1 corresponds to values of C_m and C_L very close to the desired numbers, and is considered acceptable for this phase of the design.

Figure 7.1: Cm and CL vs. Tail Incidence Angle

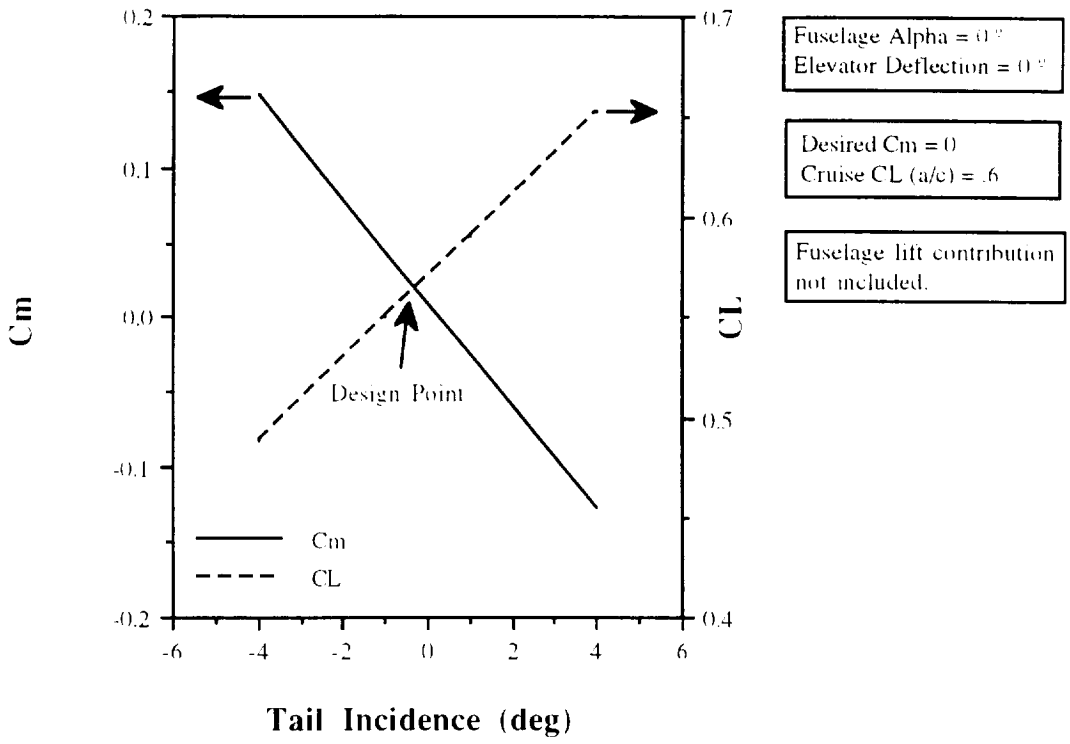

Using this tail incidence and keeping the elevator neutral, the variation of the pitching moment coefficient with angle of attack was calculated. The results are displayed in Figure 7.2 for aft and forward c.g. limits and for flaps up and down. The forward c.g. limit corresponds to an empty (no passengers) configuration. Again, the trim condition is not exactly zero due to the iterative design process. Due to the limited number of elements in LinAir, flaps and the tail could not be modeled simultaneously; therefore, the increment in C_m due to the flaps was calculated separately using a wing-only model. Figure 7.2 shows that the flaps have a nose down effect on the pitching moment, and that the amount of the effect varies with the c.g. location. The slope of the curve is designated C_{m_α} and is a measure of the stability of the configuration.

Figure 7.2: Pitching Moment Coefficient vs. Alpha for forward and aft c.g. conditions

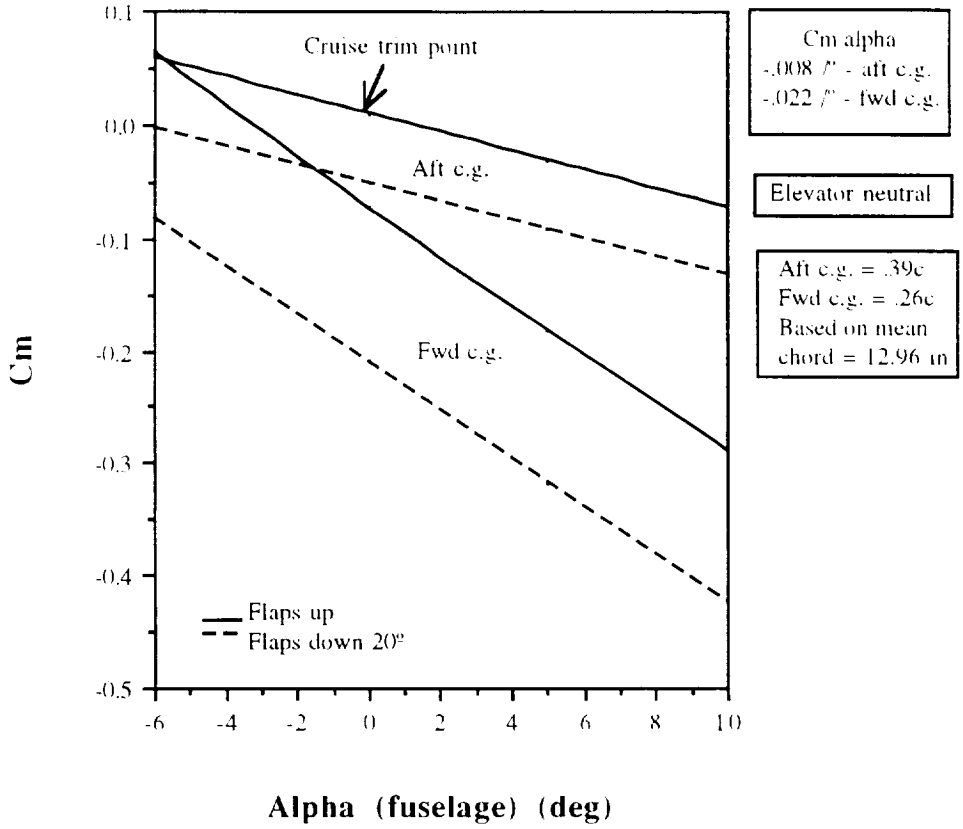

From Figure 7.2 it can be seen that the slope increases as the c.g. moves forward; thus, the forward c.g. configuration is more stable than the aft configuration. However, too much stability can make the aircraft difficult to maneuver. The static margin is a good indicator of the correct level of stability. For the design case at the aft c.g., the static margin is .2; for the forward c.g. case, the SM increases to .33. These results would provide good stability. However, a discrepancy was discovered late in the design phase which may significantly effect the handling of the aircraft. The SM calculations were based on the neutral point calculated according to Appendix B. However, LinAir can also be used to determine the static margin by plotting C_m vs. C_L. The SM is the negative of the slope of the curve. From this calculation, the static margin is only .087 for the aft c.g. and .23 for the forward c.g. Part of this discrepancy may be due to the fact that only approximate solutions were obtained as mentioned previously. However, it is difficult to accurately predict how the technology demonstrator will perform. Further studies should be conducted to determine the source of the discrepancy and to determine which method is more reliable.

7.2 Longitudinal Control

Although the aircraft is designed to be in trim at cruise with zero elevator deflection, in order to trim at other flight speeds the elevator must be employed. Deflecting the elevator does not affect the slope of the pitching moment curve, but shifts the curve up or down to change the trim point. For sufficient control at a wide range of flight speeds, the elevator should be capable of trimming the aircraft at a speed near stall and at a high speed condition. For *The Bunny*, the extreme trim conditions correspond to a fuselage angle of attack of approximately 9.5 degrees (near stall), and -6.5 degrees (corresponding to a flight speed of 50 ft/s). These points are established as the extreme limits, although the added drag created by the fuselage and elevator may prevent this speed from being reached. From Figure 7.2 it can be seen that at 9.5 degrees, the maximum ΔC_m necessary to trim is .4 for the forward c.g, flaps down condition. At negative -6.5 degrees, the maximum ΔC_m is .07 for the aft c.g., flaps up condition. The elevator was designed to provide trim at these points. The maximum ΔC_m which can be produced by the elevator is a function of elevator size and maximum deflection. A trade study indicated that for configurations of S_e and δ_e which provide equivalent ΔC_m, less drag will be produced for the configuration with a smaller elevator but larger deflection. Based on these findings and using LinAir to calculate the moments, the elevator parameters were determined and are displayed in Table 7.2.

Table 7.2: Elevator Configuration

$\frac{S_e}{S_H} = .2$
$\delta_{emax} = +18^\circ$ (up)
$= -3^\circ$ (down)

Figure 7.3 illustrates the trim at these conditions. Note that positive elevator deflection is defined as that which will produce a positive pitching moment. From this figure, it can be seen that for an angle of attack near stall with flaps down and forward c.g, deflecting the elevator up 18° will shift the curve so that trim is achieved. An important point to note is that with the flaps down at this c.g. location, trim cannot be achieved at any speed unless the elevator is deflected. The flaps on this aircraft were designed for take-off performance and are not intended for use on landing. As can be seen from these trim characteristics, if the flaps are deployed for landing at the forward c.g. location, there may not be enough elevator deflection available to produce a sufficient flare maneuver. For a high speed condition, deflecting the elevator down 3° brings the airplane into trim with

the flaps up and aft c.g. Since these points represent the extreme conditions, the airplane should be able to be sufficiently trimmed at any flight condition.

Figure 7.3: Pitching Moment Coefficient vs. Alpha for trim near stall and at high speed

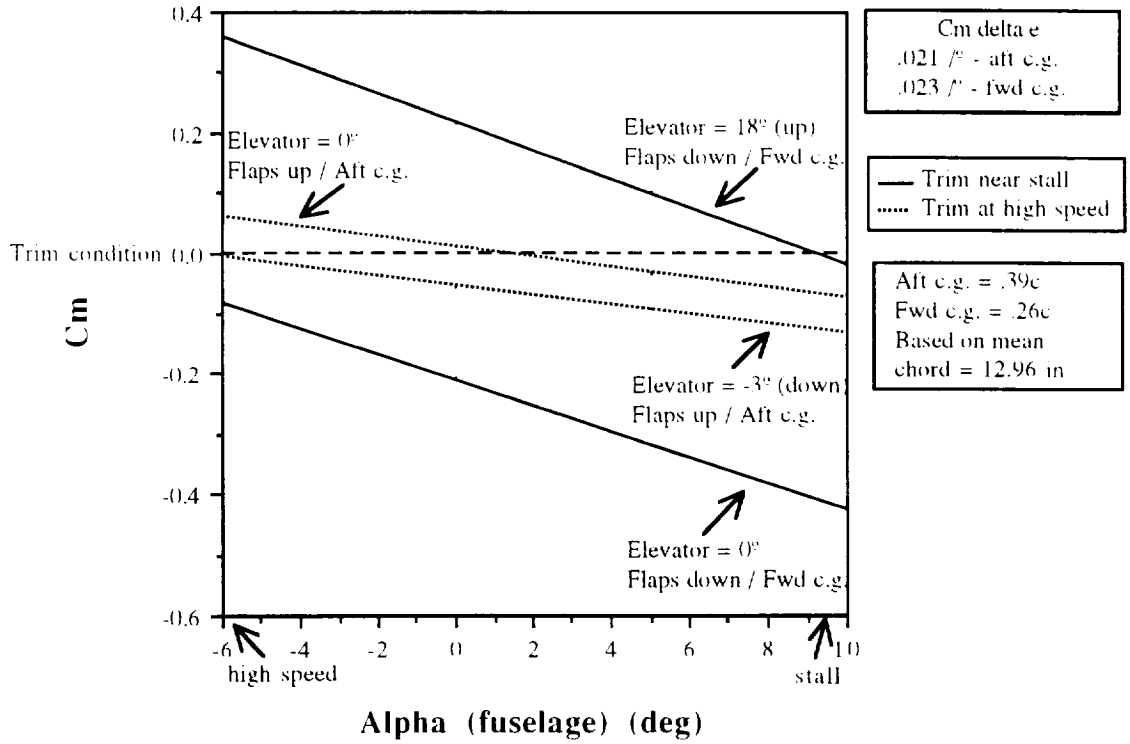

The elevator control power $C_{m\delta e}$ is also indicated on Figure 7.3. Note that for the forward c.g. condition, C_{m_α} is approximately equal to $C_{m\delta e}$. This means that for a one degree elevator deflection, the angle of attack change will be one degree. This is beneficial from a handling standpoint. For the aft c.g. configuration, however, a one degree elevator deflection produces a 3 degree change in angle of attack. Thus at the aft (design) condition, the aircraft will be more sensitive to elevator deflections and may be more difficult to handle.

7.3 Lateral/Directional Stability and Control

The Bunny uses rudder-dihedral interaction to provide roll control. The basic premise of this configuration is that the rudder can be used to induce a sideslip angle, which will in turn produce a roll moment for an aircraft with dihedral. This eliminates the need for ailerons, reducing the number of necessary servos and simplifying the construction of the wings. For this type of control, the lateral control is linked very

closely to the lateral/directional stability of the aircraft; therefore, these two areas will be considered together.

The critical factors in the lateral/directional stability and control are the roll control power $C_{l\delta r}$, the lateral stability derivative $C_{l\beta}$, and the directional stability derivative $C_{n\beta}$. The roll control power must be sufficient to allow the aircraft to maneuver through the specified course and to perform the loitering turn. A large value of $C_{l\delta r}$ means greater maneuverability with less rudder deflection. Large values of $C_{l\beta}$ and small values of $C_{n\beta}$ will lead to a large value of $C_{l\delta r}$. However, if the lateral stability derivative is too large the aircraft will respond to small sideslip angles, such as those which might be produced by a gust, with a large roll moment. This type of behavior will make the aircraft difficult to handle and is generally undesirable. If the directional stability derivative is too small, the aircraft will not return to equilibrium if disturbed to a sideslip condition. This would make the airplane stray off course easily. Thus a design trade-off had to be made between the values of $C_{l\beta}$ and $C_{n\beta}$ which provide good stability characteristics and those which produce good roll control.

In order to set these parameters, a trend study was performed. Figure 7.4 shows the variation in roll control power with rudder size ratio for a constant dihedral angle. From this figure it can be seen that roll control power increases linearly with increasing rudder size ratio up to a point, then becomes non-linear. However, neither $C_{l\beta}$ nor $C_{n\beta}$ are effected by $\frac{S_r}{S_v}$. Thus $\frac{S_r}{S_v}$ can be maximized to provide maximum control power without sacrificing stability. However, for structural reasons a sufficient portion of the vertical tail must be fixed. Since the increase in roll control power drops off where the curve becomes non-linear, a rudder size ratio of .6 was chosen as the design value.

Figure 7.4 also indicates that the roll control power increases as the vertical tail area is decreased for a given rudder size ratio. This result indicates that rudder size, rather than overall vertical tail size, has the most significant effect on the roll control. Thus maximum roll control power occurs for minimum S_v if the rudder size ratio is set. However, $C_{n\beta}$ increases with increasing S_v, such that stability will be poor if S_v is too small. Roll control power also increases with increasing dihedral angle, so that maximum control is achieved for maximum dihedral. However, $C_{l\beta}$ increases linearly with Γ, leading to poor handling at high dihedral angles. A tradeoff had to be made between good stability and sufficient control. This tradeoff is illustrated by Figure 7.5, which shows the necessary dihedral angle and tail area for a desired level of roll control.

Figure 7.4: Variation in Roll Control Power with Rudder Size Ratio for constant Dihedral Angle

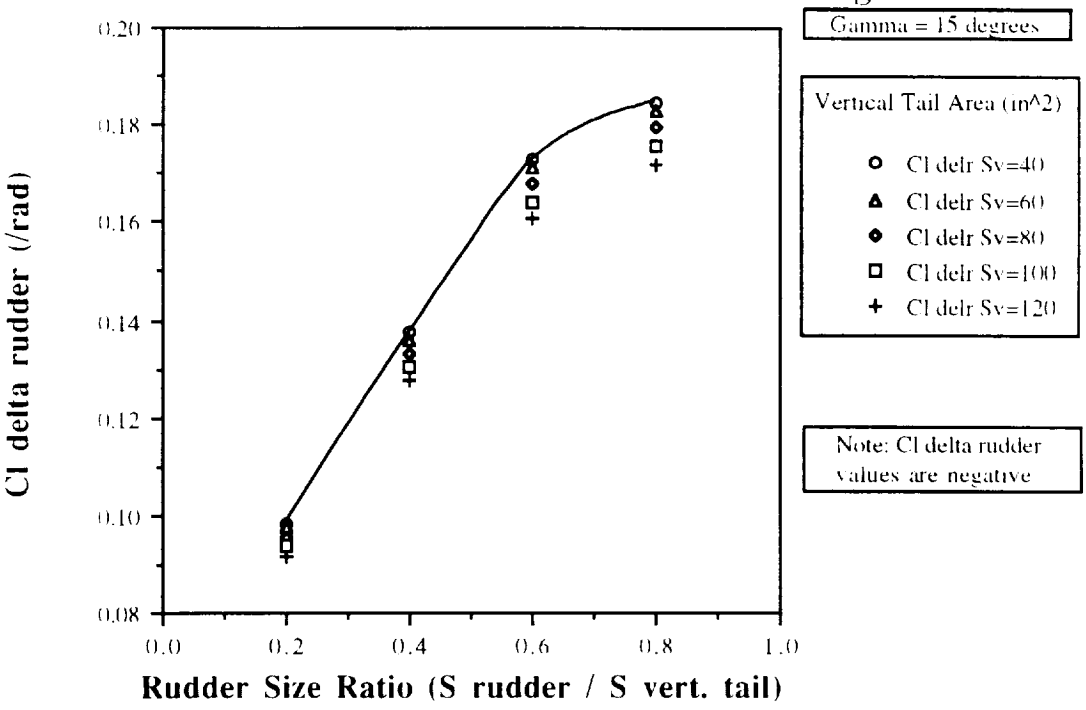

Figure 7.5: Dihedral Angle and Vertical Tail Area Necessary to Achieve Desired Roll Control Power

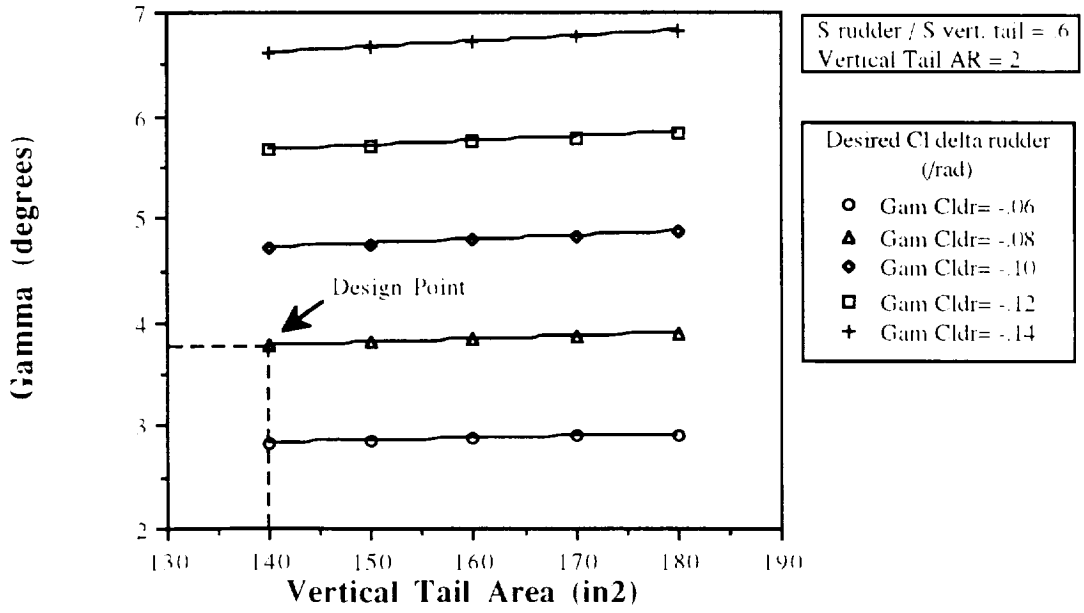

Due to the lack of flight test data for this class of aircraft, it is difficult to specify values of $C_{l\beta}$, $C_{n\beta}$, and $C_{l\delta r}$ which provide good stability and control. For this reason, it was decided to model the derivatives after the HB-40, a similar aircraft which is known to have good flying qualities. Figure 7.5 was used to select a configuration which closely approximates the HB-40. Since the vertical tail area has only a slight effect on the roll control power, this area was kept as small as possible to minimize drag. The design configuration is summarized in Table 7.3. It should be noted that the dihedral angles in Figures 7.4 and 7.5 are based on a V-dihedral configuration. However, *The Bunny* has a three-panel polyhedral configuration. Thus the value in Table 7.3 is the polyhedral angle which has the same Equivalent Dihedral Angle as the V-dihedral angle specified in Figure 7.5. The conversion was made by following the method outlined in Reference 9.

Table 7.3: Vertical Tail Configuration

Sr/Sv = .6
Sv = 140 in^2
V_v = .03
AR = 2
Polyhedral = 6° (wing)
$C_{l\delta r}$ = -.080 /rad
$C_{l\beta}$ = -.127 /rad
$C_{n\beta}$ = .111 /rad
$C_{n\delta r}$ = -.070 /rad

Although the design is modeled after the HB-40, it is difficult to predict how it will actually fly. Since the HB-40 data was based on the design report, there may be discrepancies between the data and the actual aircraft. In addition, *The Bunny* is a larger aircraft and was built to meet different requirements. With the current configuration, *The Bunny* will be slightly less stable and have less roll control than the HB-40. In addition, the effect of the change in lift of the vertical tail acting above the aircraft centerline, which was initially neglected, could be significant based on the final design, since the moment arm is approximately 8 inches. This contribution opposes the roll moment created by the dihedral effect, possibly decreasing $C_{l\delta r}$ as much as .02 /rad according to a rough calculation. A second rough calculation of the steady-state roll rate was performed based on Reference 10 (pp. 154, 108). The current configuration yields a steady-state roll rate of approximately 14 ° / second with a rudder deflection of 30 degrees. Thus it will take approximately 1.3 seconds to roll into an 18° bank for the loitering turn. This is probably a slower response than desired, but in order to increase it $C_{l\beta}$ would have to be

increased, making the aircraft very roll-sensitive to sideslip disturbances. At this stage of the design, it is felt that the roll rate can be sacrificed slightly for the sake of good lateral stability. It is recommended that the next stage of design incorporate these roll rate equations into the early phases in order to adjust the configuration for better roll control.

7.4 Control Mechanisms

The control surfaces employed by *The Bunny* are the rudder, elevator and flaps. Three servos are used to drive these control surfaces: one for the rudder, one for the elevator, and one servo with a connection to each of the flaps, which are located on either side of the fuselage. The wires will be attached to the control surfaces by small protruding horns extending from the surface. The servos will be driven on three separate remote control channels. The pilot will provide input to the radio transmitter, which will then activate the servos on board. The rudder and elevator controls on the radio transmitter return to the zero position when released, with a separate trim control to adjust the zero position if necessary. This configuration allows small step inputs to the rudder or elevator to be made easily. The flap control is also of this type, meaning that on take-off the pilot will have to hold the flap control in the flaps down position. While this will require a somewhat higher degree of pilot coordination, it will not affect the propulsion control and should not create a significant pilot workload problem.

8.0 PERFORMANCE

The emphasis in designing *The Bunny* was to attain the performance goals and requirements set in the DR&O. The most important of these was designing the aircraft to be capable of servicing all the cities of AEROWORLD. This set a takeoff and landing distance goal at a maximum of 20 ft. The aircraft was also designed to perform a sustained level 60 ft radius turn at 25 ft/s. Some of the important performance parameters are listed in Table 8.1 below.

Table 8.1

Max Takeoff Weight = 5.3 lbs	$P_{av\ max}$ = 117.9 Watts
Takeoff Velocity = 21.7 ft/s	R/C_{max} = 9.27 ft/s
C_{Lto} (α = 2.5 degrees) = 1.1	γ_{climb} = 18.6 degrees
Takeoff Distance = 16.1 ft	$\gamma_{glide\ min}$ = 3.9 degrees
Landing Distance = 53.6 ft	Max Glide Distance = 288.0 ft
Cruise Velocity = 30.0 ft/s	L/D_{max} = 13.1
Range at Cruise = 14,343 ft	R_{min} = 33.6 ft
Max Range = 14,355 ft	ϕ_{max} = 30.0 degrees
Endurance at Cruise = 478.1 s	n_{turn} = 1.15
Max Endurance = 615.8 s	Cruise Altitude = 20.0 ft

8.1 Takeoff and Landing

The takeoff and landing distances of *The Bunny* were set in the DR&O at a maximum runway length of 20 ft in order to service all cities in AEROWORLD. To achieve this goal the wing was designed using the FX 63-137 airfoil section and flaps. This produced a C_{Lto} of 1.11 at an angle of attack of 2.5 degrees and a takeoff velocity of 21.7 ft/s with the flaps deflected 20 degrees. The rolling coefficient of friction was estimated as 0.15 for the hard turf surface in Loftus. The takeoff distance was calculated as 16.1 ft at the maximum takeoff weight of 5.30 lbs (100 passengers) using the program *Takeoff* by Dr. S. Batill (Ref. 6). This value satisfies the design goal for a maximum takeoff distance of 20 ft with a factor of safety of 1.24. The cost of exceeding the takeoff distance objective was the addition of a thirteenth battery which slightly increased the weight and expense of *The Bunny*. The optimum amount of batteries to reach the maximum takeoff distance objective was between 12 and 13, but a discrete number had to be chosen and therefore 13 batteries were used. However, the capability of servicing all

airports in AEROWORLD was considered more advantageous than the weight and expense penalties.

The minimum landing distance was estimated as 53.57 ft at maximum weight using the following equation (Ref. 5):

$$LD = \frac{1.69 * W^2}{g * \rho * S * C_{l\,max} * [D + \mu * (W - L)]}$$

The instantaneous values of the lift and drag were calculated at 70% the takeoff velocity using the Shevell method. This value is much larger than the maximum runway length of 20 ft because the aircraft is not equipped with any type of braking system. A future investigation should be made regarding the addition of brakes or a drag parachute device to minimize the landing distance and fulfill the landing distance goal.

8.2 Range and Endurance

At the cruise velocity of 30 ft/s the range and endurance at maximum takeoff weight were 14,343.5 ft and 478.12 s, respectively. Figure 8.1 on the following page shows the range and endurance of *The Bunny* at maximum takeoff weight over a range of velocities. The maximum range was found to be 14,355.6 ft at a velocity of 29.0 ft/s yielding an endurance of 495.02 s. This maximum range is very close to the design cruise velocity of 30 ft/s. The maximum endurance of 615.79 s occurred at a velocity of 19.0 ft/s and with a range of 11,700.1 ft. At the cruise velocity, the values of range and endurance are greater than the values specified in the DR&O as 13,000 ft and 433 s. This is due to an excess battery capacity of over 200 mah for the batteries selected, which may be used for ground handling, taxiing and other delays that may occur. The excess capacity is a result of a thirteenth battery added to meet the takeoff distance goal. Because the takeoff distance objective was listed as a higher priority goal than the range and endurance objectives, the increased range and endurance from the initial objectives were accepted as a trade off. However, this is not considered a disadvantage because the excess range and endurance capabilities will allow *The Bunny* to be flexible in case of future design changes such as an increase in the payload weight or the addition of a more distant airport.

The relationship between range and weight was also investigated. Figure 8.2 (pg. 8-3) shows that as the passenger size was decreased from 100 to empty the range of the aircraft increased. When the aircraft is flown with 50 passengers (W = 5.05 lbs) the range increased to 14,520.83 ft and when flown empty (W = 4.8 lbs) the range increased to 14,716.57 ft.

Figure 8.1 Range and Endurance Versus Velocity

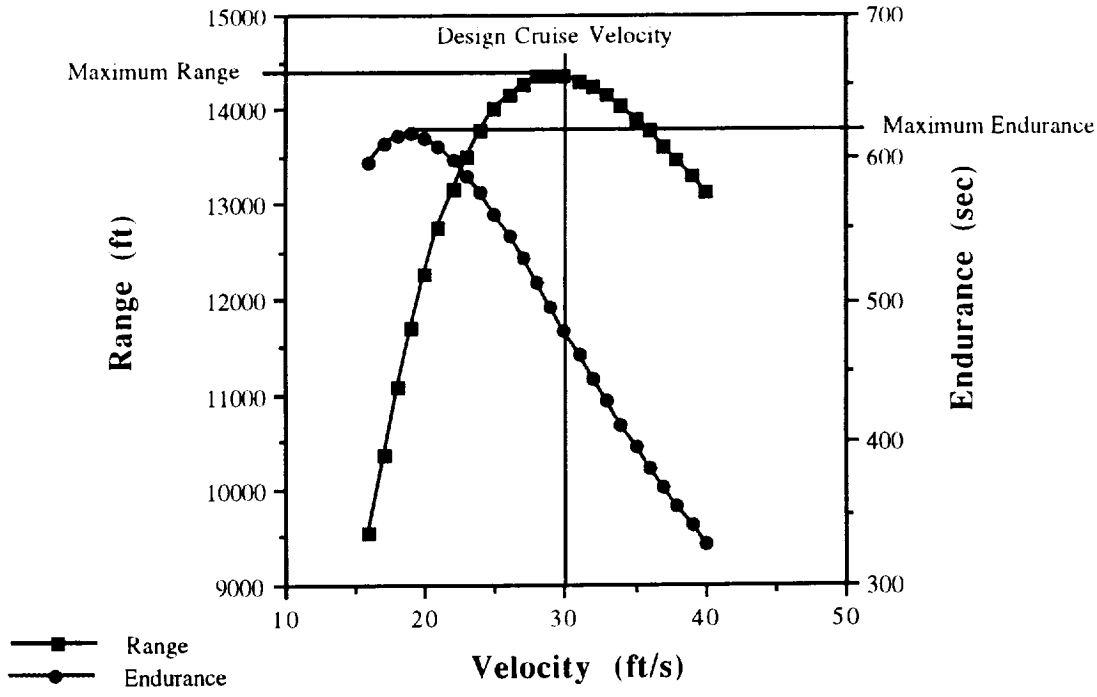

Figure 8.2 Payload Versus Range

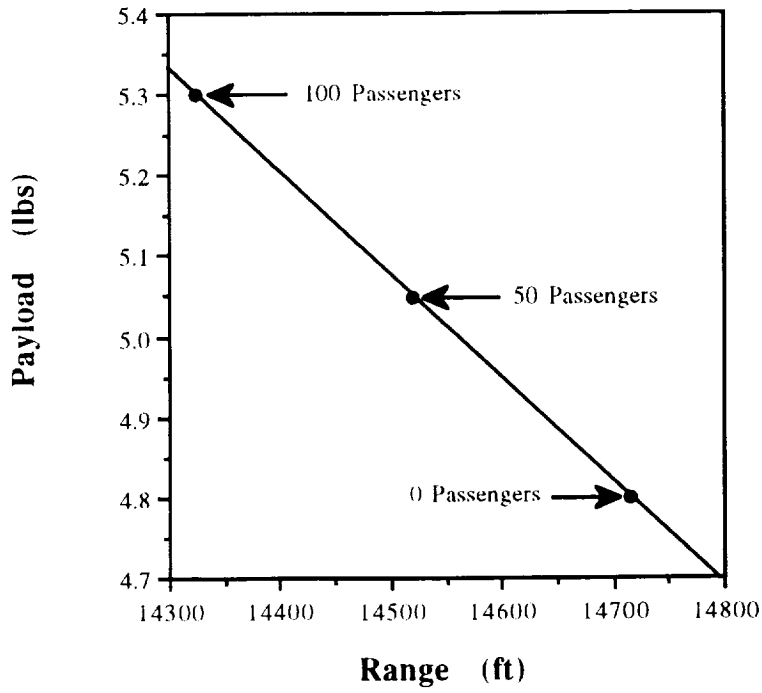

8.3 Power Available and Power Required

The power available and power required values were calculated at varying levels of voltage. The power required curve is not a function of the voltage. Figure 8.3 (pg. 8-5) shows the power available and power required curves for *The Bunny* at maximum takeoff weight. The maximum velocity of 50.0 ft/s for *The Bunny* occurs at the far right intersection of the power available and power required curves using the maximum voltage setting of 15.6 V. The minimum velocity occurs at the stall velocity of 15.95 ft/s. The power required is the power necessary to maintain steady level cruise. Between the P_{av} and P_{re} curves there is excess power which can be used to climb to a higher altitude. Figure 8.4 (pg. 8-5) illustrates the relationship between voltage and power available. As the voltage is increased the power available also increases providing a larger excess power. The maximum voltage available for the propulsion system is 15.6 volts which is used in takeoff to provide the largest rate of climb. The voltage setting should be reduced in cruise to 9.0 V where the values of P_{av} and P_{re} are nearly equal because no excess power is desired.

8.4 Climb and Glide Performance

From the power available and power required study, the rate of climb of *The Bunny* at varying voltages and velocities was determined. The maximum rate of climb equal to 9.27 ft/s occurs at the maximum voltage of 15.6 V and a velocity of 29.0 ft/s. At the cruise velocity the rate of climb decreases only 0.2% to 9.25 ft/s. Therefore, *The Bunny* will be operating near its R/C_{max} as it accelerates from the takeoff velocity of 21.7 ft/s up to the cruise velocity of 30 ft/s through its most effective range of rates of climb. At R/C_{max} *The Bunny* will climb to the cruise altitude of 20 ft in 2.2 s at a climb angle of 18.6 degrees and cover a ground distance of 59.43 ft. The total distance required to reach the cruise altitude, including the takeoff distance, is 75.53 ft. This will allow *The Bunny* to be in cruise 74.47 ft before entering the first turn of the course.

Glide performance is also an important consideration in case of motor failure because *The Bunny* is a single propeller aircraft. In the event of motor failure, the minimum glide angle is 3.97 degrees, based on the maximum lift to drag ratio of 13.1. If the power is cut at the cruise altitude of 20 ft, the maximum glide distance is 288 ft at the minimum glide angle.

Figure 8.3 Power Required and Power Available Versus Cruise Velocity

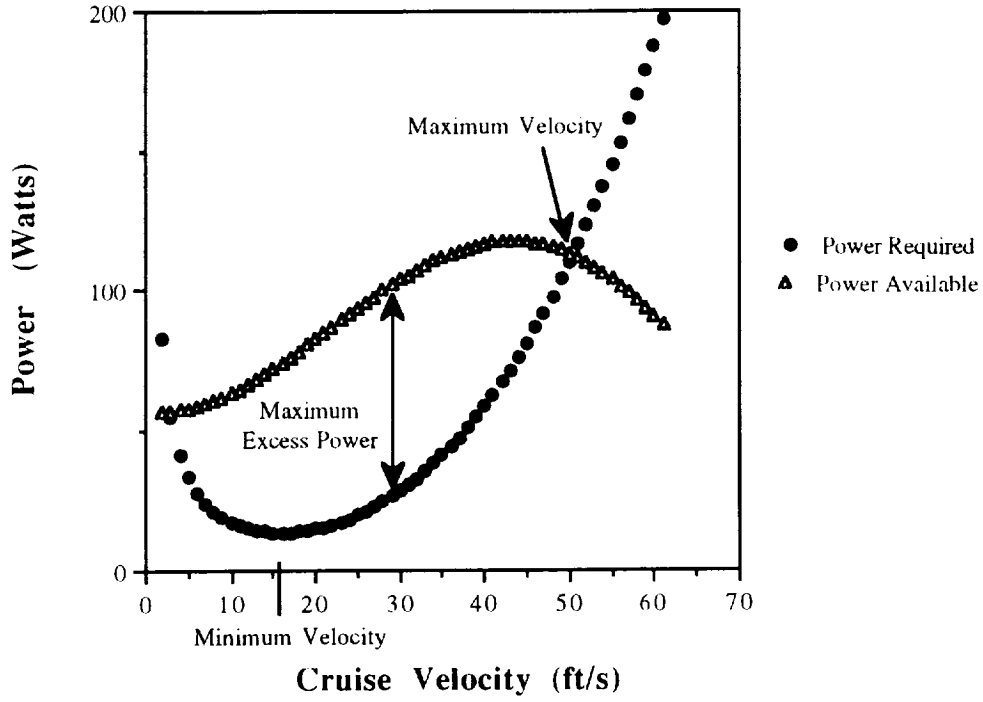

Figure 8.4 Power Required and Power Available Versus Velocity

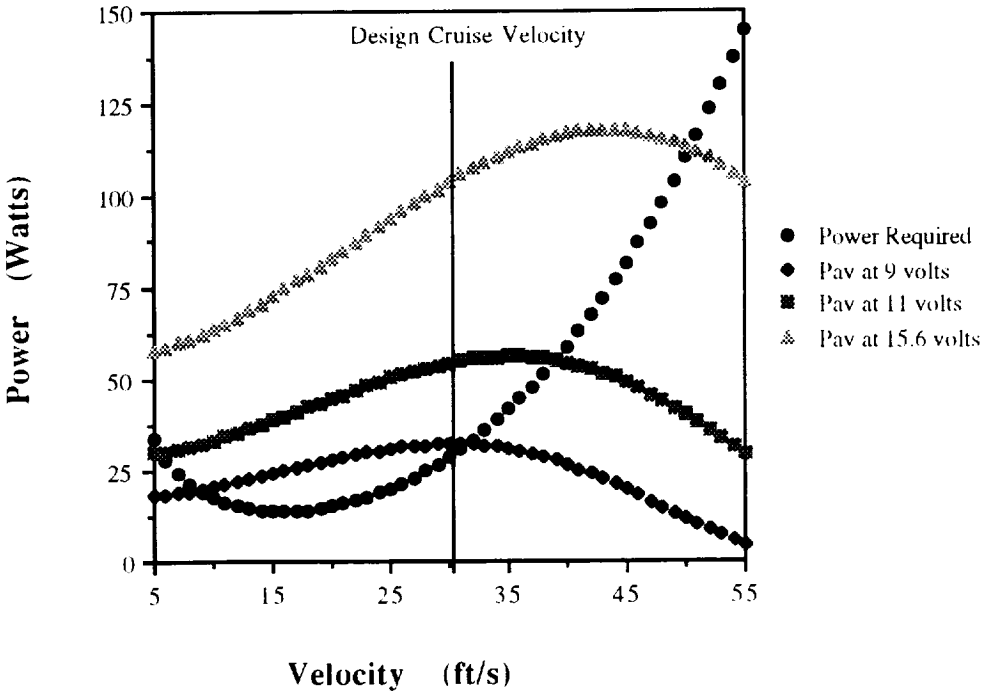

8.5 Turn Performance

From the DR&O, *The Bunny* is required to perform a sustained level turn within a 60 ft radius at 25 ft/s. At that velocity and radius, the bank angle is 17.93 degrees and the load factor is 1.05, 52% below the maximum load factor. The relationship between the bank angle, ϕ, and the load factor, n, is (Ref. 5):

$$n = \frac{1}{\cos \phi}$$

The load factor increases with increasing bank angle. Care must be taken to assure the load factor limit of 2.2, which was determined through the structural design analysis, is not exceeded due to structural limitations. At 25 ft/s the maximum bank angle which can be performed in the turn is 60 degrees for a load factor of 2.2. The minimum radius for this turn is 11.2 ft, calculated using the equation (Ref. 5):

$$R_{min} = \frac{V^2}{g * \tan \phi}$$

However, for passenger comfort the maximum bank angle is limited to 30 degrees. At this angle the corresponding turn radius is 33.6 ft, 44% less than the maximum radius of 60 ft, and the load factor is 1.15, 48% below the maximum load factor. The turn performance for *The Bunny* is targeted at a bank angle of 30 degrees yielding a minimum turn radius of 33.6 ft.

9.0 STRUCTURAL DESIGN

The structural design and analysis for *The Bunny* was based on a component by component method. The three main components examined were: (1) the fuselage structure, (2) the wing structure, and (3) the empennage structure. In order to properly analyze these components it was necessary to establish a material selection process as a means of judging the available materials. It became apparent from the rough fuselage structural model and from simple experimental material testing that the RPV's from previous years were structurally over-designed. It is believed that the lightweight fuselage construction, as well as overall construction for *The Bunny*, can decrease the weight factor of the aircraft nearly 10% - 20%. The major objective of the structural design team was to construct an aircraft frame consistent with the parameters defined by aerodynamics, stability and control, performance, etc..., which would minimize weight and optimize cost effectiveness.

9.1 Materials Selection and Structural Design

The Bunny must be a lightweight, sturdy aircraft in order to complete its mission. A variety of materials must be considered for the stress concentrations of the aircraft. The criteria for the selection of materials were: weight, cost, strength, and availability. While it was a given that the materials must be of sufficient strength and readily available to the design team, it was realized that the final airframe structure would be driven by the weight and cost parameters. With these factors under consideration, balsa wood was determined to be the preferable material due to its lower density ($0.0058 lb/in^2$) and lower cost per beam than the other available materials. Therefore, balsa wood will be used for the majority of the fuselage, tail, and much of the wing. The following is a listing of the beam bending moments to which both the fuselage and the wing are subjected, based upon the components which the fuselage must support and a simple wing loading analysis.

Beam Bending Moments:

Fuselage----------37.5 (lb - in)

Wing----------66.4 (lb - in)

Due to the fact that the main lateral spar caps of the wing undergo nearly twice the beam bending moment than the fuselage, the next step up in beam strength was necessary. Therefore, bass wood will be used for the main lateral spar caps of the wing at a slight weight and cost disadvantage. The strength attributes of the thin birch plywood will be utilized to support the wing carry-through structure and for the Wortmann airfoil ribs at the connection of the polyhedral and at the wing connection to the fuselage. Birch plywood will also be used for the I-beam web of the wing's

main lateral spar in order to maintain the shape of the weak airfoil ribs and to add beam bending strength to the main spar caps. It was the desire of the structural design team to keep the use of spruce wood to a minimum because of the weight and cost penalty. Spruce will only be employed where it is necessary to use wood screws, for the support of the landing gear, and for the main supporting beams of the engine mount. The structural design of the aircraft is based on a substructure design process. First the particular loading that the structure must endure was considered. Second, the best material which can withstand these stresses and supply ample structural integrity, with minimal weight and cost penalty was located. Finally, a detailed sizing of each of the frames of the aircraft was performed. The following is a list of some of the materials most readily available to the design team and a few of their respective densities.

Densities of various materials:

Balsa----------0.0058 (lb/in^3)
Spruce----------0.016 (lb/in^3)
Douglass Fir----------0.020 (lb/in^3)
Pine----------0.025 (lb/in^3)
Birch Plywood----------0.3696 (oz/in^3)
Monokote----------0.00349 (lb/in^3)

The grain pattern of the various materials is critical when examining the stress directions and limits because the material could be considerably stronger in one direction than another. The following listing of the stress limitations of balsa wood and spruce illustrate that the two have different grain patterns and exhibit their maximum stress limitations in different directions (this stress data taken from a previous design report).

Stress direction and limits for two materials:

	Balsa	Spruce
XX(psi)	400	6200
YY(psi)	600	4000
XY(psi)	200	750

9.2 The Wing

In order to satisfy the weight goal for the aircraft we must be able to manufacture the wing in a strong, lightweight fashion. An important design consideration was the polyhedral to be used for roll control because it posed some difficult structural and manufacturing dilemmas. The span

of the wing was designed to be sufficient to reduce the induced drag to a reasonable value by increasing the aspect ratio. Wherever possible, based on the material selection process, balsa will be used for the internal components of the wing.

The wing will have three spars: leading edge spar, main spar, and the trailing edge spar. The leading edge spar will be notched into the airfoil ribs, will be constructed of balsa, will have an approximate cross-sectional area of 3/8 in^2, and will aid in maintaining the shape of the wing. The trailing edge spar will be made of balsa and will support the flap structure on the part of the wing with no dihedral (from the root to the 1/4 span position). The main spar caps will be constructed of two beams which will be notched into the top and the bottom of the airfoil ribs at the position of greatest thickness. Each of these beams will be constructed of bass wood with a cross sectional area of 1/4in X 1/4in. The connecting posts, or I-beam web, will be necessary to supply bending moment support and to maintain the integrity of the airfoil ribs. The aforementioned structural design for the main supports of the wing was based on a simple shear and bending moment balance for the in-flight condition.

$$V(x)=-1/2(Wo + W)x + 1/2(Lo + L)x$$
$$M(x)=-(2Wo + W)x^2/b + (2Lo + L)x^2/b$$

There will be two distributed forces on the wing: the lift along the span and the weight of the wing section. Through a simple calculation of the lift and weight on the wing the following bending moment diagram was determined for the in-flight condition.

Figure 9.1

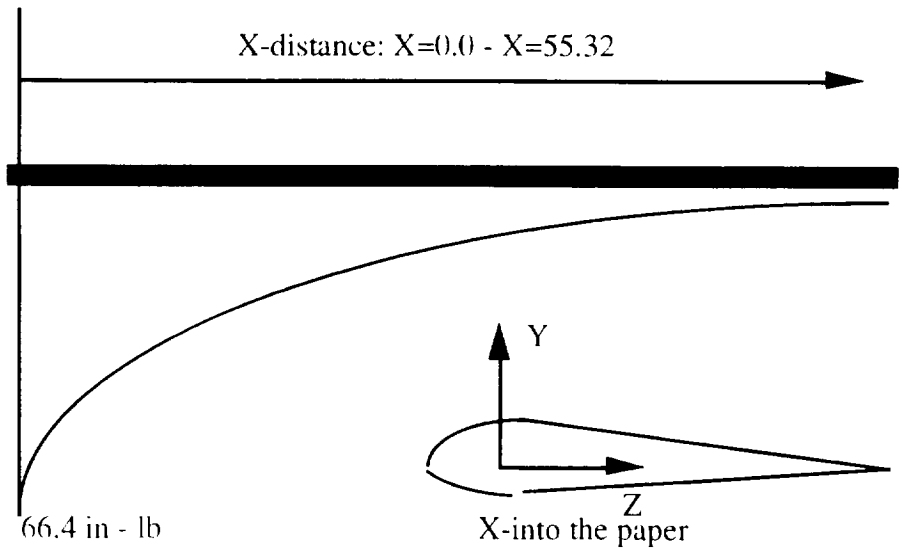

Using this analysis, the spar caps were sized and the next step was to make a best guess at the appropriate internal layout for the wing. The number of Wortmann airfoil shaped ribs total 28, with a rib spacing of 4 inches based on estimates taken from previous design data. The large number of ribs are necessary in order to maintain the shape of the leading edge and the overall wing shape. An enlarged photocopy version of the Wortmann airfoil will be used to trace the airfoil sections onto the balsa and birch plywood. Supports will be necessary for the wing at the polyhedral attachment (balsa), and supports will be needed at the wing attachment to the fuselage. The weight of the wing was determined from a rough design and was determined to be 0.9 lbs. The weight of each component was determined from a volume*density calculation. The final layout of the wing is as pictured below in Figure 9.2.

Figure 9.2

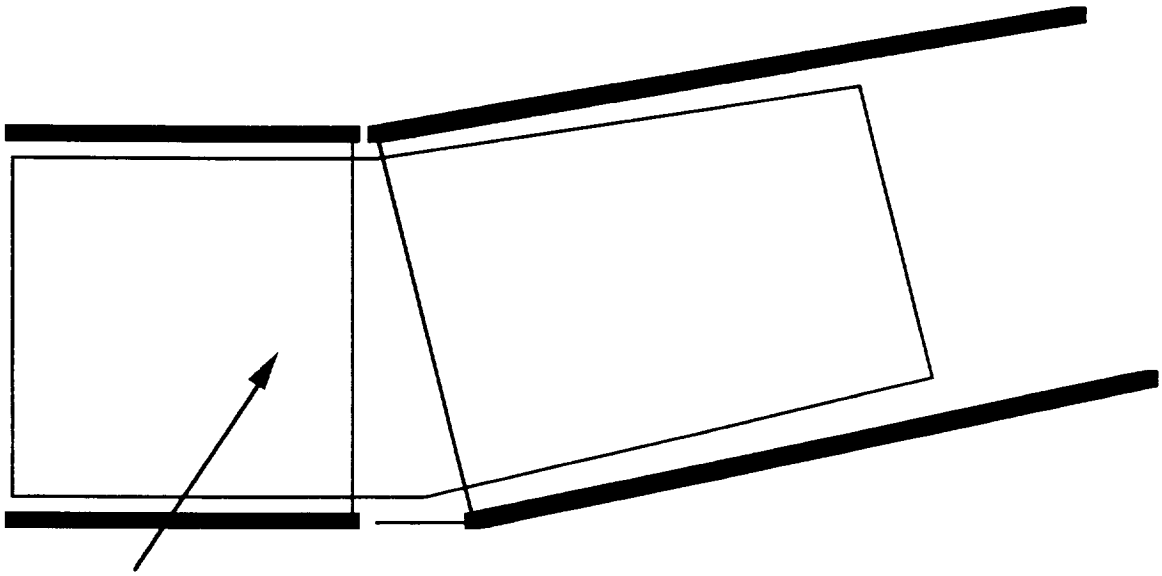

I-beam wedge for simplicity in polyhedral attachment

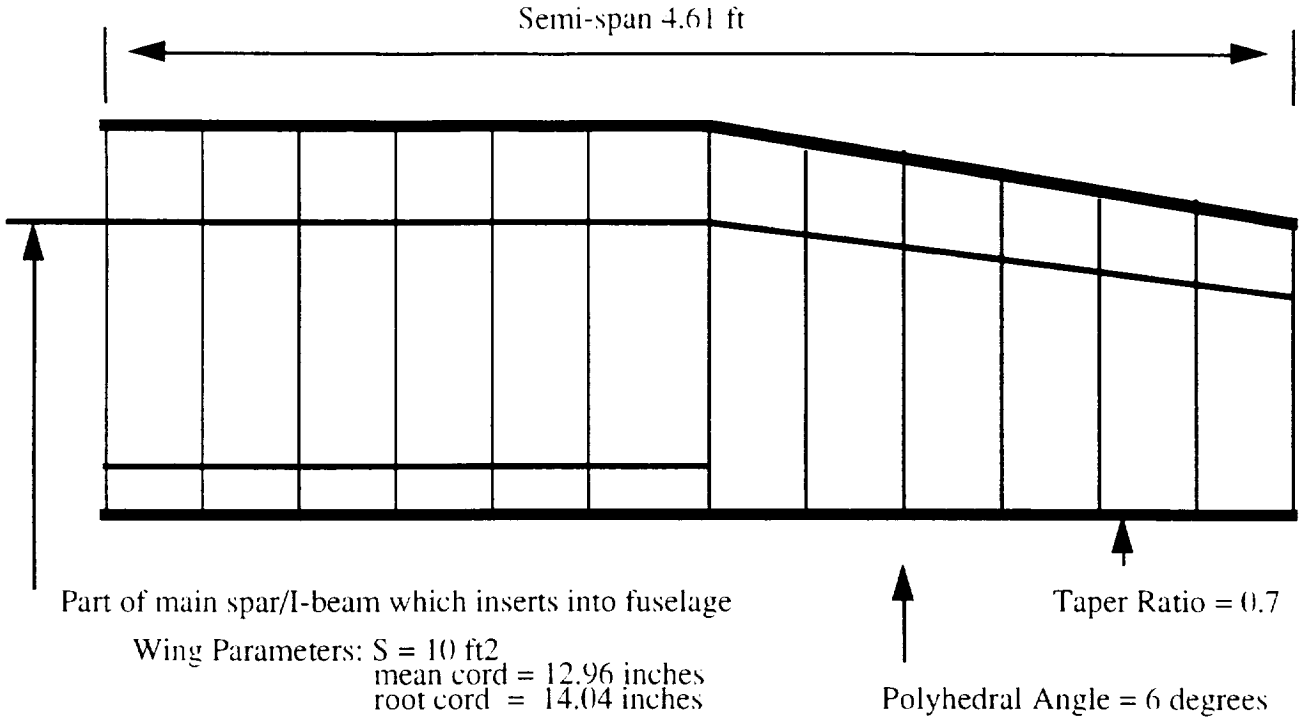

Based on Figures 9.1 and 9.2 the maximum stress which occurs at the wing root was determined from:

$$\text{stress} = MzY/Izz \quad Mz=66.4 \text{ in - lb} \quad Y=1.1 \text{ in} \quad Izz=(1/12)bh^3$$

The maximum stress at the wing root was calculated to be approximately 440 psi, which falls in the optimal material range of bass wood due to the minimum strength requirements.

9.3 The Fuselage

For the fuselage we must also minimize the weight and cost while maximizing the structural integrity and the passenger spacing. The main load carrying members of the fuselage will be the four main beams that run the entire length of the fuselage. Using the symmetric homogeneous advanced beam formula listed in section 9.2, and the calculated beam bending moment, the maximum stress in the beam can be determined. The maximum stress which each of the longerons need to provide for was approximately 225 psi, which is well within the strength capabilities of balsa wood.

The main loads on the rear of the fuselage will be produced by the empennage control surfaces, and the ultimate loads will be produced by the maximum deflections of the rudder and elevators. The overhead sections of the fuselage will be removable for passenger entry and easy

access for battery maintenance. The main fuselage structure was determined from the finite element program of Dr. Stephen Batill and from methods derived from previous RPV designs. This program demonstrated that there was a great deal of structural overkill in many of the previous RPV designs, and that a fuselage structure using balsa for nearly all of the components is all that is necessary. The side view of the fuselage structure can be seen in Figure 9.3.

Figure 9.3

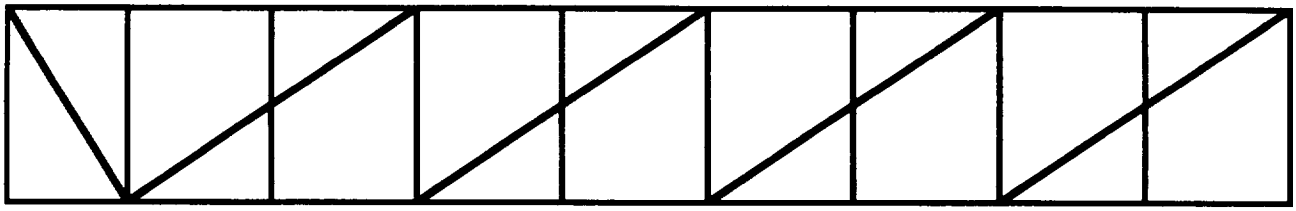

Fuselage Side View(passenger and battery pack sections only)
(all beams 3/8 in^2 balsa wood)
Fuselage Parameters: Height----------4.5 in
Main vertical beams spaced 5 in

Passenger access will be possible from the top of the fuselage, at the rear of the battery pack and servo compartment via a hinged upper fuselage frame.

The engine mount must be able to withstand a static thrust of up to 2.6 lbs, therefore all beams of the engine block will be made from spruce, while the firewalls will be made from birch plywood. Figure 9.4 illustrates the engine mount which will be able to withstand the thrust and weight of the engine and much of the avionics and battery pack.

Figure 9.4

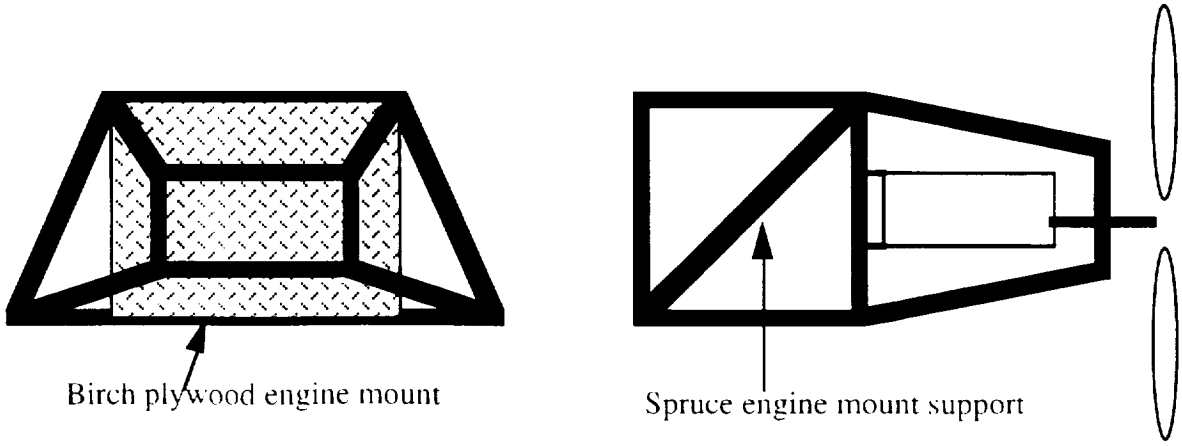

9.4 Landing Gear

Another vital load on the fuselage will be produced by the landing gear. We will use the tail-dragger configuration which will already place the wing at a slight angle of attack prior to liftoff. The position of the front tires is based on the moment balance between the weight at the center of gravity and the thrust acting at the fuselage centerline. The exact placing of all members of the landing gear was based on having a turnover angle of less than 55 degrees. The calculations for turnover angle were based on the following equations and Figures 9.5 and 9.6 (Reference 11).

Alpha=atan(A/B) X=C/tan(Alpha) Y=(D+X)sin(Alpha) Theta=atan(E/Y)

Figure 9.5

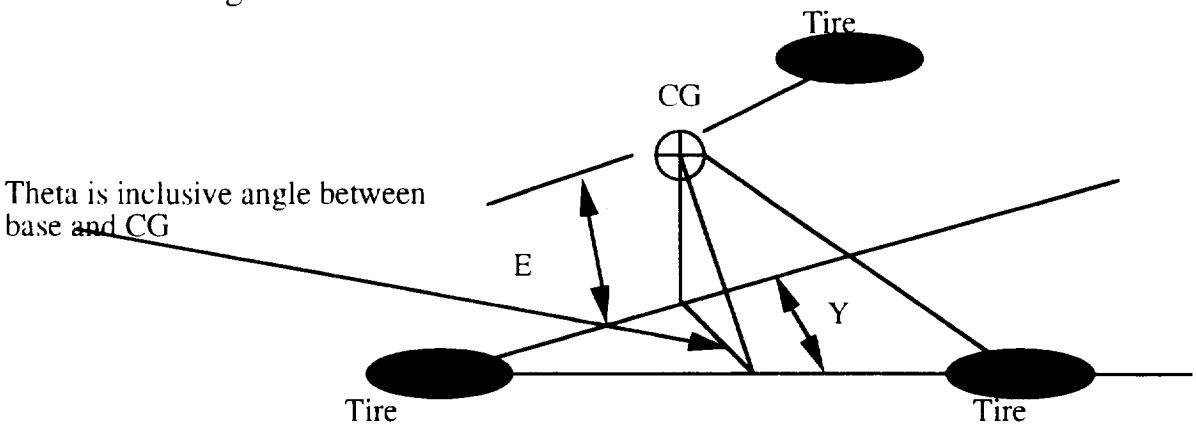

Figure 9.6

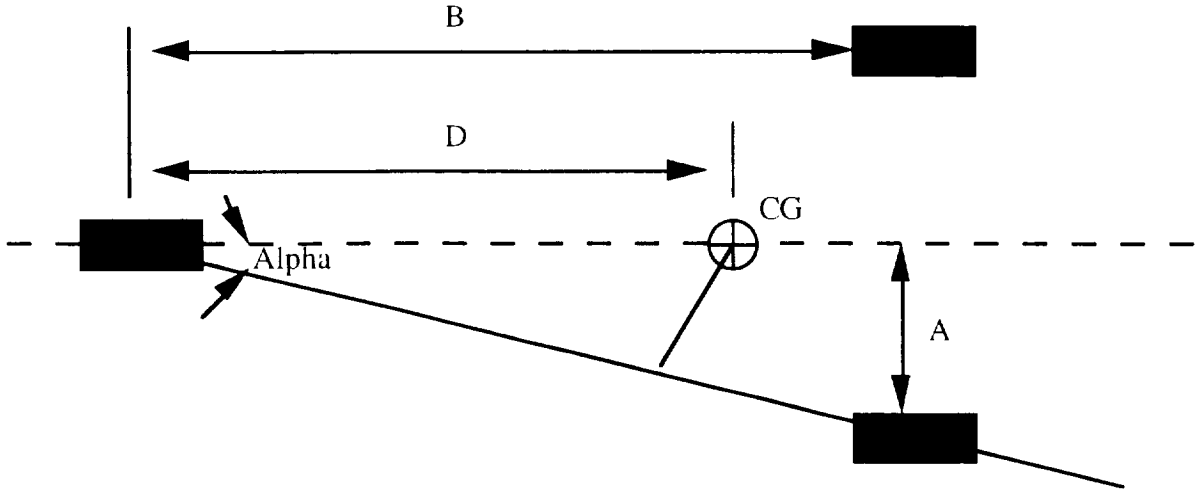

The landing gear struts must be long enough to provide for propeller clearance and for placing the airplane at the desired orientation for takeoff. The struts will be long enough to allow for an extra 1.5 inches of clearance and to allow for landing gear deflection of 1.0 inch upon impact. The struts are to be constructed from aluminum with a wire connecting the front gear to give additional support.

9.5 Empennage

The empennage will consist of a horizontal and a vertical flat plate due mainly to the ease of construction. Both of these components will be directly connected to the keel to ensure that the control surfaces are adequately supported. The horizontal tail should be out of the wake of the wing in order to bring the tail efficiency near unity. The empennage will be tapered and will employ a basic control surface design. Figures 9.7 and 9.8 illustrate the simple structural designs necessary for the horizontal and vertical tails respectively.

Figure 9.7

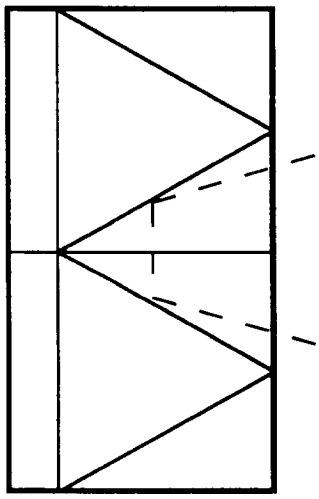

Horizontal tail parameters:
S = 2.98 ft2
AR = 2.4
b = 32.75 inches
c = 13.10 inches

Figure 9.8

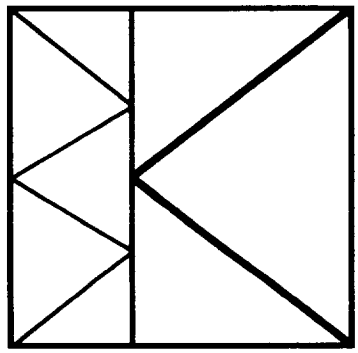

Vertical tail parameters:
S = 0.972 ft2
AR = 2.0
b = 16.7 inches
c = 8.37 inches

9.6 Loading

The structural design of the aircraft was based on a factor of safety of 1.5, and it was necessary to examine the particular aircraft loading in order to allow the airframe to fall within this safety limit. There are two types of loading that must be considered, those while the aircraft is on the ground and those while in the air. On the ground the load applied by the landing gear where they are attached to the fuselage was considered. The two distributed loads along the x and y axis of the aircraft were also examined. Along the y-axis is the weight of the wing which produces a bending moment at the root chord --M= Wing Weight*(span)/2. Along the x-axis are the landing gear, fuselage, and aircraft components. However, greater loads occur during flight, and studies were driven by the fact that most stresses will occur during this period, with the greatest stresses occurring during the turn.

The load factor for takeoff was determined from the vertical acceleration necessary to overcome the acceleration due to gravity. The equation to determine this load factor is as follows:

Takeoff $n = 1 + a/g$ (a = vertical acceleration)

A vertical acceleration of 3.0 was approximated from takeoff data and resulted in a load factor of only 1.3 at takeoff.

The load factor is greatest during the turn because the plane encounters the force due to the weight of the aircraft and the force due to increased acceleration in the turn. In the turn the load factor is affected by velocity, radius, and weight. For a sixty foot radius turn at a velocity of 25ft/sec, the maximum load factor was determined to be 2.2. With this load factor of 2.2 and the design load factor of 3.0 only a factor of safety of 1.4 was achieved. Although this falls below the required limit, the factor of safety of 1.4 was deemed sufficient by the design team.

Based on this load factor analysis and the expected ultimate loading on the aircraft, the V-n diagram was produced (Figure 9.9). Using the Clmax of 1.8 and (-) Clmax of 0.6 the curves for the load factor versus velocity were determined based on these equations and parameters:

$n = 0.5*(\text{air density})*S/W*Clmax*V$

$W = 5.5$ lbs $S = 10$ ft^2

air density = 0.00238 lb/ft^3

The upper load factor limit of 2.2 was determined from that incurred during the required turn, while the Vcruise and the Vmax limits were determined from propulsion data.

Figure 9.9

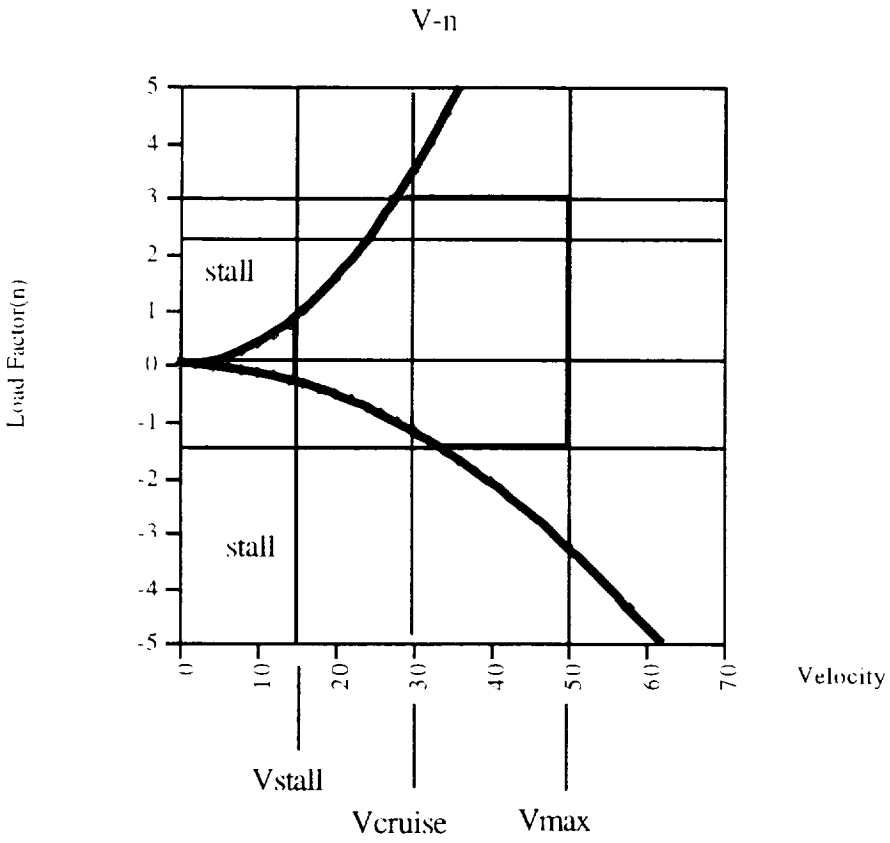

The structural design team was able to acheive the goal of weight and cost reduction through the use of light and inexpensive materials. In order to maintain the design factor of safety of 1.5 for all of the substructures, it was at times necessary to sacrifice some of the weight and cost benifits with the use of stronger materials. Overall, The Bunny will be able to turn these lightweight structural benefits into better takeoff distance and overall cruise efficiency.

10.0. ECONOMIC ANALYSIS

10.1 Cost Estimates

In order to successfully compete against the HB-40 and future entries into the AEROWORLD market, *The Bunny* must be designed and manufactured with a similar level of economic efficiency. The HB-40, the only existing AEROWORLD air transportation server, is manufactured at a cost of approximately $2300.00 per aircraft with a cost per seat per 1000 feet (CPSPK) of .9 cents operating at full capacity (40 passengers) for its full design range (17,000 feet). Attempting to be as attractive to the market as possible, *Sunshine Aeronautics* originally proposed to produce an aircraft which could operate at a CPSPK 25 % less than that of the HB-40 (.675 cents). Although this goal was termed "ambitious" by senior level management, it proved to be quite attainable after a thorough cost analysis.

The cost breakdown for production and operation of *The Bunny* is shown in Table 10.1. Once the propulsion system was selected, the fixed subsystem costs were set. As the design narrowed and geometric quantities were known, the amount of raw materials needed for manufacturing could be estimated. (Some alterations may be made to this as a detailed manufacturing plan is produced.) Estimations of manufacturing costs such as personnel, tooling, and disposal were made bringing the total cost of *The Bunny* to $1948.69, 12.4% less than the original projected cost of $2225.00 and 18% less than the cost of manufacturing the HB-40. Of course, this improved cost relies directly upon an efficient manufacturing plan with little waste and few or no material change orders.

A cost analysis was then performed as presented in Reference 1. *The Bunny* was calculated to safely perform 397 flights in its lifetime, resulting in a total depreciation cost of $4.91 per flight. For a design flight time of 453.3 seconds (7.56 minutes), the operation costs, including the flight crew costs and maintenance costs, were calculated to be $.363 per flight. For the same aforementioned flight time, the fuel cost was found to be $.992-$1.98 per flight depending on the current cost per amphour of battery usage. The above costs were added together resulting in a direct operating cost (DOC) of $6.26-$7.25 per flight.

Table 10.1: Cost Breakdown

Aircraft Cost:			
Fixed Subsystems			
Astro 15 Motor		$107.00	
Radio Transmitter		$ 75.00	
Radio Receiver		$ 35.00	
Avionics Battery Pack		$ 10.00	
Switch Harness		$ 5.00	
Servos (3)		$105.00	
Speed Controller		$ 50.00	
Batteries (13 P-90SCR's)		$ 39.00	
Motor Power Wiring (2 feet)		$ 4.00	
	Subtotal		$430.00
Raw Materials			
Fuselage Wood		$ 18.52	
Wing Wood		$ 12.54	
Landing Gear		$ 2.63	
Glue		$ 15.00	
MonoKote		$ 20.00	
	Subtotal		$ 68.69
Manufacturing			
Personnel (100 hours)		$1000.00	
Tooling		$ 350.00	
Disposal		$ 100.00	
	Subtotal		$1450.00
********	**Total Cost Per Aircraft**		**$1948.69**
Depreciation Costs:			
# of flights/lifetime		397 flights	
**********	**Depreciation Cost**		**$4.91/ flight**
Operation Costs:			
Flight Crew Costs		$ 0.3/flight	
Maintenance Costs (all coach)		$.063/flight	
**********	**Operation Costs**		**$0.363/ flight**
Fuel Costs:			
Current Draw		5.25 amps	
Cost per amphour		$1.50-$3.00	
**********	**Min. Fuel Cost**		**$0.992/ flight**
**********	**Max. Fuel Cost**		**$1.98/ flight**
Direct Operating Costs (DOC)			**$6.26/ flight-$7.25/ flight**

10.2 Cost Per Seat Per 1000 Feet

The DOC is insignificant as a means of comparison with the HB-40 due to its different design range and capacity. In order to put this DOC into perspective in relation to the size and range of the aircraft produced for comparative purposes, a parameter was defined as the cost to move each passenger seat a given distance. The cost per seat per 1000 feet (CPSPK) of the HB-40 is known to be .9 cents per flight based upon its full capacity (40 passengers) and its design range (17,000 feet). *Sunshine Aeronautics* has imposed upon itself the objective of achieving a CPSPK 25% less than that of the HB-40, or .675 cents per flight. After the above cost analysis and a review of the range and payload combinations available to *The Bunny*, it now appears that this goal is very feasible at the design range (10,000 feet) when fully loaded (100 passengers). Figure 10.1 shows the variation in CPSPK with range of flight for a fully loaded aircraft. A CPSPK of .675 cents per flight falls between the minimum and maximum calculated DOC's at the design range of 10,000 feet. In fact, *The Bunny* can fly routes as short as 7500 feet (75% of its design range) fully loaded with a CPSPK less than the HB-40 flying at its design range. If the HB-40 were to fly for 75% of its design range (12,750) it would have a CPSPK of 1.2 cents per flight, whereas that for *The Bunny* is about .9 cents per flight. Table 10.2 lists the CPSPK at the design range and half the design range for a range of passenger loads.

Figure 10.2 shows the variation of CPSPK with range for different passenger loads at the maximum direct operating cost. Note that *The Bunny* could fly at 75% capacity for its design range at a CPSPK equal to that of the HB-40. Also note the trend that CPSPK increases dramatically for ranges less than approximately 5000 feet and for a 25% capacity flight. This should have no bearing on its marketability, however, since this would be expected for any aircraft produced.

Table 10.2: Cost Per Seat Per 1000 Feet

CPSPK: (see Figures 10.1 and 10.2)	
Design Range (10,000 feet)	
100 passengers	.626-.725 cents
75 passengers	.834-.967 cents
50 passengers	1.25-1.45 cents
25 passengers	2.50-2.90 cents
Range = 5000 feet	
100 passengers	1.25-1.45 cents
75 passengers	1.67-1.93 cents
50 passengers	2.50-2.90 cents
25 passengers	5.01-5.80 cents

Figure 10.1: CPSPK variation for a fully loaded aircraft

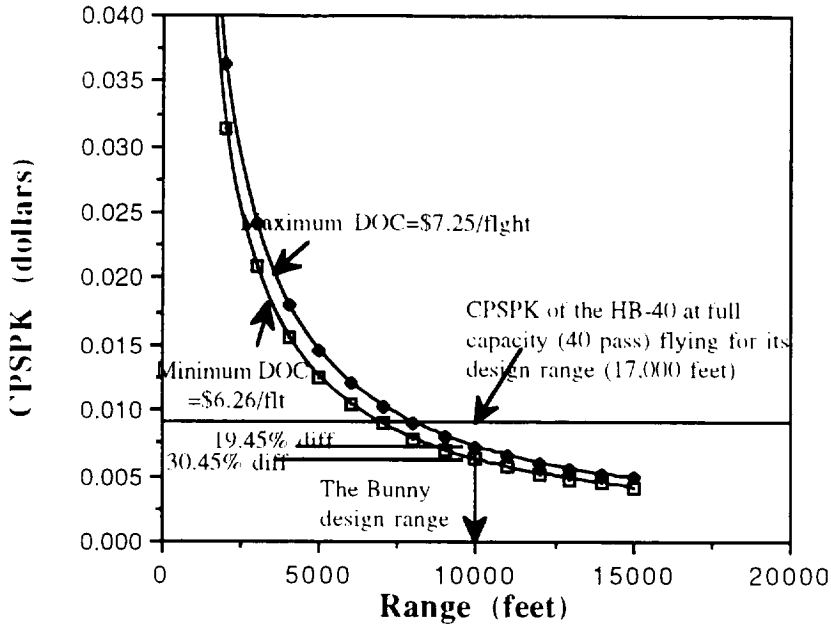

Figure 10.2: Variation of CPSPK with range for different passenger capacities (max DOC=$7.25/flght)

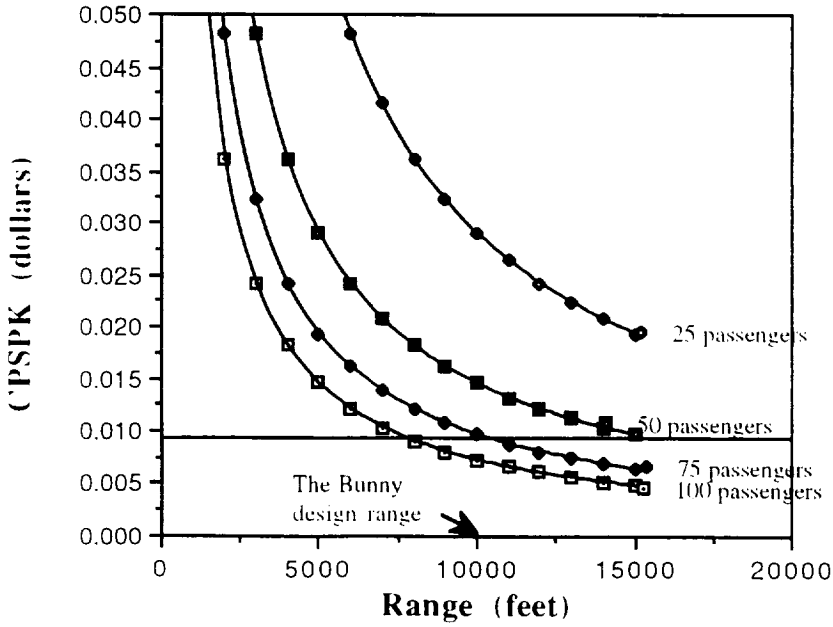

Appendix A: List of References

1. "Request for Proposals", Department of Aerospace and Mechanical Engineering, University of Notre Dame, Notre Dame, IN, 1993.

2. Miley, S.J., A Catalog of Low Reynolds Number Airfoil Data for Wind Turbine Applications, Texas A&M University, College Station, TX, 1982.

3. Roskam, Jan, Airplane Design: Part VI, Roskam Aviation and Engineering Corporation, Kansas, 1985.

4. Jensen, D.T., A Drag Prediction Methodology for Low Reynolds Number Flight Vehicles, A Master's Thesis, University of Notre Dame, 1990.

5. Nelson, Robert C., "Notes from AE 348: Flight Mechanics", Department of Aerospace and Mechanical Engineering, University of Notre Dame, IN, 1991.

6. Batill, Stephen M., "Takeoff Performance", Computer Code, Department of Aerospace and Mechanical Engineering, University of Notre Dame, IN, 1993.

7. Young, B.N., "Propeller Performance Analysis for Small Computers,", Master's Thesis, Department of Aerospace and Mechanical Engineering, University of Notre Dame, 1984.

8. Dunn, Patrick F., "Notes from AE 454: Propulsion", Department of Aerospace and Mechanical Engineering, University of Notre Dame, IN, 1992.

9. Beron-Rawdon, Blaine, "Dihedral", Model Aviation, August-November 1988.

10. Nelson, Robert C., Flight Stability and Automatic Control, McGraw-Hill, Inc., New York, 1989.

11. Currey, Norman S., Landing Gear Design Handbook, Lockheed-Georgia Company, Marietta, GA, 1982.

12. McCormick, Barnes V., Aerodynamics, Aeronautics, and Flight Mechanics, John Wiley & Sons, Inc., New York, 1979.

Appendix B: Stability and Control Analysis Methods

Part I: Longitudinal Stability

For a given center of gravity location, the static margin depends on the neutral point, which is given in Reference 10 as follows:

$$\frac{X_{np}}{\bar{c}} = \frac{X_{ac}}{\bar{c}} - \frac{C_{m_{\alpha f}}}{C_{L_{\alpha w}}} + \eta V_H \frac{C_{L_{\alpha t}}}{C_{L_{\alpha w}}} \left(1 - \frac{d\varepsilon}{d\alpha}\right) \qquad \text{B-1}$$

This model is based on a component build-up method which considers separately the contributions of the wing, fuselage, and tail to the pitching moment coefficient. Each contribution is estimated using simple theoretical models. The key assumptions made in these analyses are small angle of attack, negligible vertical distance from the c.g. to the aerodynamic center, and negligible drag from the tail. Since *The Bunny* is relatively small and will perform only limited maneuvers, these assumptions should be valid. Although the drag on the tail is not negligible, the vertical distance from the tail a.c. to the airplane c.g. is very small and thus this assumption should hold. However, the effect of drag may be important at high angles of attack. The tail efficiency was assumed to be one, but since the tail lies in the wake region of the wing, in reality the efficiency will be less than one. An elliptic lift distribution was assumed when calculating downwash effects, and the distance from the wing to the tail was not taken into account. In this analysis, $C_{m_{\alpha f}}$ was determined to be very small for the target c.g. and was neglected. The effect of the propulsion system was also neglected, although the propeller can produce a considerable moment about the c.g. at high angles of attack.

Part II: Lateral/Directional Stability and Control

The basic premise of a rudder-elevator only design is that the rudder can be used to induce a sideslip angle, which will in turn produce a roll moment for an aircraft with dihedral. This effect occurs due to the difference in angle of attack between the two sides of the wing when in a sideslip. Wing sweep also produces a roll moment, due to the difference in velocity between the wings in a sideslip. There will also be a roll moment produced due to the change in lift force acting on the vertical tail, if the aerodynamic center of the tail is off the airplane's centerline. *The Bunny* has some sweep due to taper on the outer portion of the wings; this effect was included but estimated only. The distance from the a.c. of the tail to the centerline was initially assumed to be small and this effect was neglected.

The chain rule can be used to derive an expression which relates the roll moment to the rudder deflection which produces the sideslip angle. Thus the roll control power $C_{l\delta r}$ can be written

$$C_{l\delta r} = C_{l\beta} \frac{\Delta\beta}{\Delta\delta_r} \qquad \text{B-2}$$

A relationship between the sideslip angle and the rudder deflection can be developed by assuming a steady sideslip condition. If the aircraft is flying at a given sideslip angle, the yaw moment will be zero (no additional sideslip is being created as the rudder is held in a particular deflection). The yaw moment coefficient can be expressed as

$$C_n = C_{n\delta r}\,\Delta\delta_r + C_{n\beta}\Delta\beta \qquad \text{B-3}$$

If the yaw moment is set to zero, the equation can be solved for $\frac{\Delta\beta}{\Delta\delta_r}$

$$\frac{\Delta\beta}{\Delta\delta_r} = -\frac{C_{n\delta r}}{C_{n\beta}} \qquad \text{B-4}$$

Thus the roll moment coefficient induced by a rudder deflection is

$$C_{l\delta r} = -\,C_{n\delta r} \frac{C_{l\beta}}{C_{n\beta}} \qquad \text{B-5}$$

Since $C_{n\beta}$ is typically positive while $C_{n\delta r}$ and $C_{l\beta}$ are both typically negative, $C_{l\delta r}$ will be negative. Thus for a positive rudder deflection, a negative roll moment is produced. Using the sign convention in Reference 10, this means that a left rudder deflection will produce a left roll, as might be expected.

The expressions used to calculate the stability coefficients are as follows:

$$C_{n\delta r} = -V_v \eta_v \tau C_{L\alpha v} \qquad \text{B-6}$$

(Ref. 12, p. 527)

$$C_{n\beta} = C_{n\beta wf} + V_v \eta_v C_{L\alpha v}\left(1 + \frac{d\sigma}{d\beta}\right) \qquad \text{B-7}$$

(Ref. 10, p. 70)

$$C_{l\beta} = -\frac{C_{L\alpha w}}{6}\left(\frac{1+2\lambda}{1+\lambda}\right)\Gamma - \left(\frac{1+2\lambda}{3(1+\lambda)}\right)C_L \tan\Lambda + .00917 \text{ /rad} \quad \text{B-8}$$

(Ref. 12, pp. 544, 547)

For $C_{n\delta r}$, η_v was assumed to be 1, and $C_{L\alpha v}$ was calculated based on a two-dimensional theoretical lift curve slope of 2π for a flat plate. The flap effectiveness factor τ was obtained from Reference 10 as a function of the ratio of rudder area to vertical tail area. For the coefficient $C_{n\beta}$, similar assumptions were made, with $C_{n\beta wf}$ estimated according to Reference 10 (p. 68), and the factor $\eta_v\left(1 + \frac{d\sigma}{d\beta}\right)$ calculated as a function of vertical tail area according to Reference 10 (p. 71). The expression for $C_{l\beta}$ is a summation of three factors: the dihedral effect, the wing sweep effect and a constant empirical factor for the fuselage cross-flow effect.

The above formulae are based on small-angle assumptions for the angle of attack, dihedral, and sideslip. In addition, induced drag effects which occur at low aspect ratios were neglected. The empirical calculations indicated were based on preliminary estimates of overall aircraft parameters in the early design phases and should be corrected in further design studies.

Appendix C: Data Base

Airplane	# of passengers	Weight(lbs)	vel(cruise) ft/s	Endurance(s)	Range(ft)	Fuselage Vol(in3)	Fus Length(in)
HB 40	40	4.29	30	600	17000	864	57
Initial Guess		3.81	28	240	5500	549.504	51
El Toro	51	5	28	978	25000	691.2	40
Pale Horse	30	4.98	30	646.8	20000	1416.96	51.2
	50	3.81	32	510	8000	1537.92	44
FX-90		2.75	24	479.4	12210	238.464	17
Arrow 227		5	27	558	15990	1587	58.2
Drag-n-Fly		2.73	25	193	4831	670.464	41
Dawdler		2.3187		193	5280	841.54	37
Screem-J4D		3	23	234	5500	25.92	37
Penguin		3.125	25	105.3	2609	259.2	42

Airplane	Wing Area(ft2)	Wing span(ft)	Aspect ratio	Dihedral (deg)	HTail Area(ft)	VTail Area(ft)	Battery volts
HB 40	7.34	8	8.72	7	1.01	0.42	10.8
Initial Guess	7	7	7	9	1.3	0.6	
El Toro	6.94	8.33	10	20.6 (polyhedral)	1.25	0.49	15.3
Pale Horse	7	8	9.14	10	0.97	0.46	15.6
	5.81	5	4.3		1.1	0.347	14.4
FX-90	4.38	5.84	7.79	13	0.482	0.35	
Arrow 227	9.51	10	10.52	8	1.57	0.72	14.4
Drag-n-Fly	6.02	8.5	12	12 (polyhedral)	1.05	0.5	
Dawdler	3.24	5	7.72	13	1.4	0.3437	
Screem-J4D	5.46	8	11.72	10	0.63	0.38	
Penguin	4.67	7	10.5	3	1.04	0.42	15.6

Component Weights							
Airplane	weights(ozs)						
	engine	mount	servos	prop	speed control	batteries	receiver
HB 40							
Initial Guess							
El Toro	9.05			0.5	7.5	21.3	
Pale Horse	9.12	1.12	1.28	0.8	1.76	24.16	0.96
FX-90	5.5	1	1.2	2	3.23	7.46	0.95
Arrow 227	8.9	1.91	1.2	0.54	2.66	20.55	0.95
Drag-n-Fly	8		1.2		3.23	8.24	0.95
Dawdler	6.9	1.29	1.31		1.25	6.4	0.95
Screem-J4D	6.5		1.2	1	3.23	8	0.95
Penguin	10.3	4	1.8	2	3	7	1

Airplane					
	wing	fuselage	empenage	landing gear	total
HB 40					
Initial Guess					
El Toro	14	15	3	7.1	77.45
Pale Horse	17.6	13.28	1.92	5.12	77.12
FX-90	10.5	10	3.5		45.34
Arrow 227	15.5	11	3.4	5	71.61
Drag-n-Fly	12.1	1	2.64	2	39.36
Dawdler	8.18	11.4	3.6	1	42.28
Screem-J4D	10.36	5.22	1.18	2.4	40.04
Penguin	12.5	10	1.7	2.9	56.2

Appendix D: Primary Deliverables - Figures and Tables

List of Figures and Tables

1. **Figure 8.2:** Payload vs. Range
2. **Figure 4.4:** Cl & Cd vs. Alpha for FX 63-137 Airfoil
3. **Figure 4.15:** Aircraft CL vs. Alpha (with flap deflection)
4. **Figure 4.16:** Aircraft Drag Polar
5. **Table 4.5-4.7:** Component Drag Breakdown
6. **Figure 4.17:** Aircraft L/D vs. Alpha
7. **Figure 7.2:** Pitching Moment Coefficient vs. Alpha for forward and aft c.g.
8. **Figure 8.3:** Power Required and Power Available vs. Cruise Velocity
9. **Figure 5.3:** Propeller Efficiency vs. Advance Ratio
10. **Figure 6.2:** Weight Balance Diagram
11. **Table 6.1:** Component Weight Estimates
12. **Figure 9.9:** V-n Diagram
13. **Figure 1.2:** External View - Three-view
14. **Figure 1.3:** Internal View

Figure 8.2 **Payload Versus Range**

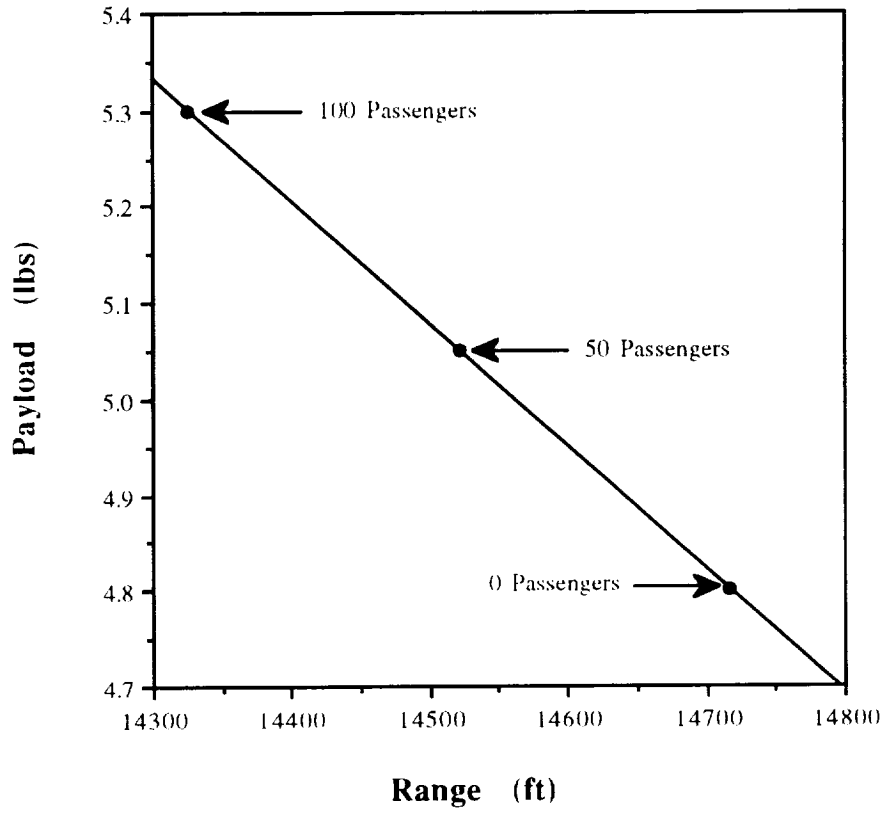

Fig. 4.4: Cl & Cd vs. Alpha for FX 63-137 Airfoil

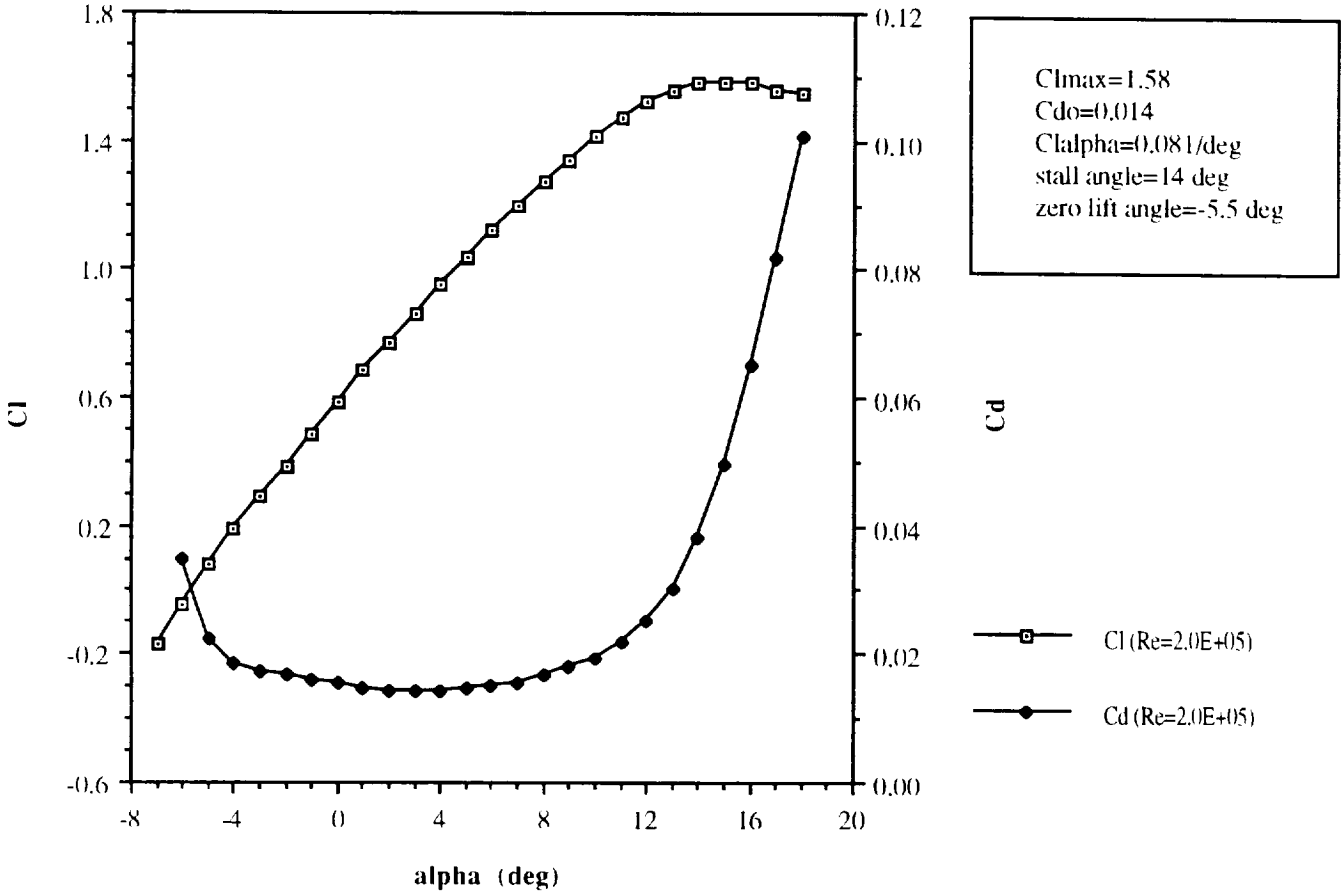

Fig. 4.15: Aircraft CL vs. Alpha (w/flap deflection)

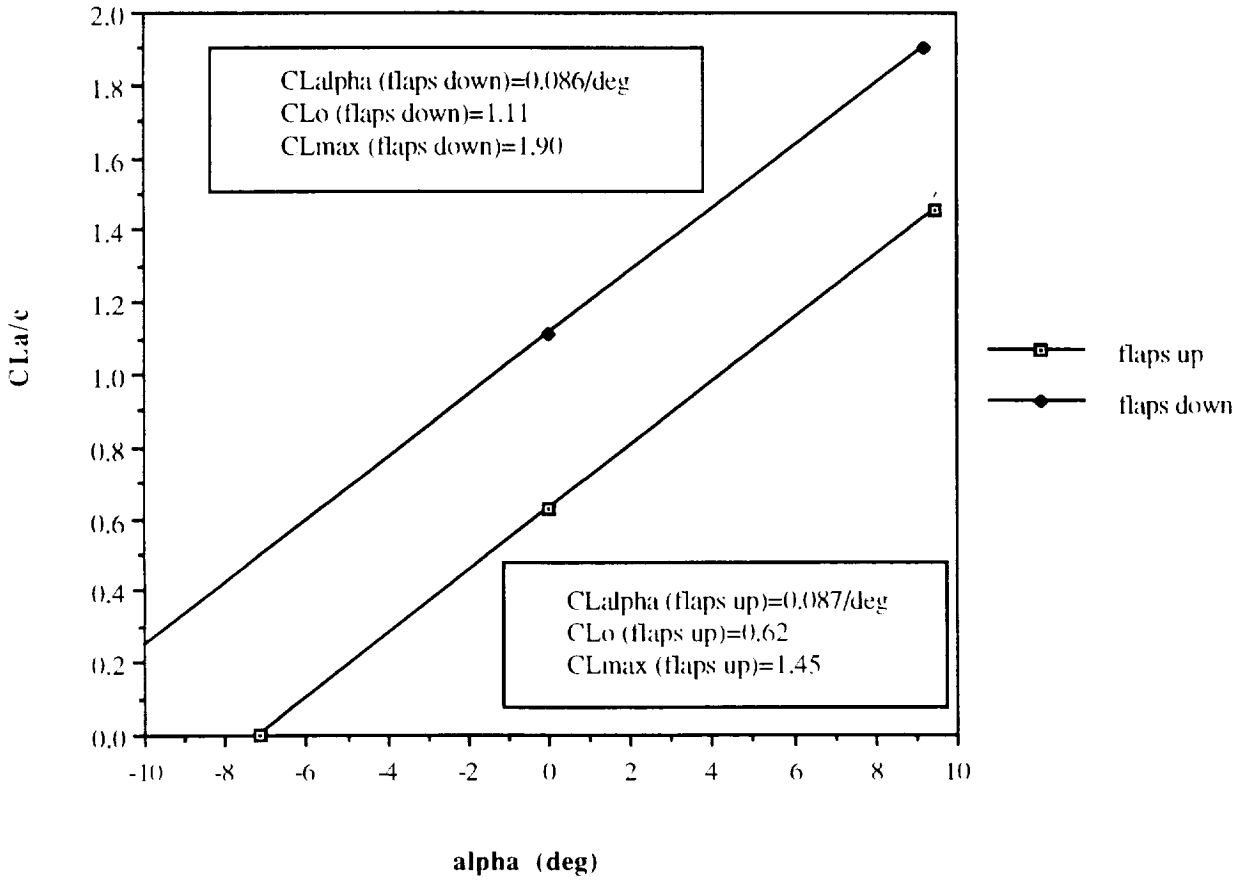

Fig. 4.16: Aircraft Drag Polar

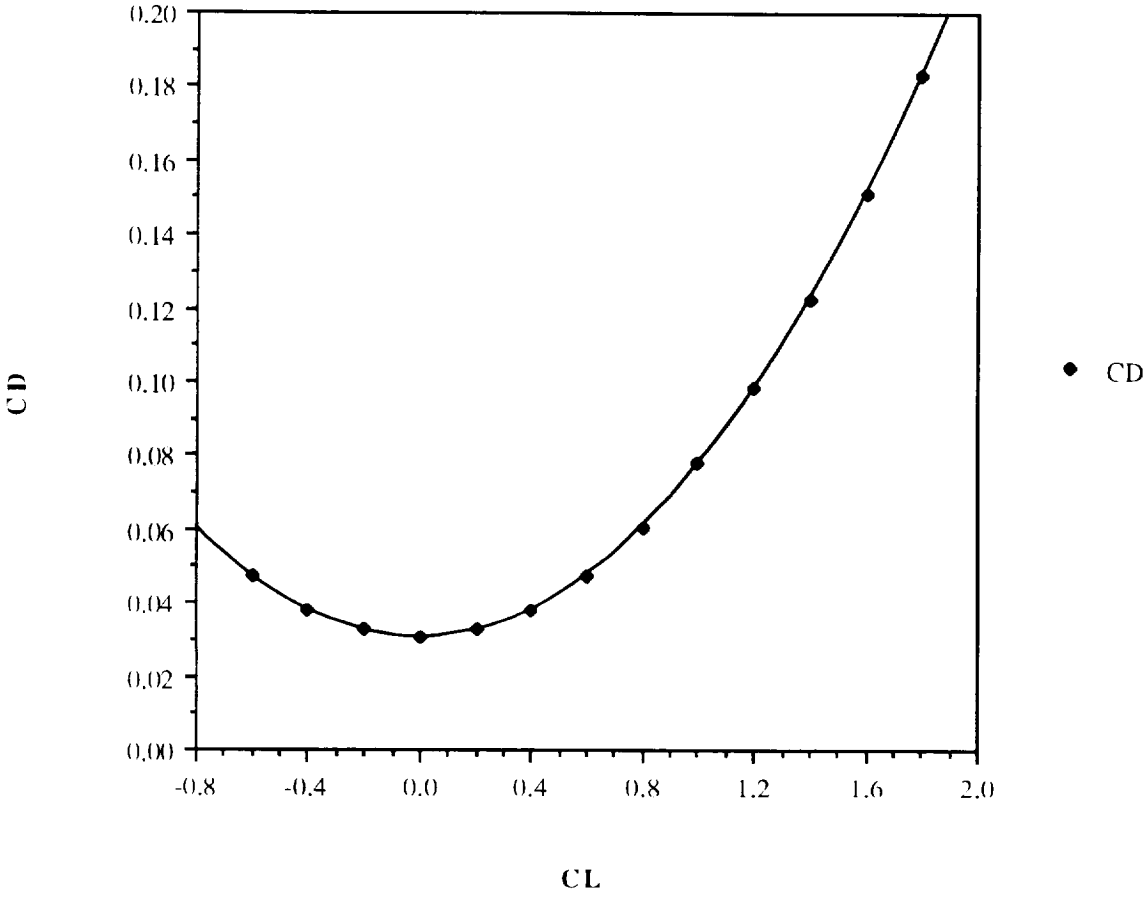

Table 4.5: Jensen's Method I Drag Estimation			
component	**S_{wet} (in^2)**	**C_{Do} Contribution**	**% Total C_{Do}**
wing	2880.0	0.0110	40.1
fuselage	1288.0	0.0049	17.9
horizontal tail	858.0	0.0032	11.7
vertical tail	340.0	0.0012	4.4
landing gear	--	0.0071	25.9
TOTAL		**0.0274**	

Table 4.6: Nelson's Component Drag Breakdown Estimation				
component	**$C_{D\pi}$**	**A_π (in^2)**	**C_{Do} Contribution**	**% C_{Do}**
wing	0.007	1440.0	0.0070	24.5
fuselage	0.110	31.5	0.0024	8.4
horizontal tail	0.008	429.0	0.0024	8.4
vertical tail	0.008	170.0	0.0009	3.1
landing gear	0.014	1440.0	0.0140	49.0
interferences			0.0006	2.1
roughness/protuberances			0.0013	4.5
TOTAL			**0.0286**	

Table 4.7: Combined Nelson/Jensen Method II Drag Breakdown Estimation				
component	**$C_{D\pi}$**	**A_π (in^2)**	**C_{Do} Contribution**	**% C_{Do}**
wing	0.007	1440.0	0.0143	38.6
fuselage	0.110	31.5	0.0024	6.5
horizontal tail	0.008	429.0	0.0024	6.5
vertical tail	0.008	170.0	0.0009	2.4
landing gear	0.014	1440.0	0.0140	37.8
interferences			0.0010	2.7
roughness/protuberances			0.0020	5.4
TOTAL			**0.0370**	

Fig. 4.17: Aircraft L/D vs. Alpha

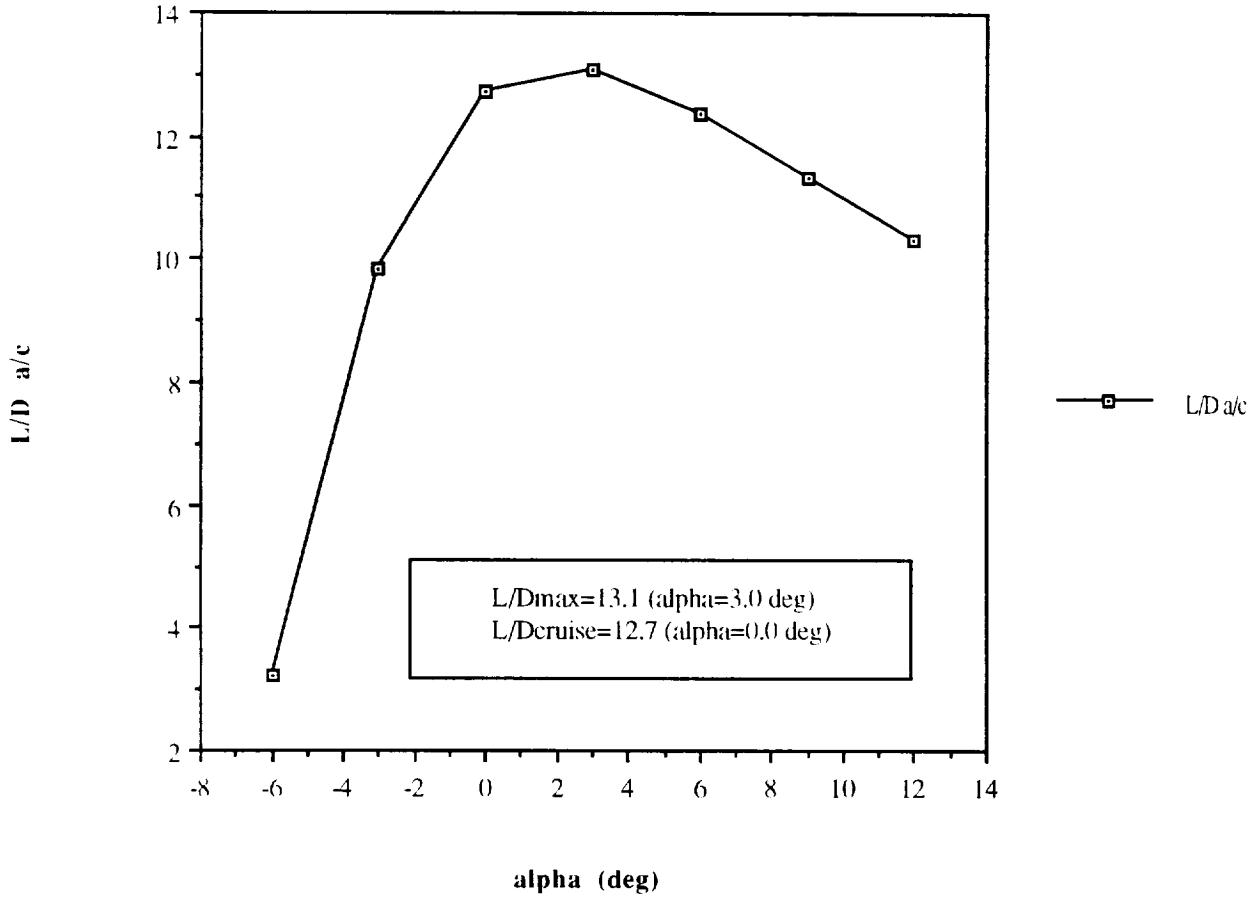

Figure 7.2: Pitching Moment Coefficient vs. Alpha for forward and aft c.g. conditions

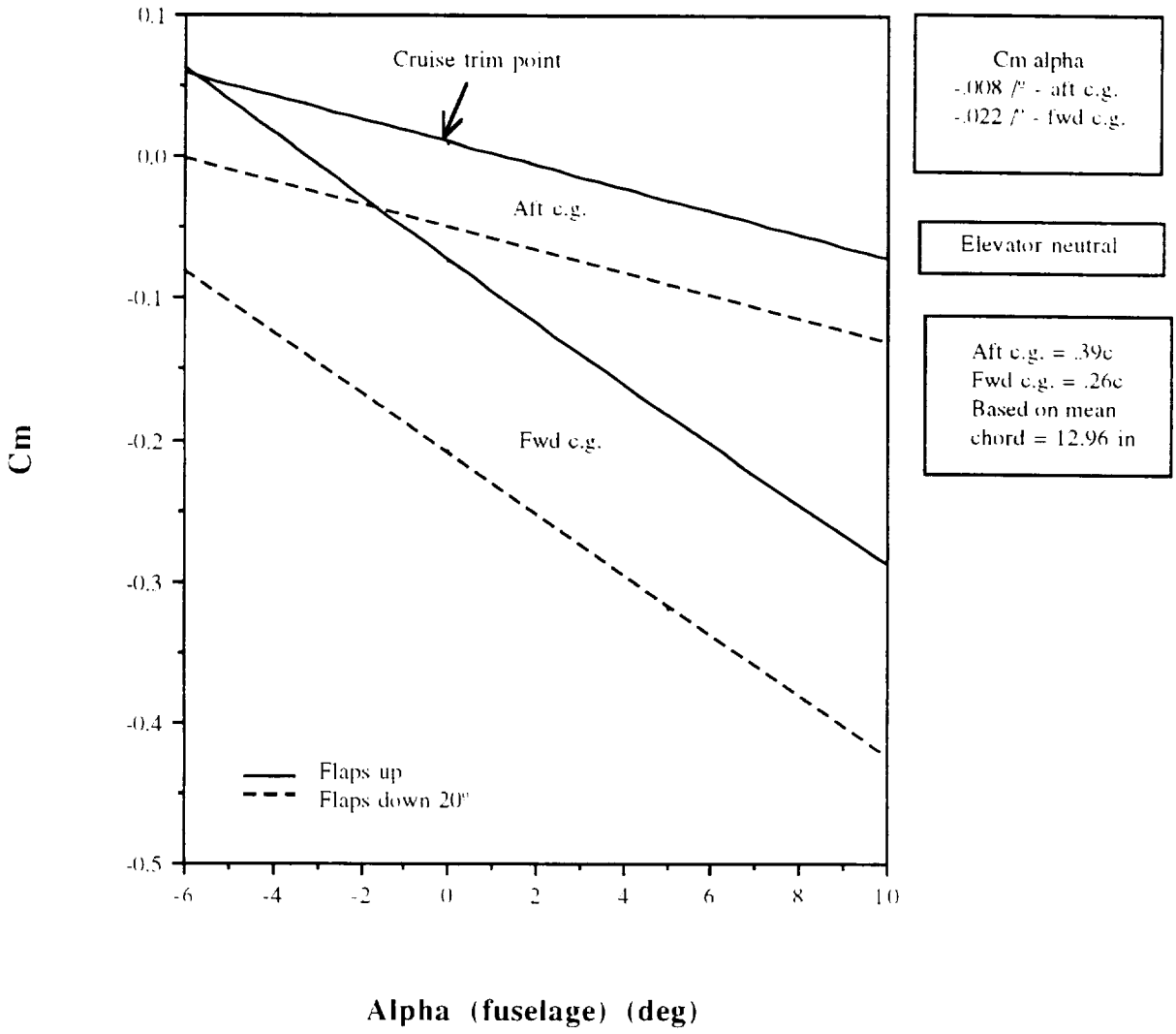

Figure 8.3 **Power Required and Power Available Versus Cruise Velocity**

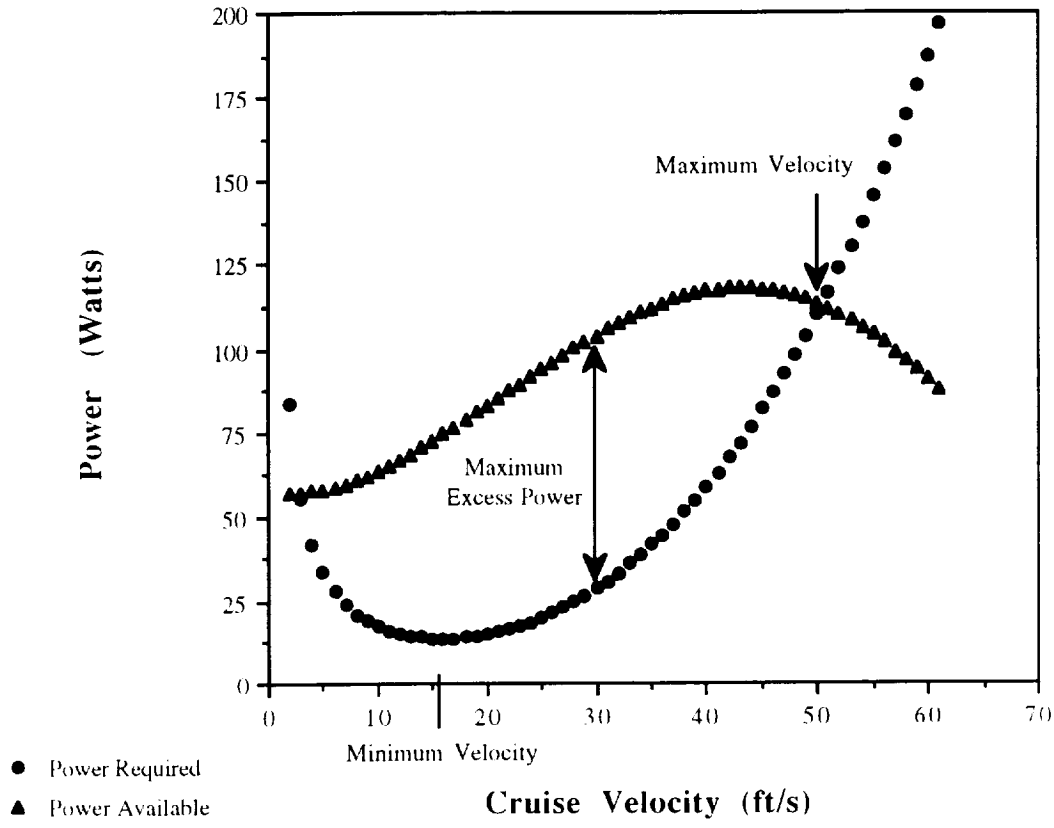

Figure 5.3: Propeller Efficiency vs. Advance Ratio

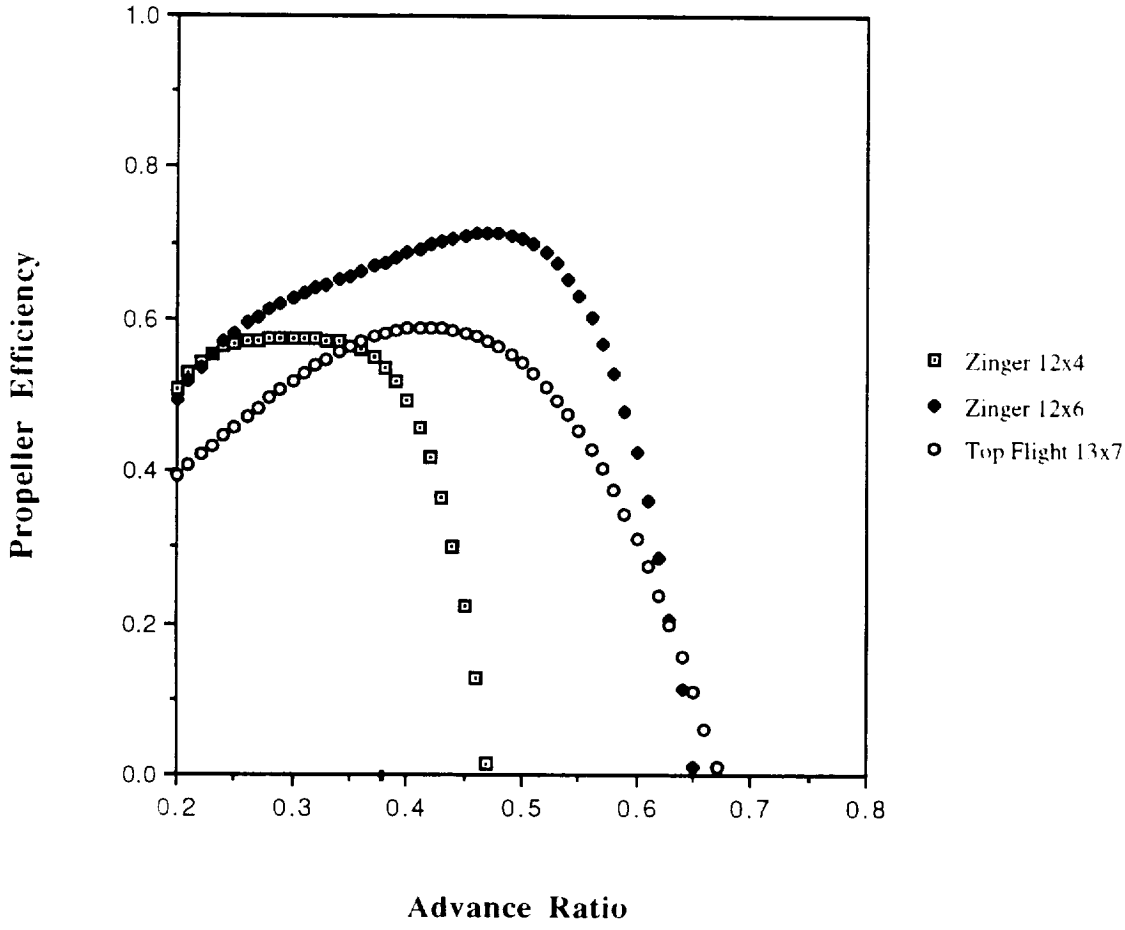

Figure 6.2: Weight Balance Diagram

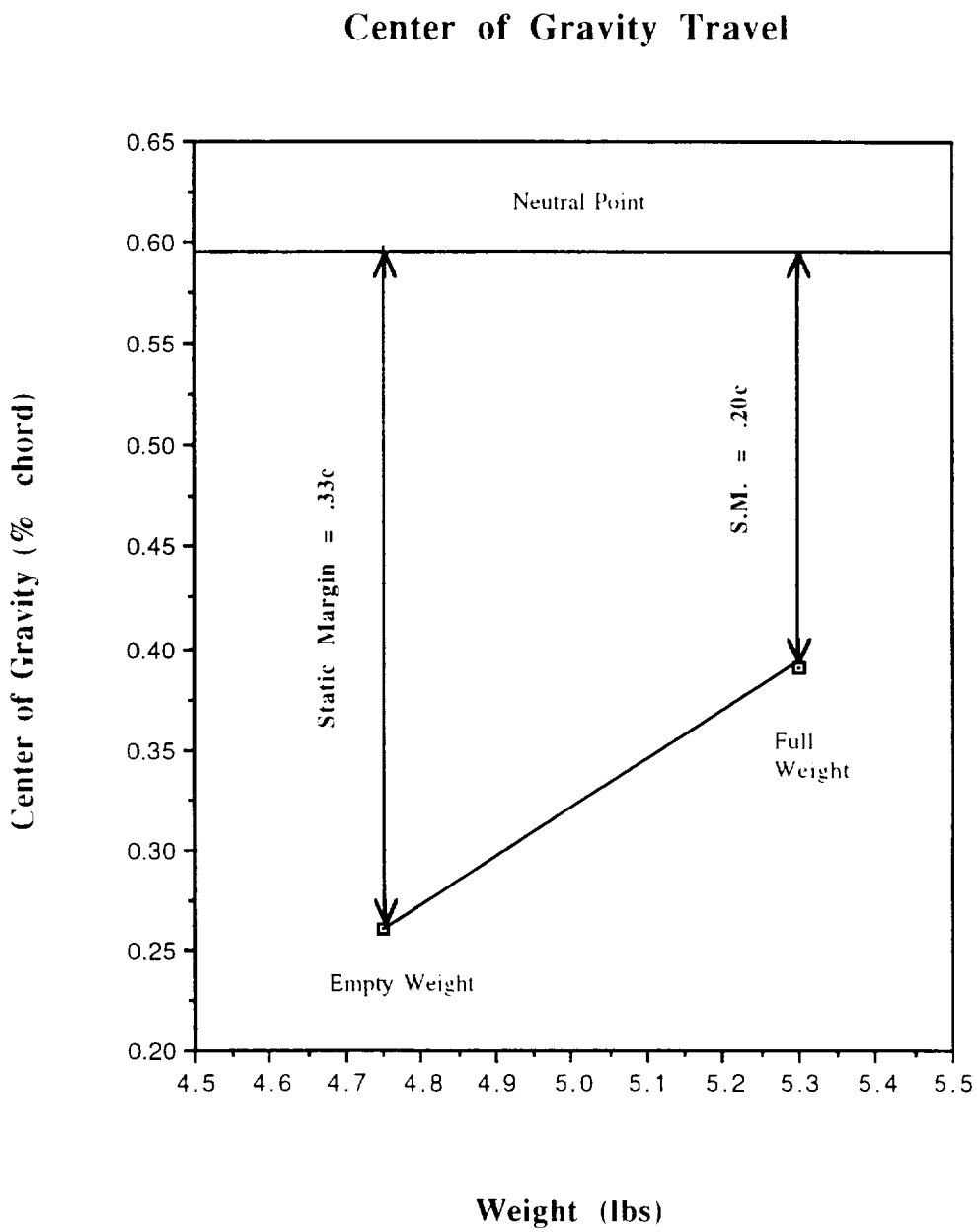

Table 6.1: Component Weight Estimates

Component	Prelim. Estimate (ounces)	Weight Fraction (%)	Final Estimate (ounces)	Weight Fraction (%)
Propulsion:				
engine	9.0	9.49	7.5	9.32
propeller	0.5	.53	.69	.86
avionics package:		27.43		29.82
speed controller	3.25		3.25	
servos	1.8		1.8	
receiver	.95		.95	
batteries	20.0		18.0	
Structure:				
wing	16.0	21.1	14.4	22.86
fuselage	24.0	25.32	11.68	14.51
empenage	4.0	4.22	6.3	7.83
landing gear	5.0	1.05	6.0	2.48
engine mount	1.5	1.58	1.12	1.39
Empty Totals	86.0		71.69	
Passenger load	8.8	9.28	8.8	10.93
Full Totals	94.8	100%	80.49	100%

Figure 9.9 : V-n Diagram

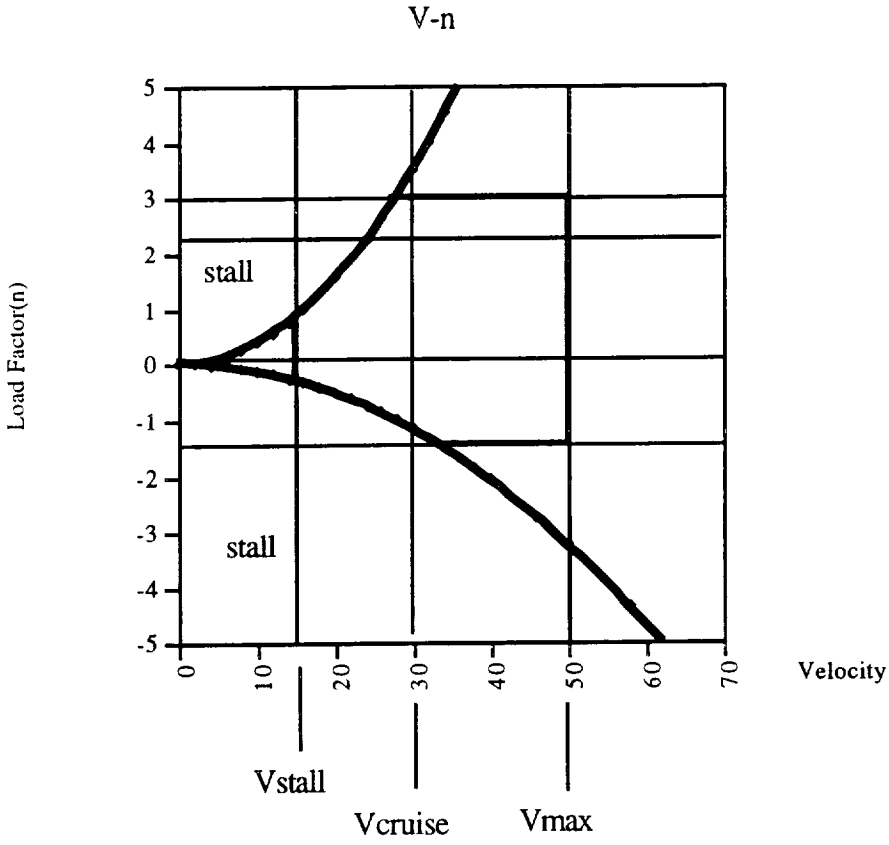

Figure 1.2: External View - Three-view

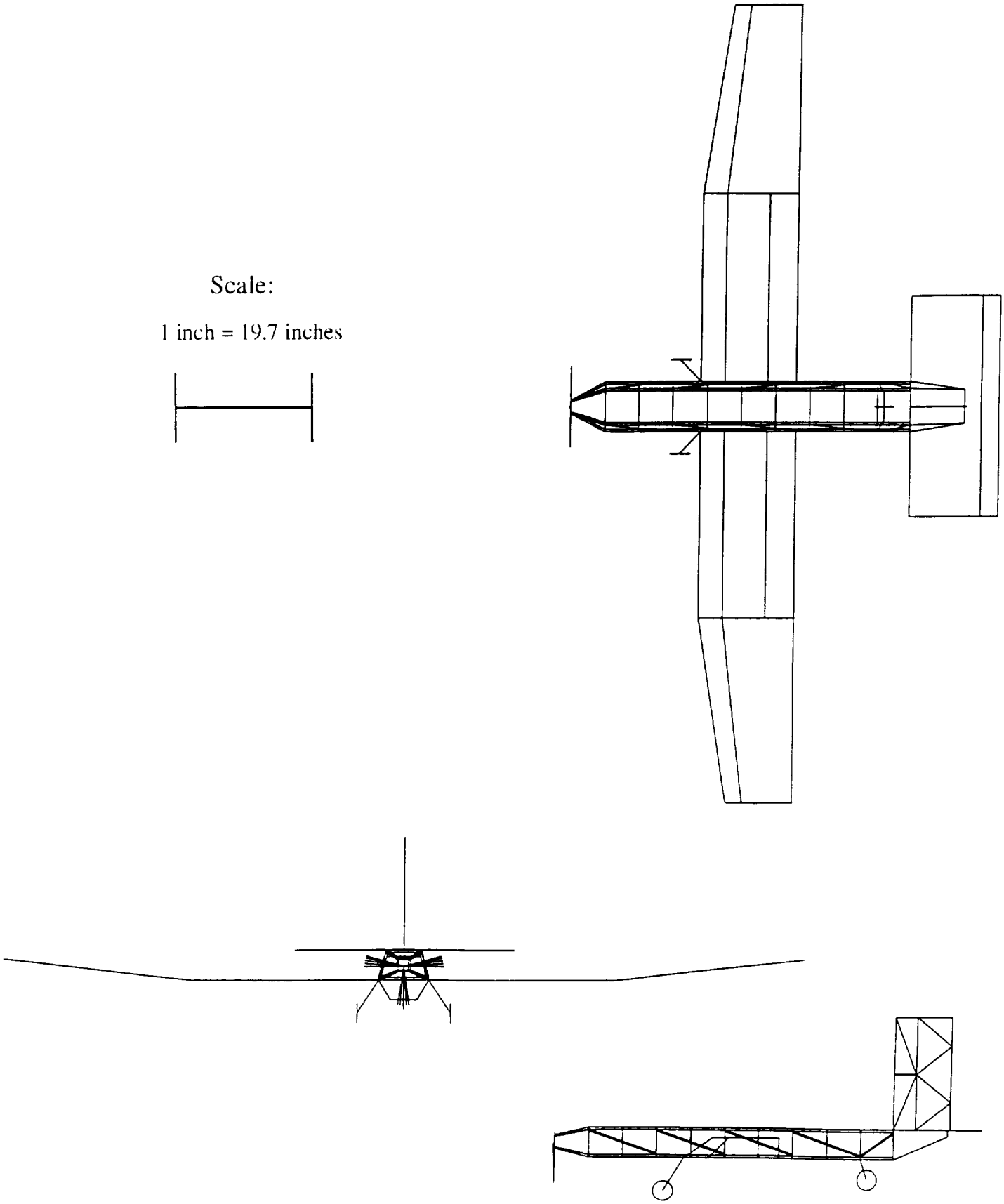

Figure 1.3: Internal View

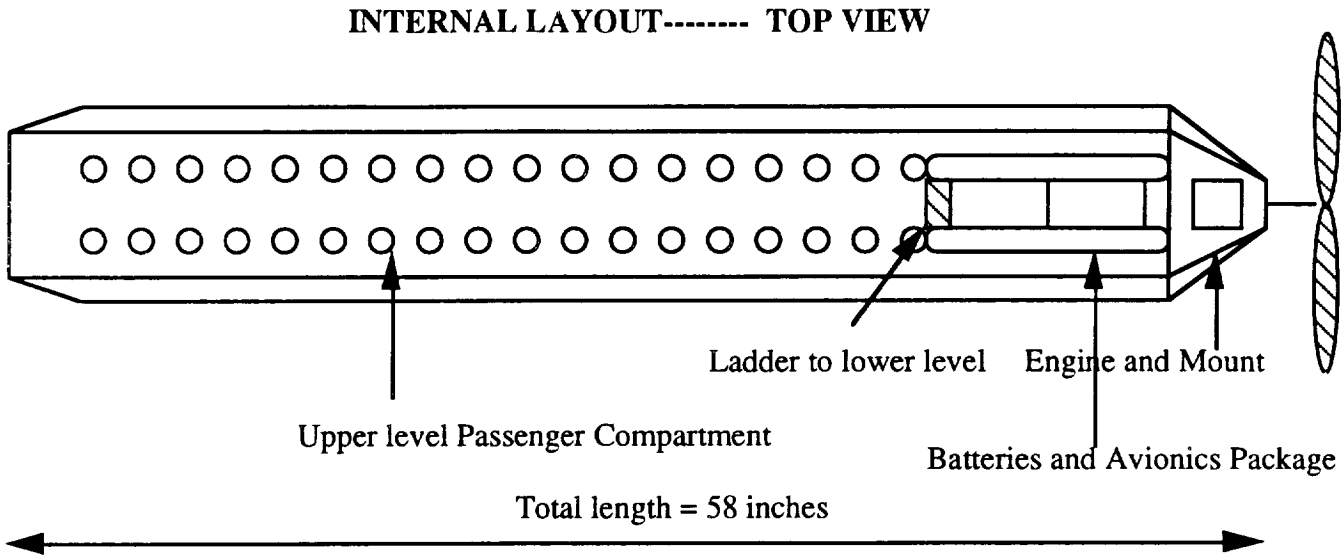

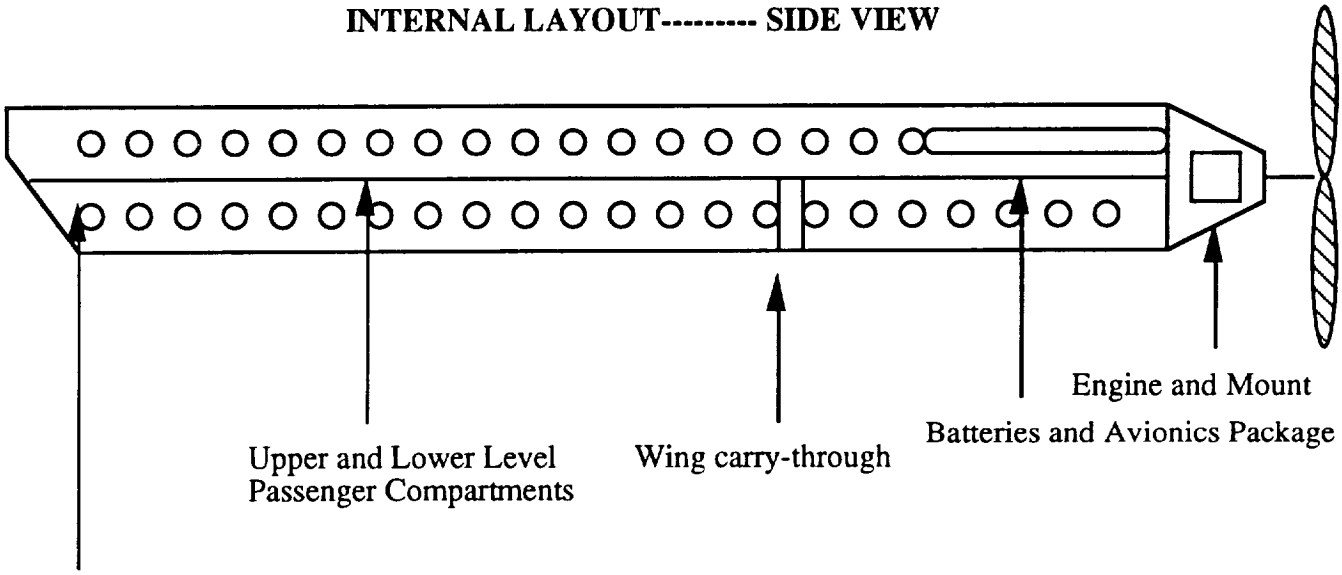

Three passenger rows on the lower deck and two passenger rows on the upper deck

The cockpit and crew are situated below the battery pack and avionics and are separated from the passengers by a main bulkhead

Appendix E: Fabrication of the Technology Demonstrator

The fabrication of the technology demonstrator took place over a two-week span following the Manufacturing Plan Review. General phases of the construction process included the allocation of raw materials and supplies, subsystem/component fabrication, structural component integration, control/propulsion system integration, Monokoting, and systems testing. Several problems and inconsistencies with the proposed design have arisen, however, and necessary adjustments have been made and are listed as follows.

E.1 Weight

Upon completion of fabrication the technology demonstrator weighed approximately 6.7 lbs, 1.4 lbs greater than our final proposed design weight of 5.3 lbs. This weight increase was due primarily to the addition of extra structural support members for the interior avionics compartment and landing gear supports for *The Bunny*. Our initial Monokote estimate was also considerably lower than that used in the fabrication process. These added material weights comprise the majority of the weight increase for *The Bunny*. This higher weight may not allow *The Bunny* to achieve some of its projected performance objectives. However, our original target weight was 6.0 lbs, and many of our initial sizing and performance calculations were made using this weight. In addition, our propulsion analysis indicates that operation of *The Bunny* will be possible for weights under 7.5 lbs. For these reasons, we feel that in spite of the increased weight, *The Bunny* will still perform to acceptable levels. Due to the added weight, the center of gravity was carefully monitored throughout the construction and assembly phases. Through simple balance analyses the center of gravity was found to be located at approximately 0.3 of the mean aerodynamic chord. Center of gravity placement at this location shall provide adequate maintainable stability and control.

E.2 Flaps

The implementation of the flap surfaces and corresponding control systems provided the singlemost time consuming obstacle in the manufacturing of *The Bunny*. Construction of the flap surfaces proceeded according to our Manufacturing Plan Review, yet several alterations had to be made. Extra Monokote had to be added to the flap/wing joint in order to strengthen the connection and allow for adequate flap rotation without translation. Our original design of bending the flexible-type pushrods from the lower level to the flap servo on the upper level proved inadequate. The outer sheath was too stiff to bend, yet the inner rod was too flexible to transmit the necessary force without the sheath. With this arrangement, the movement of the servo resulted mainly in the

bending of the pushrod, rather than the deflection of the flaps as desired. In order to correct this problem, the flap servo was moved to the lower level and a four-arm connection was used. The pushrods were connected perpendicularly to opposite arms of the servo. This allowed the rods to remain straight, and maximized the effect of the servo deflection. With this arrangement, the desired twenty degree flap deflection was able to be achieved. One other condition which added to this problem was the modification of our remote control transmitter to accommodate the flaps. The spring was removed from the flap control so that the pilot would not have to hold the flaps in the deflected position during take-off. However, this modification reduced the degree of rotation of the servo. One further recommendation for future productions of *The Bunny* is to run the pushrods straight out to the desired spanwise location, and use some type of lever device to join the pushrods to the flap control horns at a perpendicular angle. This would allow for greater deflection of the flaps, since there would be less room for bending of the rods.

E.3 Materials and Manufacturing Costs

The manufacturing costs of *The Bunny* exceeded projected totals by approximately 18.3%, amounting in a total increase in aircraft cost of approximately 14.3 % (see Table E.1 below). This increase in the projected cost of *The Bunny* can be accounted for in two major areas, materials and personnel costs. Costs projections in personnel hours were based on crude estimations from previous design reports. A detailed record of actual personhours worked on the construction of *The Bunny* proved that these projected estimates may have been inconsistent or inaccurate. Increases in the materials costs, however, were due primarily to errors in calculating the actual size and amount of materials needed. Whereas the proper size of each structural component was adequately determined, the amount of material needed to to accomplish the task of building each element was underestimated and did not take into account the size availability from the raw materials subcontractor. Subsequently, manufacturing change orders were required for the purchase of added balsa and aluminum rods for the landing gear, consisting of nearly 25% of the entire raw materials cost.

Table E.1: Final Cost of *The Bunny*				
Materials	Projected Cost	Actual Initial Cost	Manufacturing Change Orders	Actual Total Cost
	$68.69	$152.00	$50.00	$202.00
Personnel	Projected Hours	Projected Cost	Actual Hours	Actual Cost
	100	$1000.00	134	$1340.00
Tooling		Projected Cost		Actual Cost
		$350.00		$46.50
Disposal		Projected Cost		Actual Cost
		$100.00		$208.00
Manufacturing Total Cost		Projected Cost		Actual Cost
		$1518.69		$1796.50
Total Cost		**Projected Cost**		**Actual Cost**
		$1948.69		$2226.50

APPENDIX F

Manufacturing Plan and Costing

The construction of the technology demonstrator follows a systematic substructure design. A preliminary sizing estimate allowed for the purchasing of the bare-bone necessities for *The Bunny*. This preliminary design estimate was followed by the drafting of the actual size construction plans. The construction plans enabled the team to determine the final raw materials to be purchased. Using the construction plans, all of the necessary cuts were marked on every piece of wood, and labeled for ease of identification. This plan allows for all of the cutting to be completed at the beginning of the fabrication. Once the cutting is complete, the substructure fabrication may begin.

The fuselage, wing, vertical tail, and horizontal tail are all constructed separately. Each of these substructures will be completed, then assimilated to form the entire aircraft. These are some significant considerations which affected the formulation of the plan.

- Allow for larger disposal costs, thereby minimizing the possibility of an Engineering Change Order penalty
- Make all of the cuts at the beginning of the fabrication, rather than waiting until the piece is to be glued to make the cut
- The fabrication of the flaps was a major concern due to the minimal thickness at the trailing edge of the Wortmann airfoil
  (see flap diagram at end of Appendix F)
- The tapered fuselage involves the cutting of more angles, and therefore heightens the risk of uneven sizing
- 48inch longerons were used, thereby minimizing the amount of splicing in the fuselage to only two splices in the tail section
- Allow six inch hatch at the top of the fuselage for access to the avionics package and for passenger entry
- Space the side beams of the fuselage in a manner in which they can be used for support of the wing carry-through structure and may be used to support the leading edge of the wing
- Due to the large tail sizes, strengthen their support by notching them into the main fuselage longerons for the horizontal tail, and notching the vertical tail into the cross beams of the tail section
- Have one continuous elevator which when deflected upward, will not interfere with the overlapping rudder

- The polyhedral connection to the main wing will be removable in order to ease in handling for transportation

Scheduling (tasks to be completed on/by prescribed date)

April 15

- finalization of the construction plans
- cut marks on all of the pieces

April 18

- all cuts of the wood
- bare-bone construction of the fuselage
- horizontal tail
- vertical tail

April 20

- wing and polyhedral
- wing carry-through, fuselage paneling, and engine mount

April 22

- Monokoting and aircraft assimilation
- landing gear attachment

April 25

- all avionics related assembly, servo connections, push rods, etc...
- ready for Tech Demo Roll Out

Manufacturing Costs

Large Scroll saw----------$ 16.0
Raw Materials cost----------$ 140.12
Disposal Cost----------$ 200.0
Production Manhours---------- 120 hrs

Detailed Raw Materials Breakdown

MATERIAL	COST(dollars)
Balsa	
5 3/32 x 6 x 36 inches	17.00
4 1/2 x 3/8 leading edge	3.60
4 3/8 x 3/8 x 48 inches	5.12
3 1/8 x 3/8 x 36 inches	0.96
10 1/4 x 3/8 x 36 inches	6.40
Birch	
1 1/16 x 12 x 48 inches plywood	16.19
4 3/16 x 36 inch dowels	2.56
Bass	
3 1/8 x 1/4 x 36 inches	1.64
8 1/4 x 3/8 x 36 inches	8.78
Monokote	
4 rolls	35.16
Miscellaneous	42.71
	140.12

FLAP CONSTRUCTION